



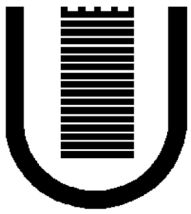

Escuela Técnica Superior de
Ingenieros de Telecomunicación

Universidad Politécnica de Valencia

Facoltà di Ingegneria

Università degli studi di Roma
Tor Vergata

Corso di Laurea in Ingegneria delle Telecomunicazioni

Tesi di Laurea Specialistica

Estimation of quality parameters of vineyards by remotely sensed data

Author: Pablo Farinós Navarro

Coordinator: Ing. Alessandro Burini

Director: Dr. Fabio del Frate

Rome, June 2007

Agradecimientos

Agradezco a mi director de proyecto, Alessandro Burini, el tiempo y la ayuda que me ha dedicado.

Quisiera agradecer a mis padres, Enrique y Carmen, la posibilidad de estudiar esta carrera universitaria, y su orientación siempre tan sabia.

También a mis amigos de la carrera todos esos grandes momentos pasados durante este tiempo.

Y especialmente a mi novia, Dora, por sus ánimos y la confianza depositada en mi.

Contents

1. Abstract

Several studies have demonstrated that it is possible, nowadays, to use high resolution satellite data (hyperspectral and multispectral) to analyze several phenomena related to agriculture, such as crops, plant status, leaf, etc...

Specifically, my final thesis has taken place on ESRIN, ESA (European Space Agency) headquarters on Rome, in collaboration with the company GEO-K, and it's focused on the vineyards of the Frascati region, in the south-east part of Rome, in Lazio region.

With multispectral very-high resolution QuickBird images (60 cm.), and hyperspectral images from sensor CHRIS on PROBA satellite, it has been calculated various vegetation indices with algorithms published on varied sources, and correlated them with real data, to obtain direct images of important parameters in farming.

It has been studied, for example, the relationship between the acidity of crops or its sugar content with the IVN index, or the hyperspectral reflection data with the Leaf Area Index, which is an important parameter for decision-making on agriculture.

The applications are innumerable, and go from the intra-field management (which zones to irrigate more, what fertilizers use in each zone and what quantity …) to the administration of controlled territories, as in the case of the guarantees of origin.

2. Introduction

2.1. Remote sensing: territorial information with satellite images

In the broadest sense, remote sensing is the measurement or acquisition of information of an object or phenomenon, by a recording device that is not in physical or intimate contact with the object. In practice, remote sensing is the utilization at a distance (as from aircraft, spacecraft, satellite, or ship) of any device for gathering information about the environment. Thus an aircraft taking photographs, Earth observation and weather satellites, monitoring of a pregnancy via ultrasound, and space probes are all examples of remote sensing. In modern usage, the term generally refers to techniques involving the use of instruments aboard aircraft and spacecraft, and it is distinct from other imaging-related fields such as medical imaging or photogrammetry.

There are two kinds of remote sensing. Passive sensors detect natural energy (radiation) that is emitted or reflected by the object or scene being observed. Reflected sunlight is the most common source of radiation measured by passive sensors. Examples of passive remote sensors include the eye, optical telescopes, and radiometers. Active sensors, on the other hand, provide their own source of energy to illuminate the objects they observe. An active sensor emits radiation in the direction of the target to be investigated. The sensor then detects and measures the radiation that is reflected or backscattered from the target. RADAR is a widely known form

of active remote sensing. In RADAR, the instrument emits a radio wave and senses the returned energy that was reflected from the target. Since the speed of light is known and the time delay between emission and return is measured, the distance to the target can be determined. Altimeters and Lidar are other examples of active remote sensing.

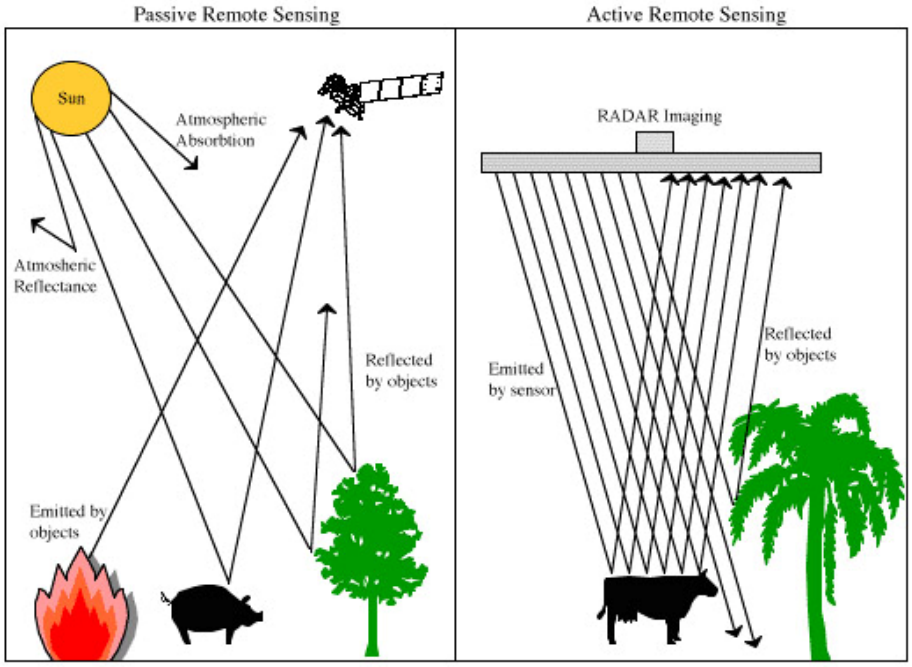

Figure 1: Passive/Active Remote Sensing

With remote sensing we can study dangerous or difficult to reach regions, such as area hit by hurricane or wildfire. Using remote sensing we can better understand water patterns of the whole Amazon region without organizing an expensive explorative mission, or we can take measurements from polar regions and oceans' depths. Taking measurements remotely also ensures that we won't interact with the object under study.

The instruments aboard orbiting satellites can collect data such as temperature, electromagnetic spectrum, energy output, heat, and light from the Earth's surface and atmosphere. Satellite data, in conjunction with analysis of Earth system data from other sources, provides us with enough information to predict many of the Earth's processes.

This information is utilized for the purposes of protecting the environment, land use, improving natural resources management, enhancing economic security and national safety, to name a few.

2.1.1. History

Beyond the primitive methods of remote sensing our earliest ancestors used (ex.: standing on a high cliff or tree to view the landscape), the modern discipline arose with the development of flight. The balloonist G. Tournachon (alias Nadar), who made photographs of Paris from his balloon in 1858, is considered to be the first aerial photographer. Messenger pigeons, kites, rockets and unmanned balloons were also used for early images. These first, individual images were not particularly useful for map making or for scientific purposes.

Systematic aerial photography was developed for military purposes beginning in World War I and reaching a climax during the Cold War with the development of reconnaissance aircraft such as the U-2.

The development of artificial satellites in the latter half of the 20th century allowed remote sensing to progress to a global scale. Instrumentation aboard various Earth observing and weather satellites such as Landsat, the Nimbus and more recent missions such as RADARSAT and UARS provided global measurements of various data for civil, scientific, and military purposes. Space probes to other planets have also provided the opportunity to conduct remote sensing studies in extra-terrestrial environments, synthetic aperture radar aboard the Magellan spacecraft provided detailed topographic maps of Venus, while instruments aboard SOHO allowed studies to be performed on the Sun and the solar wind, just to name a few examples.

Further strides were made in the 1960s and 1970s with the development of image processing of satellite imagery. Several research groups in Silicon Valley including NASA Ames Research Centre, GTE and ESL Inc. developed Fourier transform techniques leading to the first notable image enhancement of aerial photographs.

2.1.2. Data acquisition techniques

In order to coordinate a series of observations, most sensing systems need to know where they are, what time it is, and the rotation and orientation of the instrument. High-end instruments now often use positional information from satellite navigation systems. The rotation and orientation is often provided within a degree or two with electronic compasses. Compasses can measure not just azimuth (i.e. degrees to magnetic north), but also altitude (degrees above the horizon), since the magnetic field curves into the Earth at different angles at different

latitudes. More exact orientations require gyroscopic pointing information, periodically realigned perhaps from a star.

The resolution determines how many pixels are available in measurement, but more importantly, higher resolutions are more informative, giving more data about more points. However, more resolution occasionally yields less data. For example, in thematic mapping to study plant health, imaging individual leaves of plants is actually counterproductive. Also, large amounts of high resolution data can clog a storage or transmission system with useless data, when a few low resolution images might be a better use of the system.

Data may be acquired through a variety of devices depending upon the object or phenomena being observed. Most remote sensing techniques make use of emitted or reflected electromagnetic radiation of the object of interest in a certain frequency domain (infrared, visible light, microwaves). This is possible due to the fact that the examined objects (plants, houses, water surfaces, air masses...) reflect or emit radiation in different wavelengths and in different intensities according to their current condition. Some remote sensing systems use sound waves in a similar way, while others measure variations in gravitational or magnetic fields.

- **RADIOMETRIC**

Radar may be used for ranging and velocity measurements of either hard targets (i.e. an aircraft) or distributed targets (such as a cloud of water vapour in meteorology, or plasmas in the ionosphere).

Laser and radar altimeters on satellites have provided a wide range of data. By measuring the bulges of water caused by gravity, they map features on the seafloor to a resolution of a mile or so. By measuring the height and wave-length of ocean waves, the altimeters measure wind speeds and direction, and surface ocean currents and directions.

LIDAR LIght Detection And Ranging - Using a laser pulse, ground based LIDAR may be used to detect and measure the concentration of various chemical in the atmosphere, while airborne LIDAR can be used to measure heights of objects and features on the ground more accurately than with radar technology.

Radiometers and photometers are the most common instrument in use, collecting reflected and emitted radiation in a wide range of frequencies. The most common are visible and

infrared sensors, followed by microwave and rarely, ultraviolet. They may also be used to detect the emission spectra of various chemical species, thus providing information on chemical concentrations in the atmosphere.

Stereographic pairs of aerial photographs have often been used to make Topographic maps. Satellite imagery has also been used.

Thematic mappers take images in multiple wavelengths of electro-magnetic radiation (multi-spectral) and are usually found on earth observation satellites, including (for example) the Landsat program or the IKONOS satellite. Maps of land cover and land use from thematic mapping can be used to prospect for minerals, measure land usage, and examine the health of plants, including entire farming regions or forests.

- **GEODETIC**

Satellite measurements of minute perturbations in the Earth's gravitational field (geodesy) may be used to determine changes in the mass distribution of the Earth, which in turn may be used for geological or hydrological studies.

- **ACOUSTIC**

Sonar may be utilized for ranging and measurements of underwater objects and terrain.

Seismograms taken at different locations can locate and measure earthquakes (after the fact) by comparing the relative intensity and precise timing.

2.1.3. Data processing

Generally speaking, remote sensing works on the principle of the inverse problem. While the object or phenomenon of interest (the state) may not be directly measured, there exists some other variable that can be measured (the observation), which may be related to the object of interest via some (usually mathematical) model. The common analogy given to describe this is trying to determine the type of animal from its footprints. For example, while it is impossible to directly measure temperatures in the upper atmosphere, it is possible to measure the spectral emissions from a known chemical species (such as carbon dioxide) in that region. The frequency of the emission may then be related to the temperature in that region via various thermodynamic relations.

The quality of remote sensing data consists of its spatial, spectral, radiometric and temporal resolutions. Spatial resolution refers to the size of a pixel that is recorded in a raster image - typically pixels may correspond to square areas ranging in side length from 1 to 1000 metres. Spectral resolution refers to the number of different frequency bands recorded - usually, this is equivalent to the number of sensors carried by the satellite or plane. For example, Landsat images have seven bands, including several in the infra-red spectrum. Radiometric resolution refers to the number of different intensities of radiation the sensor is able to distinguish. Typically, this ranges from 8 to 14 bits, corresponding to 256 to 16,384 intensities of colour, in each band. The temporal resolution is simply the frequency of flyovers by the satellite or plane, and is only relevant in time-series studies or those requiring an averaged or mosaic image. This may be necessary to avoid cloud cover. Finally, some people also refer to the "economic resolution", that is, how much data you get or are able to process per unit money.

In order to generate maps, most remote sensing systems expect to convert a photograph or other data item to a distance on the ground. This almost always depends on the precision of the instrument. For example, distortion in an aerial photographic lens or the platen against which the film is pressed can cause severe errors when photographs are used to measure ground distances. The step in which this problem is resolved is called georeferencing, and involves matching up points in the image (typically 30 or more points per image) with points in a precise map, or in a previously georeferenced image, and finally "warping" the image to reduce any distortions. From the early 1990s, most satellite images are sold fully georeferenced.

In addition, images may need to be radiometrically and atmospherically corrected. Radiometric correction gives a scale to the pixel values, e.g. the scale of 0 to 255 will be converted to actual radiance values. Atmospheric correction eliminates atmospheric haze by rescaling each frequency band so that its minimum value (usually realised in water bodies) corresponds to a pixel value of 0.

Interpretation is the critical process of making sense of the data. Traditionally, this was performed by a human being, perhaps with a few measurement tools and a light table, but nowadays the analyses are becoming increasingly sophisticated and automated.

Old data from remote sensing is often valuable because it may provide the only long-term data for a large extent of geography. At the same time, the data is often complex to interpret, and bulky to store. Modern systems tend to store the data digitally, often with lossless compression. The difficulty with this approach is that the data is fragile, the format may be archaic, and the data may be easy to falsify. One of the best systems for archiving data series is

a computer-generated machine-readable ultrafiche, usually in typefonts such as OCR-B, or as digitized half-tone images. Ultrafiches survive well in standard libraries, with lifetimes of several centuries. They can be created, copied, filed and retrieved by automated systems. They are about as compact as archival magnetic media, and yet can be read by human beings with minimal, standardized equipment.

2.2. Precision agriculture

Agriculture dominates the world's land use decisions. The urgent need for doubling farm production over the next 25 years on less land with less water through further intensification would inevitably involve substantial social, economic, and environmental costs. Identification of tools to minimize such costs through enhanced productivity and economic profits while simultaneously conserving the environment is, therefore, crucial. Precision agriculture (PA) is one of such tools catching worldwide attention.

PA is defined and termed in many ways, but the underlying concept remains the same. In simple terms, PA can be defined as a holistic and environmentally friendly strategy in which farmers can vary input use and cultivation methods—including application of seeds, fertilizers, pesticides, and water, variety selection, planting, tillage, harvesting—to match varying soil and crop conditions across a field. This definition suggests that there are at least three elements critical to the success of PA: information, technology, and management.

It has been long recognized that crops and soils within a field and/or region are both spatially and temporally variable. Growers tried to manage such variability to a limited extent mainly by intuition.

Developments in geo-spatial information and communication technologies especially in the late twentieth century have made it possible, however, to manage such variability much more precisely than before. PA, therefore, differs from conventional farming as it involves determining variation more precisely and linking spatial relationships to management actions, thereby allowing farmers to look at their farms, crops and practices from an entirely new perspective, thus leading to:

- Reduction in costs.

- Optimization of yields and quality in relation to the productive capacity of each site.
- Better management of the resource base.
- Protection of the environment.

PA also provides a framework of information with which farmers can make rational management decisions. In the future, PA may even enable us to trace farm products to their genetics and environmental conditions thereby providing a significant degree of control over food quality and safety.

2.2.1. Stages on PA

Field adoption of PA may be represented as a five-step cyclical process including data collection, diagnostics, data analysis, precision field operations, and evaluation (Figure 2).

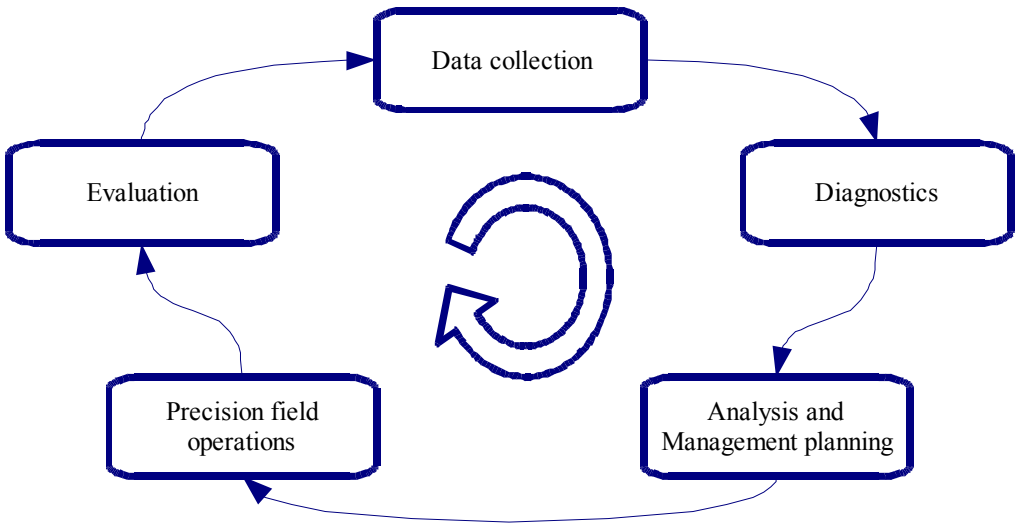

Figure 2: Stages on Precision Agriculture

The evaluation of economic profitability, safety, and environmental impacts of precision field operations becomes a part of the data collection process for the next season. The PA system can be considered, therefore, the agricultural system of the twenty-first century, as it symbolizes a better balance between reliance on traditional knowledge and information-and management-intensive technologies.

Precision agriculture promises to revolutionize farming as it offers a variety of benefits in profitability, productivity, sustainability, crop quality, environmental protection, on-farm quality of life, food safety, and rural economic development. In the short term, the diagnostic and database-building benefits are considerable. Growers can predict and correct problems such as water and nutrient stresses, diseases, and pests more efficiently. Database-building benefits will be in the form of accurate farm record keeping of inputs, property, machinery and labour, and efficient monitoring of environmental quality through recording the amounts and location of input applications. In the long term, farmers can optimize yields through finding locations that produce maximum profit margins, and through avoiding introduction of inappropriate cropping systems. Knowledge on crop response enables more precise targeting of external inputs, information on spatial and temporal response of varieties may help in selecting right genotypes and observations of consistent poor performance of a cropping system may encourage the withdrawal of such systems.

On a regional level too, spatial and temporal characterization of farms can help identify emerging trends in factors that impact sustainability, either in geographically adjoining regions or in specific agro-ecological zones, and to target possible solutions. Building geo-referenced databases for each field in a region will help identify causes and factors that underlie productivity features in each cropping system, and provide a synthesis within and among fields of the extent and severity of factors that constrain or enhance sustainability. For instance, data gathered in PA systems can help in identifying areas with high pollution potential. Adoption of PA on a large scale increases opportunities for skilled employment in farming, and provides new tools for evaluating multi-functional character of agriculture.

At least three criteria are required for implementation of PA:

- Clear evidence of significant spatial and temporal variability in soil and crop conditions within a field and in fields within a region.

- Ability to identify and quantify such variability. It is possible to identify variation even with conventional techniques (e.g., based on grower intuition) but positioning and information technologies are of great help in quantifying such variation. Indeed, successful adoption of PA depends upon blending the best of farmer's knowledge on field variability with information and communication technologies.

- Ability to reallocate inputs and adjust management practices to improve productivity and profitability while minimizing environmental degradation. For instance, if data on

precise weed distribution is available, spot- or patch- spraying of herbicides can be done instead of whole-field treatments.

The development of cost-effective techniques to discern such information, to develop site-specific or field-specific recommendations and data analysis tools, and to determine the appropriate scales of analysis and measurement are, therefore, prerequisites for PA.

It is important to note that PA principles and technologies are applicable in a variety of conditions irrespective of cropping system (mono- and multiple cropping), farm size (small and large), farming method (organic and chemical farming), crop type (field crops, horticultural crops, genetically engineered [GE] and non-GE crops), method of water management (rained and irrigated), and input levels in a system. The principles are applicable in livestock industry and forestry too. The driving forces for adoption of PA include economic pressures, environmental concerns and social/demographic changes, and vary with each context hence the method of implementation too varies. The overall profitability from adopting PA, however, varies. For example, although small farms are conducive to intensive agriculture and PA, small farmers are severely handicapped in using modern technologies because of restrictions on capital, market, and human skills.

Applying PA in cropping systems of one area often can have positive impact on other areas. For example, simple field- or site-specific measures (e.g., reduced tillage, input reallocation in fields) aimed at minimizing erosion and nutrient runoff of upland watersheds can have dramatic effects on sustainability of systems in lowlands.

It is important to note PA is not necessarily appropriate for every situation. For example, grain yield maps and soil fertility maps can help us determine and then vary optimal rate of fertilizers for each management unit. However, many pest and disease problems are more dependent on short-term weather patterns and do not follow consistent patterns across a field. Indeed for some pests, it may be best to always spray the entire field because even a few survivors could rapidly multiply, spread to the rest of the field and continue to cause problems. In such cases, precision spraying of pesticides is of little use. Insect and disease patterns across a field also can have a large temporal variation because of their temperature-dependence. In such cases, timing of pesticide application is more important than variable application. In contrast, perennial weeds such as Canada thistle, velvet leaf, and quack grass grow in the same patches year after year. Application of precision spraying techniques in such cases would be more cost-effective than blanket applications.

2.2.2. Tools for PA implementation

To achieve the ultimate goal of optimizing productivity and profitability in each unit of land, three basic requirements must be met:

- Ability to identify each field location
- Ability to collect, interpret, and analyze data at an appropriate scale and frequency
- Ability to adjust input use and farm practices to maximize benefits from each location.

Global Positioning Systems (GPS), geographic information systems (GIS), remote and proximal sensing, variable rate technology (VRT) and decision support systems (DSS) are employed to meet these needs (Figure 3).

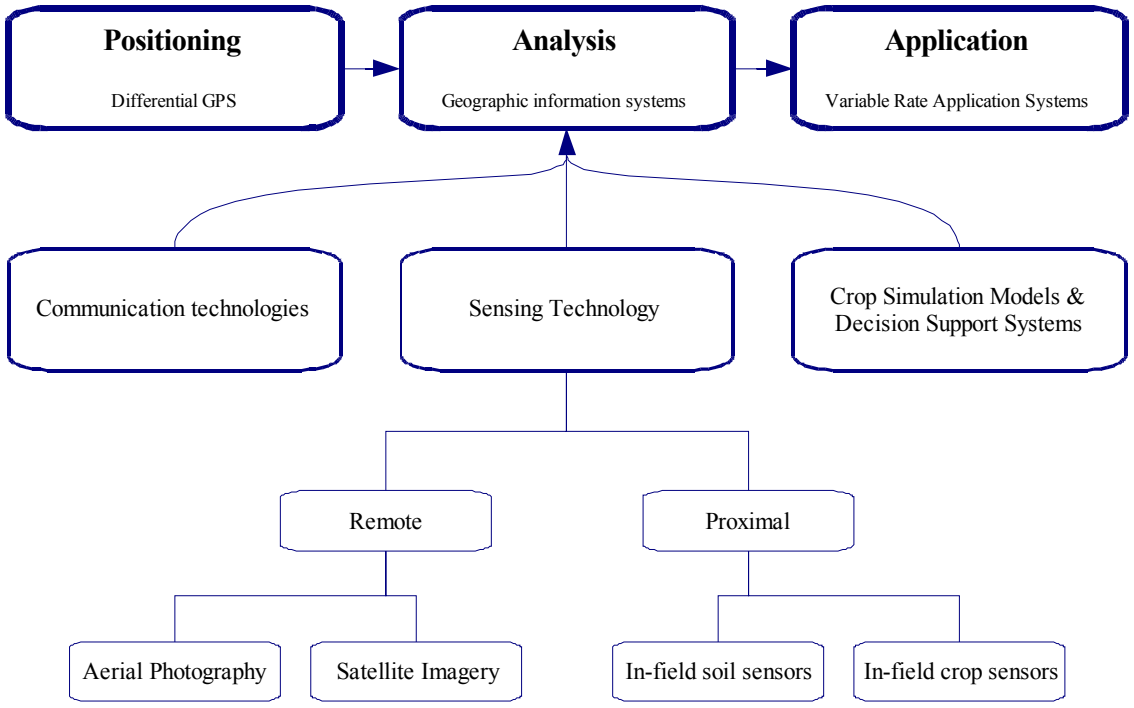

Figure 3: Tools for implementation of precision agriculture

- **GPS**

GPS is a worldwide radio-navigation system formed from a constellation of 24 satellites and their ground stations, which provides geospatial accuracy to farm practices by enabling farmers to identify each field site. With the decision by the U.S. government to turn off selective

availability (an artificial error introduced into the satellite data to reduce the positional accuracy to 100 meters) effective May 1, 2000, GPS accuracy has considerably improved to about 20 meters. However, differential GPS (GPS receiver used along with a ground reference station) is necessary to get accuracy of 1-3 m critical for yield mapping, crop scouting, and variable input applications. GPS can also be used to create field boundary and topography maps. A series of maps with each field identified with the crop grown in each season can help in tracking crop rotations in a region from year to year.

- **GIS**

GIS is a software application for computerized data storage, retrieval, and transformation and is used to manage and analyze spatial data. Data may be derived for different fields from various sources including existing digital maps, data digitized from maps and photographs, topographic surveys, soil or crop sampling, and sensor data with location information derived by using GPS. GIS can display analyzed data in maps that allow better understanding of interactions among yield, fertility, pests, weeds, and other factors, and decision making based on such spatial relationships. A GIS for PA contains base maps such as land ownership, crop cover, soil type, topography, N, P, K, and other nutrient levels, soil moisture, pH, etc. Data on rotations, tillage, nutrient, and pesticide applications, yields, etc., is also stored. GIS is used to create fertility, weed and pest intensity maps, and for making prescription maps that show recommended application rates of farm chemicals at various field locations.

- **REMOTE SENSING**

Low-flying aircraft and satellites have become a major source of spatial data due to reduction in both cost and time of image acquisition and delivery. Although the use of remote sensing in agriculture is several decades old, improvements in spatial, spectral, and temporal resolutions of recent satellites (e.g., IKONOS or QuickBird) and systems such as airborne videography, and recent developments in new hyper-spectral sensors are increasingly becoming useful to determine size, location, and cause of variation. Imagery can show all fields in a region and spot anomalies related to crop vigour and biomass much earlier than ground inspections, thereby improving the efficiency of crop scouting in large fields and allowing prompt remedial treatments. Temporal changes in vigour, as determined from NDVI [Normalized Difference Vegetation Index] analysis of images acquired at critical times, can be used to characterize spatial and temporal dynamics of crop performance and predict crop yields. Upon integration of imagery with other data layers in a GIS, maps can be prepared. GPS receivers can then be used to locate weak spots and apply corrective measures. Likewise, images of different crops planted

in rotation can reveal distinct crop vigour responses due to agronomic strategies adopted in previous crops. Imagery can also be used to monitor land use changes at regional level. In several tropical countries, cloud cover persists for most part of the cropping season and in such cases acquisition of radar imagery may be useful.

We can include here the named "proximal sensing": technologies employing electronic in-field crop and soil sensors to quantify variability in crop and soil conditions, that are also in development. Soil sensors for testing pH, EC (electrical conductivity), Ncontent and organic matter are currently in use in North America.

- **VRT**

VRT provides "on-the-fly" delivery of field inputs. A GPS receiver is mounted on a truck so that a field location can be recognized. An in-vehicle computer with the input recommendation maps controls the distribution valves to provide a suitable input mix by comparing to the positional information received from the GPS receiver. VRT systems are either map-based or sensor-based. VRT has been largely used for applying N, P, K, lime, pesticides and herbicides.

Variable rate seeders and variable rate irrigation systems are currently being studied. Systems such as manure applicators, which enable precise application of animal wastes, are also in development.

- **COMMUNICATION TECHNOLOGIES**

Technologies such as fax, cable TV, and the Internet (World Wide Web) offer capability to send, receive, and aggregate information at much lower costs than ever before. For example, transmitting a remotely sensed image of a field with crop stress zones, or digital photos of problem areas via the Internet can enable the grower to take prompt in-season remedial measures. Likewise, posting to the Web sites of crop yield maps in different rotations over two to three years enables crop consultants to examine and evaluate them in preparing appropriate recommendations. In this context, image compression technologies will be increasingly useful.

- **CROP MODELS AND DSS**

These provide an integrated framework for assessing the degree of sustainability of a farming system. They can be used for understanding yield variability in both space and time so as to optimize production, indicate future trends, and prescribe suitable actions to minimize environmental impact. Process-oriented crop simulation models, integrate the effects of temporal and multiple stress interactions on crop growth processes under different environmental and management conditions. Use of models with GIS permits mapping of adaptation zones for individual crops and rotation systems and help in targeting sustainable practices to defined regions.

Recent advances in Web-based GIS can provide access to spatial analysis of cropping systems through the Web in a scalable, threaded format. As an example, Pl@nteInfo showed that it is possible to build a Web-based DSS, in which personalized advice on farm conditions can be given in real-time to farmers.

In several developed countries, customized services in PA such as grid soil sampling, yield mapping, variable rate application of fertilizers and pesticides are now offered through the private sector. Custom services can decrease the cost and increase the efficiency by distributing capital costs for specialized equipment over more land and by using the skills of PA specialists more effectively.

3. Objectives

This final year thesis is included in a bigger investigation project carried out by the firm GEO-K, in ESRIN, headquarters of the European Spatial Agency (ESA) in Rome. The work has been full-time developed from January to May 2007.

The project consists on the description and extraction of several outstanding parameters on vineyard agriculture in Frascati, southeast of Rome, by means of the processing of several commercial and experimental satellite images, as QuickBird's or Proba's. The aim is to establish a reliable work system, fast and optimized, to obtain maps that can be very useful for decision-making in the management of these vineyards, which belong to a Controlled Guarantee of Origin of Italian vines, Frascati.

Frascati DOC (*Denominazione di Origine Controllata*), includes the Frascati, Grotaferrata and Monte Porzio Catone districts.

Figure 4: Frascati DOC zone

Specifically, I've obtained maps of the grape acidity and brix degree within these vineyards and also I've extracted and analyzed Leaf Area Index maps from the entire zone.

The process followed to achieve those objectives has been:

- Discussion over the optimal parameters to obtain in the studied zone, and request of the georeferenced ground truth data.
- Documentation phase about the decided parameters, and about the Vegetation Indices (VIs) to apply in the study.
- Treatment and correction of raw satellite images.
- From the treated images, obtaining of the vegetation index maps.
- Correlation of the obtained VIs with the ground truth data, in the points where they have been taken, and decision of the better index to represent each parameter.
- Decision of the regression method applicable (lineal, polynomial …), trying to minimize the dispersion parameters calculated.
- Final obtaining of the image of each parameter, such as acidity or brix degree.

3.1. Acidity and its influence in wine

Acids give wines their characteristic crisp, slightly tart taste. Alcohol, sugars, minerals, and other components moderate the sourness of acids and give wines balance. Some acids are naturally present in the base ingredients of wines, while others are by-products of fermentation.

Natural acids have the freshest, purest acid tastes. Among grapes they are tartaric, malic and citric. Oxalic acid, found for example in rhubarb, is another natural acid. Fermentation acids have milder, more complex tastes. The major fermentation acids are lactic, succinct and acetic.

Acidity greatly influences the taste of wine. If the wine total acidity is too low, it tastes flat and dull. If it is too high, it tastes too tart and sour.

The principal acids found in grapes, and therefore wine, are tartaric acid, potassium hydrogen tartrate (cream of tartar), malic acid and potassium hydrogen malate. Tartaric acid and potassium hydrogen tartrate are predominant in wine. Since potassium hydrogen tartrate and potassium hydrogen malate are derivatives of tartaric and malic acids, respectively, only tartaric and malic acids will be discussed with the understanding that their derivatives are also present in wine. The relative amounts of tartaric and malic acids vary depending on the grape variety and on where the grapes are grown. For example, in Burgundy, the Chardonnay has a lower concentration of malic acid than the Chardonnay grown in the Napa Valley of California.

Both tartaric and malic acids are non-volatile which means that they do not evaporate or boil off when the wine is heated. This is to be distinguished from volatile acidity (VA) in wine that represents acetic acid (vinegar). Acetic acid does boil off when heated and high VA is undesirable in a wine. A VA of 0.03-0.06% is produced during fermentation and is considered a normal level.

- **CLIMATE: ACID AND SUGAR**

Tartaric and malic acids are produced by the grape as it develops. In warm climates, these acids are lost through the biochemical process of respiration. Therefore, grapes grown in warmer climates have lower acidity than grapes grown in cooler climates. For example, Chablis (France) produces grapes with high acid because the climate is very cool, while Napa Valley produces grapes with lower acidity because the climate is warmer.

Sugar production is the complete opposite of acid production. The warmer the climate the higher the sugar content of the grapes. Sugar content of grape juice is expressed in percent (%) or ° Brix (e.g., 24 % sugar is equal to 24 ° Brix).

In summary, warmer climates result in high sugar and low acid whereas cooler climates result in low sugar and high acid. The Chablis region of France is a very cool region and normally produces grapes with low sugar and high acid. The big concern in Chablis is getting enough sunlight and warmth to get reasonable sugar levels. In low sugar years, they are allowed to add sugar to the grape juice. The process is called chaptalization.

- **MEASURING THE ACIDITY**

The total acidity (TA) of a wine is measured assuming all the acid is tartaric. This allows one to determine a value for total acidity that is consistent. A high TA is 1.0%. Most people would find this level of acidity too tart and too sour for consumption. A low TA, as 0.4%, results in flat tasting wine that is more susceptible to infection and spoilage by micro organisms. Most red table wines are about 0.6% total acid. White wines are usually a little higher.

In contrast, pH is related to an acid's strength in solution and is measured on a logarithmic scale; on the pH scale, 7 is neutral, numbers above 7 are alkaline and increase ascending, and numbers below 7 are acidic and increase descending. In other words, a pH of 9 is more alkaline than a pH of 8, while a pH of 4 is more acidic than a pH of 5. Because the measurements are logarithmic, a pH of 4 is 10 times more acidic that a pH of 5. The pH can be measured with a pH meter, an instrument that determines pH quickly and easily. It represents the active acidity of the wine. If the pH of a wine is too high, say 4.0 or above, the wine becomes unstable with respect to micro organisms. Low pH inhibits micro organism growth. Tartaric acid is sometimes added to fermenting grape juice in California to insure that an acceptable final pH can be realized, since some acid is lost during fermentation thus reducing the total acidity and raising the pH.

Although TA and pH are interrelated, they are not the same thing. A solution containing a specific quantity of a relatively weaker acid such as malic will have a different (higher) pH than a solution containing the same quantity of a stronger acid such as tartaric. So, another way of thinking of pH is to say that the acid in a solution with a pH of 4 is 10 times *stronger* than the acid in a solution with a pH of 5.

The measurable range of interest in acidity is a pH of approximately 2.5 to 4.5 for must and wine and a TA of 0.50-0.85%. A typical premium California Chardonnay has a total acidity of 0.58 grams per 100 mL (0.58%) and a pH of 3.4.

3.2. Brix and its importance in crops

The Brix scale is a system used to measure the sugar content of grapes and wine. The Brix (sugar content) is usually determined by a hydrometer, which indicates a liquid's specific gravity (the density of a liquid in relation to that of pure water). Each degree Brix is equivalent to 1 gram of sugar per 100 grams of grape juice. The grapes for most table wines have a Brix reading of between 20° to 25° at harvest. About 55 to 60 percent of the sugar is converted into alcohol. The estimated alcohol that a wine will produce (called potential alcohol) is estimated by multiplying the Brix reading by 0.55. Therefore, a 20° Brix will make a wine with about 11 percent alcohol.

The Brix scale was originally derived by Antoine Brix by recalculating Balling's scale to a reference temperature of 15.5°C. The Brix scale was subsequently recalculated again, and now uses a reference temperature of 20°C. Brix can be approximated as $261.3 \cdot (1 - 1/g)$, where g is the specific gravity of the solution at 20°C. Other systems used are the Balling and the Plato scales.

The Balling scale was developed by German chemist Karl Balling. It refers to the concentration of a sucrose solution, as the weight percentage sucrose at 17.5°C.

The Plato scale which measures in Plato degrees is also a refinement of the Balling scale. It uses a reference temperature of 17.5°C and a slightly different modulus, with the approximation $260*(1 - 1/g)$, where g is the specific gravity of the solution at 17.5°C.

The three scales are often used interchangeably since the differences are minor. Brix is primarily used in fruit juice, wine making and the sugar industry. Plato is primarily used in brewing. Balling still appears on older saccharimeters, and is still used in the South African wine industry.

Brix is used in the food industry for measuring the approximate amount of sugars in fruit juices, wine, soft drinks and in the sugar manufacturing industry. Different countries use the scales in different industries; in the UK brewing is measured with specific gravity X 1000, European brewers use Plato degrees, and US industries use a mix of specific gravity, Brix, degrees Baumé and Plato degrees.

For fruit juices, one degree Brix is about 1-2% sugar by weight. This usually correlates well with perceived sweetness.

Since Brix is related to the concentration of dissolved solids (mostly sucrose) in a fluid it is therefore related to the specific gravity of the liquid. Because the specific gravity of sucrose solutions is well known, it can also be measured by refractometers.

3.3. Leaf area index and its significance in plantations

One of the key "vital signs" of Earth's vegetation is the total green leaf area for a given ground area. Knowing the total leaf area in a plant canopy helps scientists determine how much water will be stored and released by an ecosystem, how much leaf litter it will generate, and how much photosynthesis is going on. It also helps scientists understand the flow of energy among the various layers of vegetation, the atmosphere, and the ground, which in turn affects climate.

The Leaf Area Index or LAI is the ratio of total upper leaf surface of a crop divided by the surface area of the land on which the crop grows. The LAI is a dimensionless number.

The LAI is used to predict the photosynthetical primary production and as a reference tool for crop growth. As such, LAI plays an essential role in theoretical production ecology. An inverse exponential relation between LAI and light interception, which is linearly proportional to the primary production rate, has been established:

$$P = P_{\max} \cdot \left(1 - e^{-c \cdot LAI}\right)$$

Equation 1: Primary production function

In which P_{max} designates the maximum primary production and c designates a crop-specific growth coefficient. This inverse exponential function is called the primary production function.

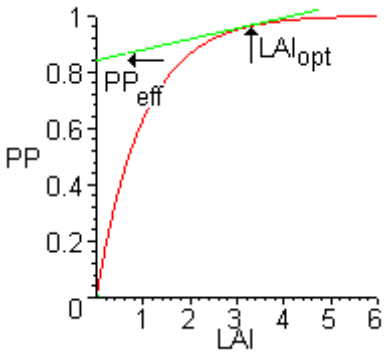

Graphic 1: Effective primary production, obtained from leaf area index

A higher LAI corresponds to a higher leaf mass and therefore a higher respiration rate of the crop. As follows from the primary production function, an increased LAI increases primary production by only a fraction. The optimum LAI is thus those in which any increase in primary production is exactly offset by the increase in respiration rate, which can be found by equalising the derivatives of the respiration function (linearly dependent on leaf biomass, hence on LAI) and the primary production function and solving for LAI. Plants have a crude but effective system to regulate their leaf mass. Mature leafs cannot act like assimilate sinks, but must be self-sufficient. As a result, all leafs which are net consumers of assimilates eventually die off and the final crop LAI closely resembles optimum LAI. Typically, this optimum LAI equals to less than 3 for succulent leafs up to 5 or 6 for thin leafs.

4. Available dataset

4.1. Available images description

To achieve the objectives enounced on section 3, a large dataset has been employed. We have used QuickBird imagery, data from sensor CHRIS on ESA's satellite PROBA, and all the information on the Frascati cadastre database, with shape images, boundary information, etc…

4.1.1. QuickBird images

QuickBird is a high-resolution commercial earth observation satellite, owned by DigitalGlobe and launched in 2001 as the first satellite in a constellation of three scheduled to be in orbit by 2008. QuickBird collects the highest resolution commercial imagery of Earth, and boasts the largest image size and the greatest on-board storage capacity of any other satellite. The satellite collects panchromatic (black & white) imagery at 60-70 centimetres resolution and multispectral imagery at 2.4- and 2.8-meter resolutions.

At this resolution, detail such as buildings and other infrastructure, or the biggest trees in a crop, are easily visible. However, this resolution is insufficient for working with smaller objects such as a number plate on a car. The imagery can be imported into remote sensing image processing software, as well as into GIS packages for analysis. The imagery can also be used as a backdrop for mapping applications, such as Google Earth and Google Maps.

- **SATELLITE AND SENSORS DESIGN AND SPECIFICATIONS**

QuickBird was designed and built by Ball Aerospace & Technologies Corp., Kodak, and Fokker Space. By utilizing proven technology from each supplier, QuickBird is a satellite system built from space-qualified components.

Aspect	Specifications
Launch information	Date: October 18, 2001 Launch Window: 1851-1906 GMT (1451-1506 EDT) Launch Vehicle: Delta II Launch Site: SLC-2W, Vandenberg Air Force Base, California
Orbit	Altitude: 450 km 98 degree sun-synchronous inclination Revisit frequency: 3-7 days Orbit time: 93.4 minutes
On board storage	128 Gigabit capacity
Swath	Nominal swath width: 16.5 km at nadir Accessible swath: 544 km (±30º off nadir) Areas of interest: -Single area: 16.5km x 16.5 km -Strip: 16.5 km x 165 km
Spacecraft	Fuelled for 7 years 950 kg, 3,04 m length

Table 1: QuickBird satellite specifications

Aspect	Specifications
Bands	PAN: 450-900nm Blue: 450-520 nm Green: 520-600 nm Red: 630-690 nm Near Infrared: 760-900 nm
Resolution	PAN: 0.6 m Multispectral: 2.4m
Dynamic Range	11 bits per pixel
Reference	http://www.digitalglobe.com/about/quickbird.html

Table 2: QuickBird sensor characteristics

- **EXAMPLE IMAGERY**

Below are showed some QuickBird images examples used in this project (zone of Frascati), of the two types: Panchromatic and Multispectral. The difference in resolutions is noticeable.

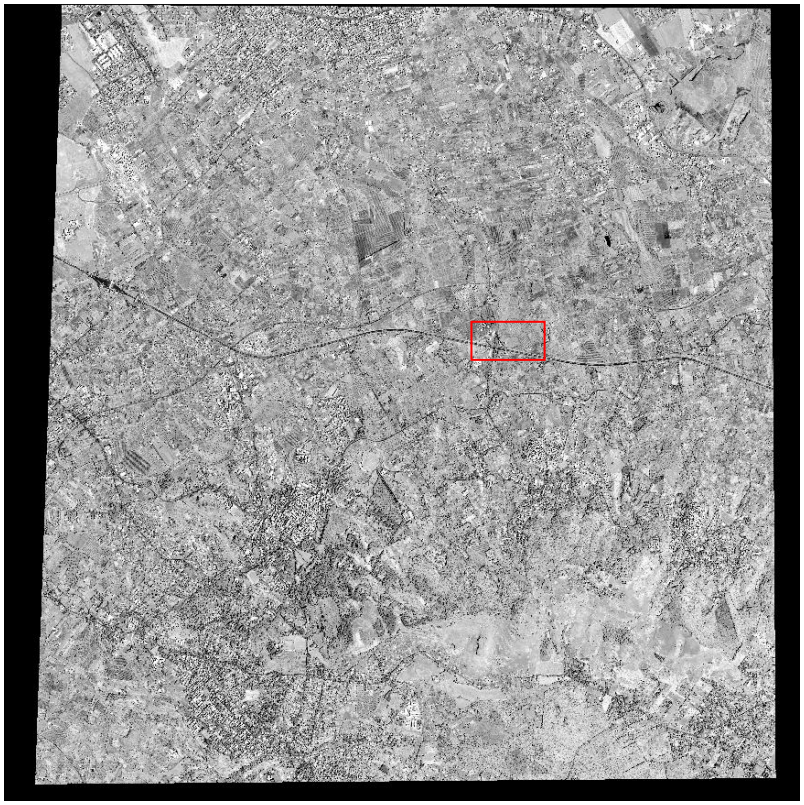

Image 1: Example of panchromatic QuickBird image used

Image 2: The zone emphasized on the previous image at complete resolution (60 cm)

Image 3: Example of multispectral QuickBird image used, in true colour composition (R,G,B)=(Band3,Band2,Band1)

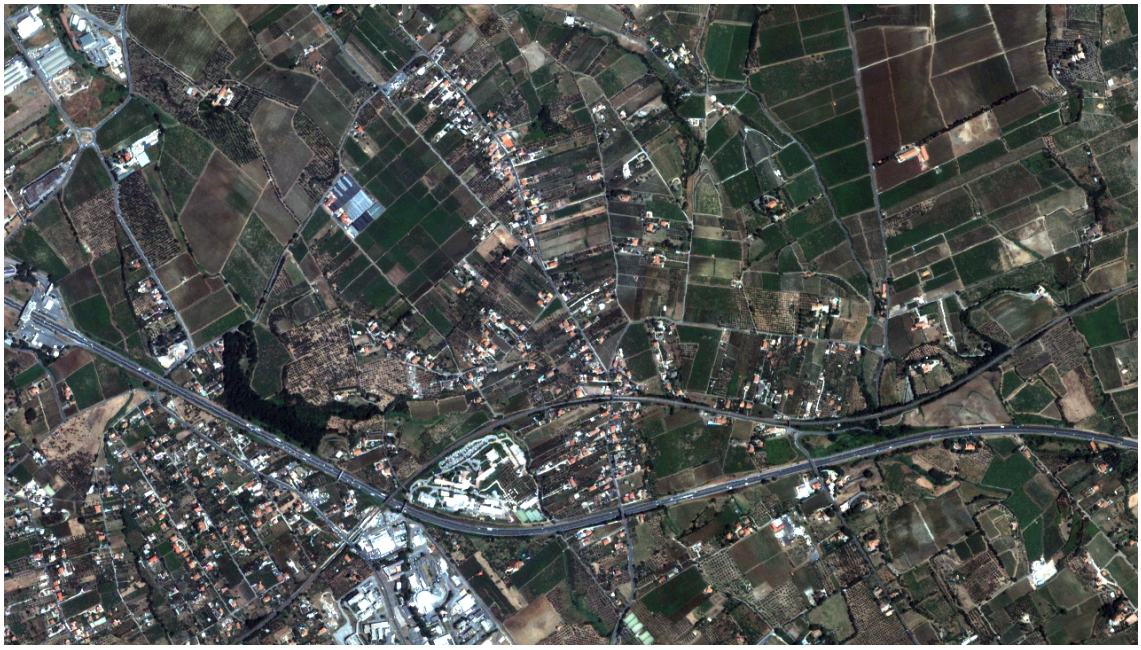

Image 4: The zone emphasized on the previous image at complete resolution (2.4 m)

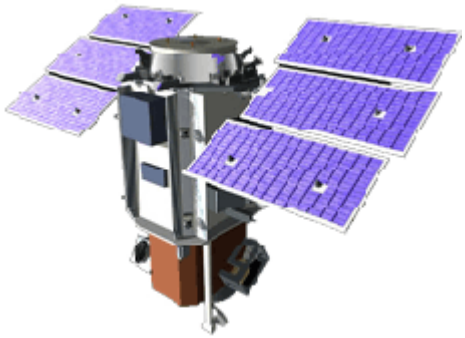

Figure 5: QuickBird satellite

4.1.2. Chris images

PROBA (Project for On-Board Autonomy) is a satellite launched by ISRO in 2001 as part of the ESA's MicroSat program. This small (40×60×80 cm; 94kg) boxlike system, with solar panel collectors on its surface, has remarkable image-making qualities. It has a hyperspectral system (200 narrow bands) that image at 30 m resolution, plus three in the visible that have 15 m resolution.

The Project for On-Board Autonomy (Proba) was originally a technology demonstration mission of the European Space Agency, started in mid-1998 and funded within the frame of ESA's General Support Technology Programme.

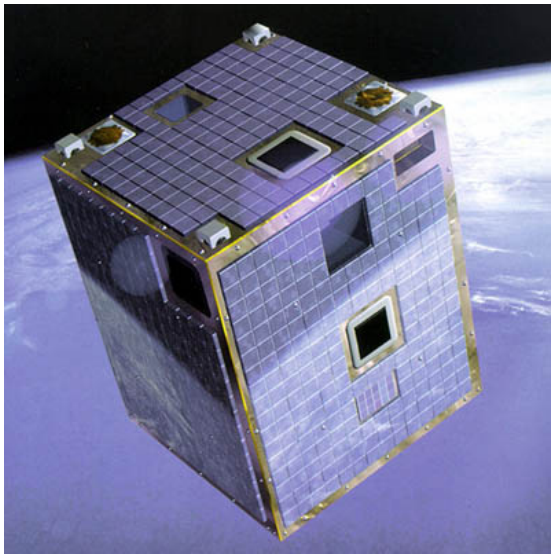

Figure 6: Proba satellite

Intended as a one-year mission, Proba has provided data successfully ever since its launch on 22nd Oct 2001. Hosting two Earth Observation instruments CHRIS and HRC, Proba is since 2004 managed by ESA's Ground Segment Department within the Directorate of Earth Observation at ESA/ESRIN.

- **SATELLITE AND SENSORS DESIGN AND SPECIFICATIONS**

Aspect	Specifications
Launch	Date: 2001 October 22 Launch site: Sriharikota (India) Launch vehicle: PSLV Mass: 94 kg Volume: 80 x 60 x 60 cm
Orbital characteristics	Orbit: Virtually circular, sun-synchronous Altitude: 829 km Inclination: 98.7º Orbital period: 101.3 minutes Equatorial crossing time: 10:30 am Platform revisit period: 14 days
Pointing capability	Across track: ±30º Along track: ±60º

Table 3: Probe satellite specifications

Aspect	Specifications
Spatial characteristics	Swath width: 18.6 km Typical image area: 19 km x 19 km
Spectral characteristics	Spectral range: 410 nm – 1050 nm Spectral resolution: 1.25 nm – 11 nm
Bands and resolution	Full swath width: 18 bands @ 25 m 50-62 bands @ 50 m Half swath width: 37 bands @ 25 m
Data characteristics	Data per typical scene: 131 Megabits Quantization: 12 bits

Table 4: Chris sensor characteristics

CHRIS acquires a set of up to five images of each target during each acquisition sequence; these images are acquired when Proba is pointing at distinct angles with respect to the target. CHRIS products include five formal CHRIS imaging modes, classified as modes 1 to 5:

- MODE 1: Full swath width, 62 spectral bands, 773nm / 1036nm, nadir ground sampling distance 34m @ 556km

- MODE 2 WATER BANDS: Full swath width, 18 spectral bands, nadir ground sampling distance 17m @ 556km

- MODE 3 LAND CHANNELS: Full swath width, 18 spectral bands, nadir ground sampling distance 17m @ 556km

- MODE 4 CHLOROPHYL BAND SET: Full swath width, 18 spectral bands, nadir ground sampling distance 17m @ 556km

- MODE 5 LAND CHANNELS: Half swath width, 37 spectral bands, nadir ground sampling distance 17m @ 556km

The images used in this project correspond to MODE 3- LAND CHANNELS, in which the bands are configured as follows.

Band	Min (nm)	Max (nm)	Mid (nm)	Width (nm)
L1	438	447	442	9
L2	486	495	490	9
L3	526	534	530	9
L4	546	556	551	10
L5	566	573	570	8
L6	627	636	631	9
L7	656	666	661	11
L8	666	677	672	11
L9	694	700	697	6
L10	700	706	703	6
L11	706	712	709	6
L12	738	745	742	7
L13	745	752	748	7
L14	773	788	781	15
L15	863	881	872	18
L16	891	900	895	10
L17	900	910	905	10
L18	1002	1035	1019	33

Table 5: Band configuration in the operating mode 3 of sensor CHRIS

- **EXAMPLE IMAGERY**

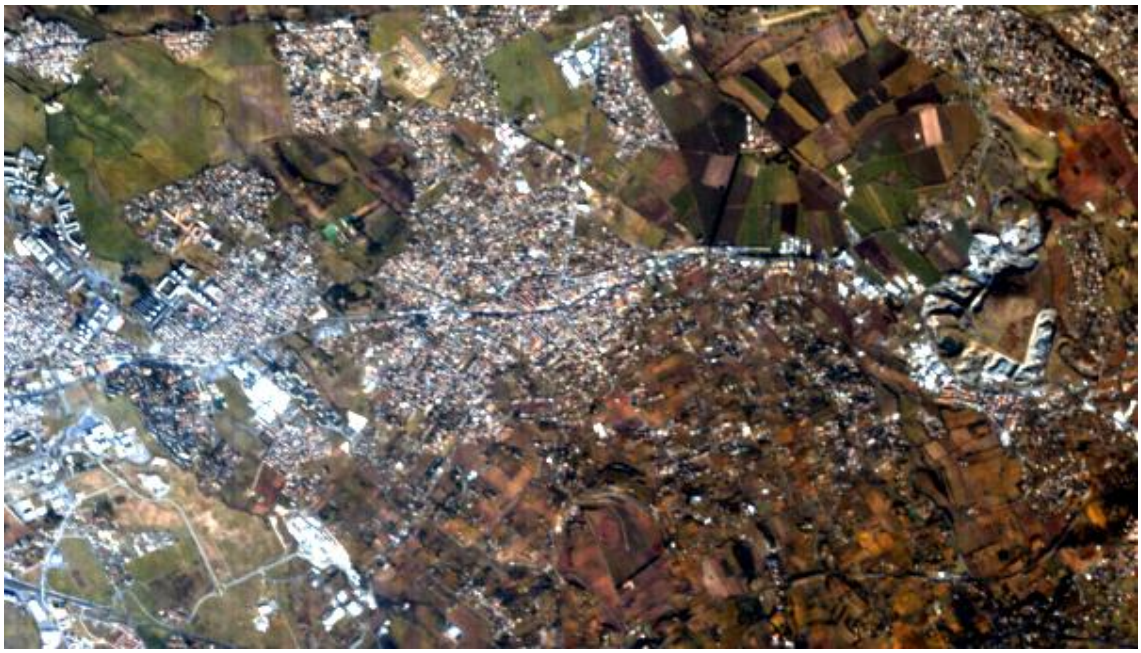

Image 5: Chris image example of Frascati: Mode 3, Resolution 17 m

4.1.3. Shapefile data

We have also available the data of the Frascati's cadastre in shapefiles. In this kind of files, there are georeferenced boundaries drawing the form of each vineyard, and also a lot of information of each one of them.

Thereby, we can see the distribution of Frascati DOC vineyards, and by clicking on them, it is possible to access to the related database obtaining information such as the field number identification, the city council (*comune*) where it has been registered and the year, the perimeter and area, the number of crops, the density of implant, the type of wine installation (*filare, tendone,…*), etc…

Image 6: Shapefile with the margins of Frascati DOC vineyards

Attributes of Unità_vitate_doc.shp

Particella	Shape	Comune_nom	Area	Perimeter	Num_ceppi	Superf_mq	Density	Sup_map	Anno_dic	Anno_inp
00315	Polygon	Roma	398.325390000000030	83.324349999999995	104	390.00	2667	398.00	1998	1993
00303	Polygon	Roma	601.992100000000050	125.395880000000010	150	600.00	2500	601.00	1998	1983
00140	Polygon	Frascati	1617.951360000000000	200.481519999999990	1264	1618.00	7812	1615.00	1998	1956
00338	Polygon	Roma	1767.722790000000000	267.652769999999980	884	1768.00	5000	1765.00	1998	1978
00578	Polygon	Frascati	2687.127810000000000	253.182199999999990	490	3062.00	1600	2682.00	1998	1974
00412	Polygon	Roma	1202.315250000000100	219.296280000000000	700	1260.00	5556	1200.00	1998	1995
00324	Polygon	Roma	340.399890000000030	79.639399999999995	106	395.00	2684	340.00	1998	1993
00413	Polygon	Roma	42.650820000000003	31.536860000000001	25	45.00	5556	43.00	1998	1995
00004	Polygon	Roma	6850.675059999999600	349.803220000000010	913	7680.00	1189	6839.00	1998	1980
01150	Polygon	Roma	6471.766529999999900	331.839990000000000	3398	6795.00	5001	6461.00	1998	1965
00154	Polygon	Frascati	4149.357119999999700	329.147969999999990	664	4149.00	1600	4142.00	1998	1996
00311	Polygon	Roma	519.020359999999980	98.106049999999996	231	519.00	4451	518.00	1998	1963
00177	Polygon	Frascati	2415.193299999999900	219.727250000000000	483	2415.00	2000	2411.00	1998	1992
00323	Polygon	Roma	352.577519999999990	81.755420000000001	94	355.00	2648	352.00	1998	1993
00001	Polygon	Roma	1997.641270000000100	237.704990000000010	357	2234.00	1598	1994.00	1998	1975
00107	Polygon	Frascati	339.504920000000030	90.648679999999999	106	357.00	2969	339.00	1998	1996
00486	Polygon	Roma	1688.330470000000100	163.518000000000000	1103	1688.00	6534	1685.00	1998	1965
00383	Polygon	Roma	521.575100000000020	103.307779999999990	100	530.00	1887	521.00	1998	1993
01150	Polygon	Roma	2521.812800000000200	241.909050000000010	1323	2645.00	5002	2517.00	1998	1965
00083	Polygon	Frascati	725.045589999999950	143.141789999999990	484	870.00	5563	724.00	1998	1980
00391	Polygon	Frascati	332.304590000000020	104.821659999999990	346	332.00	10422	332.00	1998	1940
00414	Polygon	Roma	44.350709999999999	36.725160000000002	14	44.00	3182	44.00	1998	1990
00397	Polygon	Roma	1152.253539999999900	338.344290000000000	1371	1535.00	8932	1536.00	1999	1968
00414	Polygon	Roma	48.297719999999998	34.575069999999997	28	50.00	5600	48.00	1998	1995
00412	Polygon	Roma	1441.672300000000000	230.674749999999990	444	1442.00	3079	1439.00	1998	1990
00135	Polygon	Frascati	5644.349290000000100	359.008940000000000	1763	5925.00	2976	5635.00	1998	1996
00340	Polygon	Roma	1422.641290000000000	255.401670000000000	712	1423.00	5004	1421.00	1998	1960
00347	Polygon	Roma	350.408279999999990	79.095259999999996	110	410.00	2683	350.00	1998	1993

Figure 7: ARCGIS view example of some cadastre parameters included in the shapefiles

4.2. Satellite's imagery data format

In this section I will describe the file types that I have used in the treatment and analysis of the satellite imagery available in this project. Mainly, excluding the intermediate files needed for some applications or processes, I have used GeoTIFF, shapefiles, and the ENVI files.

4.2.1. GeoTIFF

The widespread application of Geographical Information System (GIS) packages worldwide needs standardization of remote sensing satellite digital image data products' formats and its contents. Geographic Tagged Image File Format (GeoTIFF) format is an effort towards this. The Aldus-Adobe's public domain Tagged Image File Format (TIFF) is one of the widely used raster file formats, which is platform independent and has provision for extension.

The basic idea was to exploit the extensibility feature of TIFF, which allows to officially registering new TIFF Tags in order to create a well established structured format/space for a variety of geographic information. It uses a small set of reserved TIFF tags to store a broad range of georeferencing information, catering to geographic as well as projected coordinate systems needs. Projections include Universal Transverse Mercator (UTM), US State Plane and National Grids, as well as the underlying projection types such as Transverse Mercator, Lambert Conformal Conic, etc.

- **TIFF FILE STRUCTURE**

TIFF format is a widely accepted versatile raster data format in the world today. TIFF is a suitable format for storage, transfer, display, and printing of raster images such as clipart, logotypes, scanned documents etc... The TIFF imagery file format can be used to store and transfer digital satellite imagery, scanned aerial photos, elevation models, and scanned maps.

TIFF is a tag-based file format for storing and interchanging raster images. Aldus Corporation published the first version of TIFF specification in 1986, after a series of meetings with various scanner manufactures and software developers. TIFF is to describe and store raster image data. The main advantages of TIFF are its suitability for a wide range of applications and its independence of computer's architecture, operating system, and graphics hardware. It is reasonably compact and handles black-and-white, greyscale, and colour images, allowing the

user to adjust the unique characteristics of a scanner, monitor, or printer. TIFF allows colour resolution up to 48 bits (a 16-bit field each for R, G, and B), either as full RGB colour or in a 64k-color palette .The TIFF 6.0 specifications, released in June 1992, are taken as reference by GeoTIFF.

The TIFF format has a three-level hierarchy. From highest to lowest, the levels are:

- A file Header. The TIFF file begins with an 8-byte header, which gives basic information about the file such as byte order (Little Endian or Big Endian), TIFF file ID or Version Number, and a pointer to first IFD.

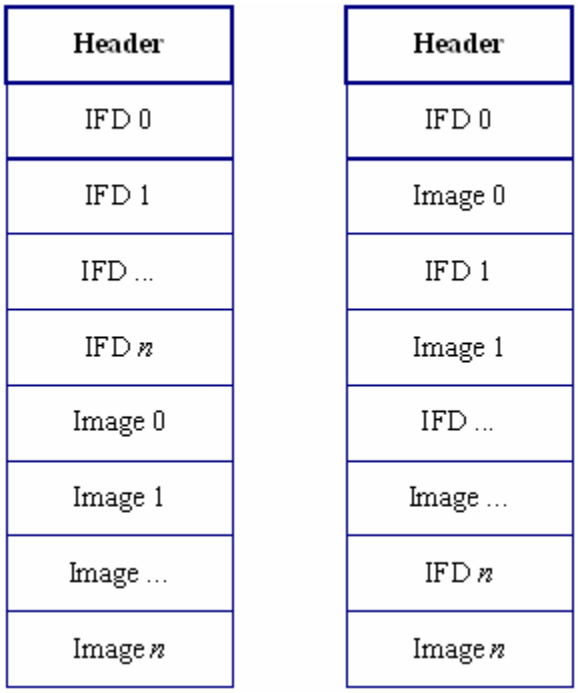

Figure 8: Two possible physical arrangements of data in a TIFF file

- One or more directories called IFD (Image File Directories), containing codes and their data, or pointer to the data. Most likely, the next structure in the file after the header will be the first (or only) IFD, but not necessarily. From here on, everything is found by following pointers. So, the first IFD is located by the header's pointer. An IFD consists of 12-byte entries, typically tagged pointers. The structure of an IFD and its entries is shown on Table 6. The first two bytes are tag, which, if public, may be looked up in the specification. These codes are assigned by the TIFF administrator (Aldus Developer's Desk), in blocks of five. This tag concept has been extended to support GeoTIFF. The

next two bytes comprise a code indicating the type of data in the pointed field. The 4-byte field specifies the number of values in the data field, not the number of bytes.

Offset (bytes)	Length (bytes)	Description
0	2	Tag
2	2	Type of data
4	4	Count field
8	4	Data pointer or data field

Table 6: TIFF IFD entry structure

- Data. The final four bytes of an IFD are usually a pointer to the start of a data field. Sometimes, however, this field contains not a pointer, but the actual data.

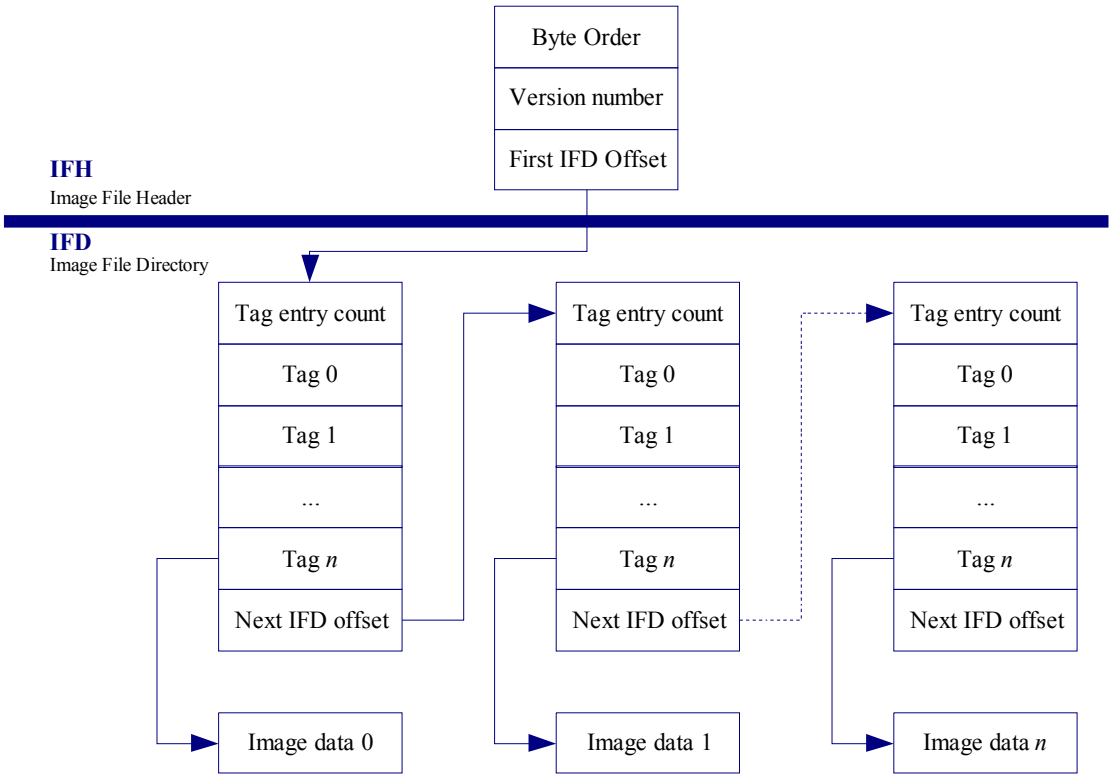

Figure 9: Logical organization of a TIFF file

- **GEOTIFF DESCRIPTION**

The GeoTIFF specification defines a set of TIFF tags provided to describe all "Cartographic" information associated with TIFF imagery that originates from satellite imaging systems, scanned aerial photography, scanned maps, digital elevation models, or as a result of geographic analyses. Its aim is to allow means for tying a raster image to a known model space or map projection.

GeoTIFF format fully complies with the TIFF 6.0 specifications, and its extensions do not in any way go against the TIFF recommendations, nor do they limit the scope of raster data supported by TIFF.

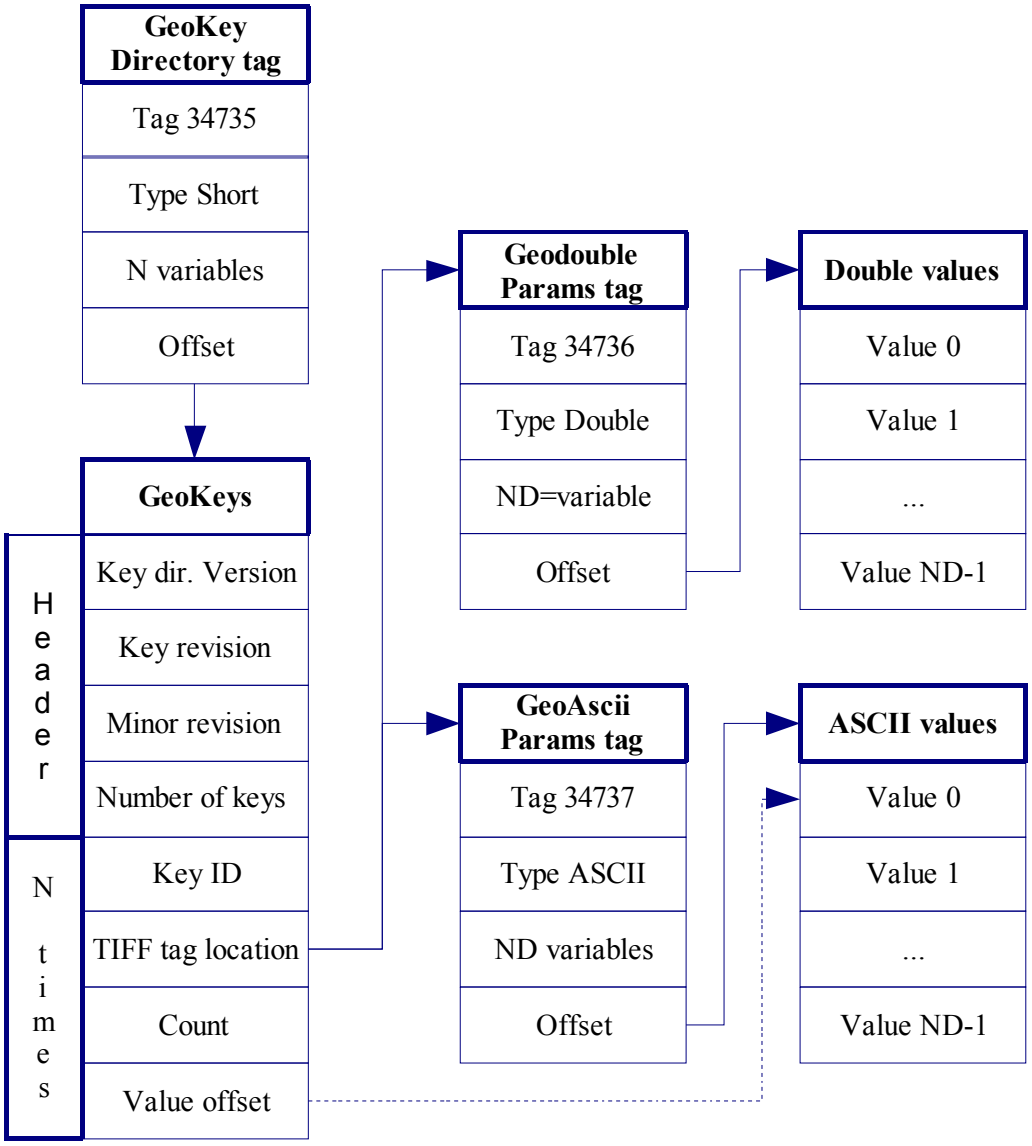

Figure 10: The Geokey concept for access to all geo-related parameters via a few TIFF tags.

GeoTIFF uses a "MetaTag" (GeoKey) approach to encode dozens of information elements into just six tags, taking advantage of TIFF platform-independent data format representation to avoid cross-platform interchange difficulties. These keys are designed in a manner parallel to standard TIFF tags, and closely follow the TIFF discipline in their structure and layout. New keys may be defined as needs arise, within the current framework, and without requiring the allocation of new tags from Aldus/Adobe.

GeoTIFF format uses numerical codes to describe projection types, coordinate systems, datums, ellipsoids, etc. The projection, datums and ellipsoid codes are derived from the EPSG list compiled by the Petrotechnical Open Software Corporation (POSC), and mechanisms for adding further international projections, datums and ellipsoids have been established. The GeoTIFF information content is designed to be compatible with the data decomposition approach used by the National Spatial Data Infrastructure (NSDI) of the U.S. Federal Geographic Data Committee (FGDC).

A GeoTIFF file is a TIFF 6.0 file, and inherits the file structure as described in the corresponding portion of the TIFF spec. All GeoTIFF specific information is encoded in several additional reserved TIFF tags, and contains no private Image File Directories (IFD's), binary structures or other private information invisible to standard TIFF readers.

As almost all standard GIS and Image Processing packages support GeoTIFF, it has emerged as a standard image file format for various GIS applications worldwide. The TIFF flexibility to add new Tags and portability has given a lot of scope for GeoTIFF expansion in future. Now major GeoTIFF data providers are Department of Space (DOS) India, Space Imaging, and SPOT. Since major remote sensing data providers in the world today provide data in GeoTIFF format it has high potential user base for GIS applications where spatial data is one of the major input.

4.2.2. ENVI files

ENVI uses a generalized raster data format consisting of a simple flat binary file and a small associated ASCII (text) header file. This approach permits ENVI's flexible use of nearly any image format, including those with embedded header information. All data types are supported in their native formats (byte, signed and unsigned integer, long integer, floating point, double precision, 64-bit integer, unsigned 64-bit integer, complex, or double complex). The generalized raster data is stored as a binary stream of bytes either in BSQ, BIP, or BIL formats.

- BSQ (Band Sequential Format). In its simplest form, the data is in BSQ format, with each line of the data followed immediately by the next line in the same spectral band. This format is optimal for spatial (X, Y) access of any part of a single spectral band.

- BIP (Band Interleaved by Pixel Format). Images stored in BIP format have the first pixel for all bands in sequential order, followed by the second pixel for all bands, followed by the third pixel for all bands, etc., interleaved up to the number of pixels. This format provides optimum performance for spectral (Z) access of the image data.

- BIL (Band Interleaved by Line Format). Images stored in BIL format have the first line of the first band followed by the first line of the second band, followed by the first line of the third band, interleaved up to the number of bands. Subsequent lines for each band are interleaved in similar fashion. This format provides a compromise in performance between spatial and spectral processing and is the recommended file format for most ENVI processing tasks.

The extension of the ENVI header file is hdr. However, the image file does not have an associated extension, so the file names are usually a simple characters string.

The ENVI header file contains information used to read an image data file and is normally created the first time a data file is accessed by ENVI. The separate ENVI text header file provides information to ENVI about the dimensions of the image, the imbedded header if present, the data format, and other pertinent information. The required information is entered interactively or is automatically created with file ingest, and can be edited and changed later. It is possible to generate an ENVI header outside ENVI using a text editor.

The file starts with the text string "ENVI" to be recognized by ENVI as a native file header. Keywords within the file are used to indicate critical file information. The following are valid keywords:

Keyword	Explanation
description	a character string describing the image or processing performed
samples	number of samples (pixels) per image line for each band
lines	number of lines per image for each band
bands	number of bands per image file
header offset	refers to the number of bytes of imbedded header information present in the file (for example 128 bytes for ERDAS 7.5 .lan files). These bytes are skipped when the ENVI file is read

file type	refers to specific ENVI defined file types such as certain data formats and processing results. The available file types are listed in the filetype.txt file described below. The file type ASCII string must match an entry in the filetype.txt file verbatim, including case
data type	parameter identifying the type of data representation, where 1=8 bit byte; 2=16-bit signed integer; 3=32-bit signed long integer; 4=32-bit floating point; 5=64-bit double precision floating point; 6=2x32-bit complex, real-imaginary pair of double precision; 9=2x64-bit double precision complex, real-imaginary pair of double precision; 12=16-bit unsigned integer; 13=32-bit unsigned long integer; 14=64-bit signed long integer; and 15=64-bit unsigned long integer
interleave	refers to whether the data are band sequential (BSQ), band interleaved by pixel (BIP), or band interleaved by line (BIL)
sensor type	refers to specific instruments such as Landsat TM, SPOT, RadarSat, etc. The available sensor types are listed in the sensor.txt file described below. The sensor type ASCII string defined here must match one of the entries in the sensor.txt file verbatim., including case
byte order	describes the order of the bytes in integer, long integer, 64-bit integer, unsigned 64-bit integer, floating point, double precision, and complex data types; Byte order=0 is Least Significant Byte First (LSF) data (DEC and MS-DOS systems) and byte order=1 is Most Significant Byte First (MSF) data (all others - SUN, SGI, IBM, HP, DG)
x start and y start	parameters define the image coordinates for the upper-left hand pixel in the image. The values in the header file are specified in "file coordinates," which is a zero-based number
map info	lists geographic coordinates information in the order of projection name (UTM), reference pixel x location in file coordinates, pixel y, pixel easting, pixel northing, x pixel size, y pixel size, Projection Zone, North or South for UTM only.
projection info	parameters that describe user-defined projection information. This keyword is added to the ENVI header file if a user-defined projection is used instead of a standard projection. This information can be used to read this file in installations of ENVI that do not contain this user-defined projection in its map_proj.txt file
default bands	if set, indicates which band numbers to automatically load into the Available Bands List's greyscale or R, G, and B text boxes every time the file is opened. By default, a new image is automatically loaded when a file that has default bands defined in its header is opened. If only 1 band number is used, then a greyscale image is loaded
wavelength units	text string indicating which units the wavelengths are in
reflectance scale factor	the value that, when divided into your data, would scale it from 0 - 1 reflectance
z plot range	values indicating the default minimum and maximum values for Z plots
z plot average	values indicate the number of pixels in the X and Y directions to average for Z plots
z plot titles	allows entry of specific X and Y axis titles for Z plots
data ignore value	currently used only in ENVI programming (see ENVI_FILE_QUERY for more information)
pixel size	indicates X and Y pixel size in meters for non-georeferenced files
default stretch	determines what type of stretch (% linear, linear range, Gaussian, equalize, square root) is used when the image displays
band names	allows entry of specific names for each band of an image

wavelength	lists the centre wavelength values of each band in an image. Units should be the same as those used for the FWHM and set in the wavelength units parameter
fwhm	lists full-width-half-max values of each band in an image. Units should be the same as those used for wavelength and set in the wavelength units parameter
bbl	lists the bad band multiplier values of each band in an image, typically zero for bad bands and one for good bands
data gain values	gain values for each band
data offset values	offset values for each band

Table 7: Valid keywords on ENVI header file

4.2.3. Shapefiles

The ESRI Shapefile is a popular geospatial vector data format for geographic information systems software. It is developed and regulated by ESRI as a (mostly) open specification for data interoperability among ESRI and other software products. A "shapefile" commonly refers to a collection of files with ".shp", ".shx", ".dbf", and other extensions on a common prefix name (i.e., "lakes.*"). The actual shapefile relates specifically to files with the ".shp" extension; however this file alone is incomplete for distribution, as the other supporting files are required.

A Shapefile is a digital vector storage format for storing geometric location and associated attribute information. This format lacks the capacity to store topological information. The Shapefile format was introduced with ArcView GIS version 2 in the beginning of the 1990s. It is now possible to read and write Shapefiles using a variety of free and non-free programs.

Shapefiles are simple because they store primitive geometrical data types of points, lines and polygons. These, for example, could represent water wells, lakes and rivers, respectively. Each item may also have attributes that describe the items, such as the name or temperature. These primitives are of limited use without any attributes to specify what they represent. Therefore, a table of records will store properties/attributes for each primitive shape in the Shapefile. Shapes (points/lines/polygons) together with data attributes can create infinitely many representations about geographical data. Representation provides the ability for powerful and accurate computations.

While a Shapefile must be considered as a whole, a "Shapefile" is actually a set of files. Three individual files are mandatory and these store the core data. There are a further 8 optional individual files which store primarily index data to improve performance. Each individual file should conform to the MS DOS 8.3 naming convention (8 character filename prefix, fullstop, 3 character filename suffix such as shapefil.shp) in order to be compatible with past applications that handle shapefiles. For this same reason, all files should be located in the same folder.

Mandatory files:

- .shp - the file that stores the feature geometry
- .shx - the file that stores the index of the feature geometry
- .dbf - the database of attributes

Optional files:

- .sbn and .sbx - store the spatial index of the features
- .fbn and .fbx - store the spatial index of the features for shapefiles that are read-only
- .ain and .aih - store the attribute index of the active fields in a table or a theme's attribute table
- .prj - the file that stores the coordinate system information, using well-known text
- .shp.xml - metadata for the shapefile
- .atx - attribute index for the .dbf file in the form of <shapefile>.<columnname>.atx (ArcGIS 8 and later)
- **FILE STRUCTURE**

The main file (.shp) contains the primary reference data in the Shapefile. The file consists of a single fixed length header followed by one or more variable length records. Each of the variable length records includes a record header component and a record contents

component. A detailed description of the file format is given in the ESRI Shapefile Technical Description.

The main file header is fixed at 100 bytes in length and contains 17 fields (nine 4-byte fields and eight 8-byte fields):

- Bytes 0-3: File code (always hex value 0000270A)
- Bytes 4-23: (Unused)
- Bytes 24-27: File length
- Bytes 28-31: Version
- Bytes 32-35: Shape type (see below)
- Bytes 36-99: Bounding box as minimum and maximum values for X, Y, Z, M.

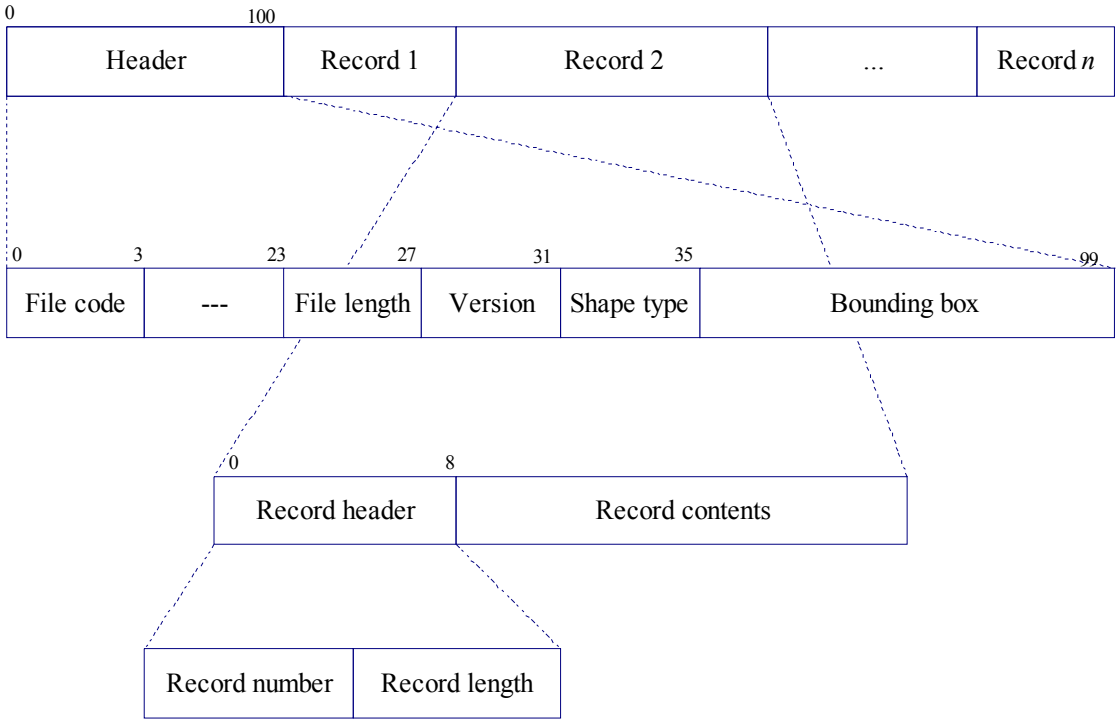

Figure 11: Shapefile structure

The variable length record header is fixed at 8 bytes in length and simply contains 2 fields with data for record number and content length.

The variable length record contents depend entirely upon the Shape Type (included in the main file header) for which there is a one to one correspondence.

Shape Type	Value	Fields
Null Shape	0	Shape Type
Point	1	Shape Type, X, Y
Polyline	3	Shape Type, Box, NumParts, NumPoints, Parts, Points
Polygon	5	Shape Type, Box, NumParts, NumPoints, Parts, Points
MultiPoint	8	Shape Type, Box, NumPoints, Points
PointZM	11	Shape Type, X, Y, Z, M
PolylineZ	13	Mandatory: Shape Type, Box, NumParts, NumPoints, Parts, Points, Z range , Z array Optional: M range, M array
PolygonZ	15	Mandatory: Shape Type, Box, NumParts, NumPoints, Parts, Points, Z range, Z array Optional: M range, M array
MultiPointZ	18	Mandatory: Shape Type, Box, NumPoints, Points, Z range, Z array Optional: M range, M array
PointM	21	Shape Type, X, Y, M
PolylineM	23	Mandatory: Shape Type, Box, NumParts, NumPoints, Parts, Points Optional: M range, M array
PolygonM	25	Mandatory: Shape Type, Box, NumParts, NumPoints, Parts, Points Optional: M range, M array
MultiPointM	28	Mandatory: Shape Type, Box, NumPoints, Points Optional Fields: M range, M array
MultiPatch	31	Mandatory: Shape Type, Box, NumParts, NumPoints, Parts, PartTypes, Points, Z range, Z array Optional: M range, M array

Table 8: Shape types and fields on a Shapefile

The file with .dbf extension stores attributes for each shape in the xBase (dBase) format, which has an open specification. First shape in the file corresponds to the first record in the dbf and so on.

Finally, the file with .sbn extension contains part of ArcView's spatial index. In case this file is outdated, ArcView will not display the shapefile correctly. It will appear like a lot of features have been deleted. To recreate the spatial index in ArcView, a few steps can be done: Go to the table → Select the Shape field → Select Field → Remove Index from the menu → Select Field → Create Index from the menu.

5. Vegetation study

5.1. Vegetation and its reflectance properties

Analyzing vegetation using remotely sensed data requires knowledge of the structure and function of vegetation and its reflectance properties. This knowledge enables you to link vegetative structures and their condition to their reflectance behaviour in an ecological system of interest. Vegetation reflectance properties are used to derive vegetation indices (VIs), which are used to analyze various ecologies. VIs are constructed from reflectance measurements in two or more wavelengths to analyze specific characteristics of vegetation, such as total leaf area and water content.

A VI is a simple measure of some vegetation property calculated from reflected solar radiation measurements made across the optical spectrum. The solar-reflected optical spectrum spans a wavelength range of 400 nm to 3000 nm. Of this range, the 400 nm to 2500 nm region is routinely measured using a variety of optical sensors ranging from multispectral (for example, Landsat TM, SPOT MSS, QuickBird) to hyperspectral (for example, AVIRIS, HyMap, Hyperion, CHRIS).

Vegetation interacts with solar radiation differently from other natural materials, such as soils and water bodies. The absorption and reflection of solar radiation is the result of many interactions with different plant materials, which varies considerably by wavelength. Water, pigments, nutrients, and carbon are each expressed in the reflected optical spectrum from 400

nm to 2500 nm, with often overlapping, but spectrally distinct, reflectance behaviours. These known signatures allow scientists to combine reflectance measurements at different wavelengths to enhance specific vegetation characteristics by defining VIs.

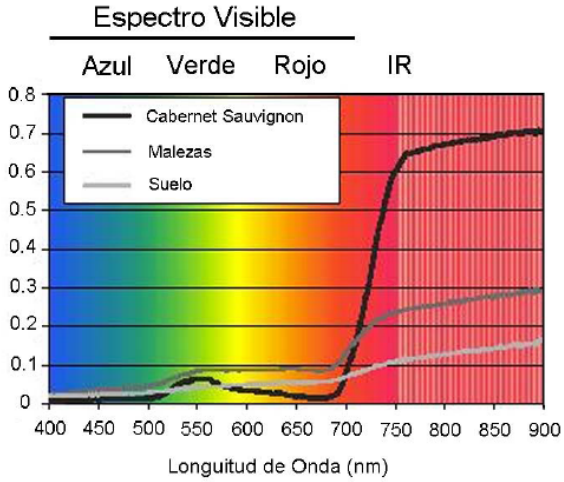

Graphic 2: Example of spectral signature of Cavernet Sauvingnon grape compared with weeds or simple soil

The optical spectrum is partitioned into four distinct wavelength ranges:

- Visible: 400 nm to 700 nm
- Near-infrared: 700 nm to 1300 nm
- Shortwave infrared 1 (SWIR-1): 1300 nm to1900 nm
- Shortwave infrared 2 (SWIR-2): 1900 nm to 2500 nm

The transition from near-infrared to SWIR-1 is marked by the 1400 nm atmospheric water absorption region in which satellites and aircraft cannot acquire measurements. Similarly, the SWIR-1 and SWIR-2 transition is marked by the 1900 nm atmospheric water absorption region.

Vegetation is divided into the following general categories:

- Plant Foliage
- Canopies

- Non-Photosynthetic Vegetation

5.1.1. Plant foliage

Plant foliage, including leaves, needles, and other green materials often look similar to the casual observer, but they vary widely in both shape and chemical composition. The chemical composition of leaves can often be estimated using VIs, but doing so requires some knowledge of the basic composition of leaves and how they change under different environmental conditions.

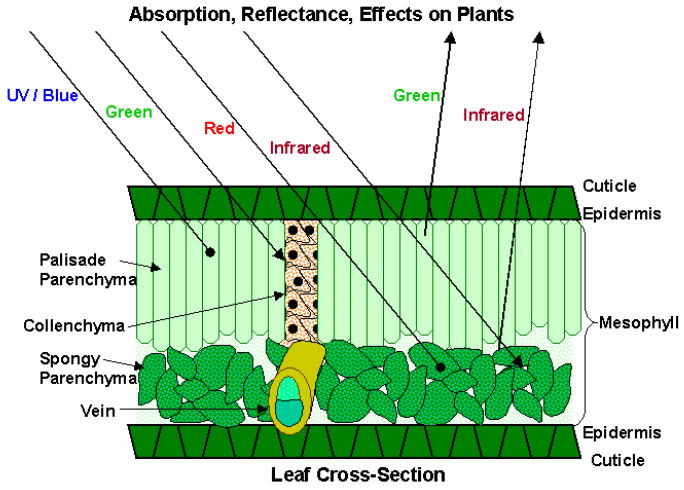

Figure 12: Diagrammatic cross section of a leaf, showing interaction with incident energy.

In Figure 12 we can see that incident blue and red wavelengths are absorbed by chlorophyll in the process of photosynthesis, incident green wavelengths are partially reflected by chlorophyll, and incident IR energy is strongly scattered and reflected by cell walls in the mesophyll.

The most important leaf components that affect their spectral properties are:

- Pigments
- Water
- Carbon

- Nitrogen

These components are described in the sections that follow. Other components (such as phosphorus, calcium, and so forth) are significant to plant function, but they do not directly contribute to the spectral properties of leaves, and therefore cannot be directly measured using remotely sensed data.

- **PIGMENTS**

There are three main categories of leaf pigments in plants: chlorophyll, carotenoids, and anthocyanins. These pigments serve a variety of purposes, and are critical to the function and health of vegetation, though the relative concentrations of these pigments in vegetation can vary significantly. Vegetation with a high concentration of chlorophyll is generally very healthy, as chlorophyll is linked to greater light use efficiency or photosynthetic rates. Conversely, carotenoid and anthocyanin pigments often appear in higher concentrations in vegetation that is less healthy, typically due to stress or the onset of senescence (dormant or dying vegetation that appears red, yellow, or brown).

Chlorophyll, the most well-known and most important pigment, causes the green colour of healthy plant leaves. It is primarily responsible for photosynthesis, the process by which plants take up carbon dioxide (CO_2) from the atmosphere and convert it into organic forms such as sugar and starch. Chlorophyll concentrations in leaves are broadly correlated with photosynthetic rates. Chlorophyll-a and -b pigments are the most closely associated with photosynthesis.

Carotenoids are a group of pigments containing alpha-carotene, beta-carotene, and xanthophyll pigments (for example, zeaxanthin). Carotene is the yellow-orange pigment found in tree leaves as they change from green to brown (as seen during autumn). Carotenoid pigments have multiple functions, but they are generally found in higher concentrations in plant leaves that are either stressed (seen in drought or nutrient depletion), senescent, or dead. Carotenoids assist the process of light absorption in plants, and help protect plants from the harmful effects of very high light conditions.

Anthocyanins also have multiple functions, but are typically related to changes in foliage. Anthocyanins are reddish pigments abundant in both newly forming leaves and leaves undergoing senescence. Anthocyanins also serve to protect leaves from damage due to ultraviolet radiation.

As a group, leaf pigments only affect the visible portion of the shortwave spectrum (400 nm to 700 nm), though the affects vary depending upon the type of pigment. Graphic 3 shows the absorption of each pigment type as a function of wavelength throughout the visible range.

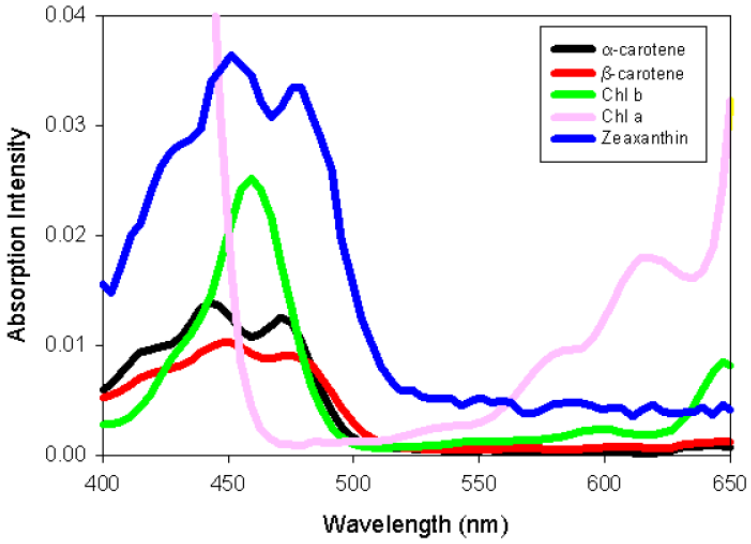

Graphic 3: Relative Light Absorption Intensity of Some Leaf Pigments

- **WATER**

Plants of different species inherently contain different amounts of water based on their leaf geometry, canopy architecture, and water requirements. Among plants of one species, there is still significant variation, depending upon leaf thickness, water availability, and plant health. Water is critical for many plant processes, in particular, photosynthesis. Generally, vegetation of the same type with greater water content is more productive and less prone to burn.

Leaf water affects plant reflectance in the near-infrared and shortwave infrared regions of the spectrum (see Graphic 4). Water has maximum absorptions centred near 1400 and 1900 nm, but these spectral regions usually cannot be observed from airborne or space-based sensors due to atmospheric water absorption, preventing their practical use in the creation of VIs. Water features centred on 970 nm and 1190 nm are pronounced and can be readily measured from hyperspectral sensors. These spectral regions are generally not sampled by multispectral sensors.

- **CARBON**

Plants contain carbon in many forms, including sugars, starch, cellulose, and lignin. Sugars and starch are immediate products of photosynthesis; they are moved to other locations in plants to construct cellulose and lignin. Cellulose is primarily used in the construction of cell walls in plant tissues. Lignin is used for the most structurally robust portions of plants, such as leaf vacuoles, veins, woody tissue, and roots. Cellulose and lignin display spectral features in the shortwave infrared range of the shortwave optical spectrum (SWIR).

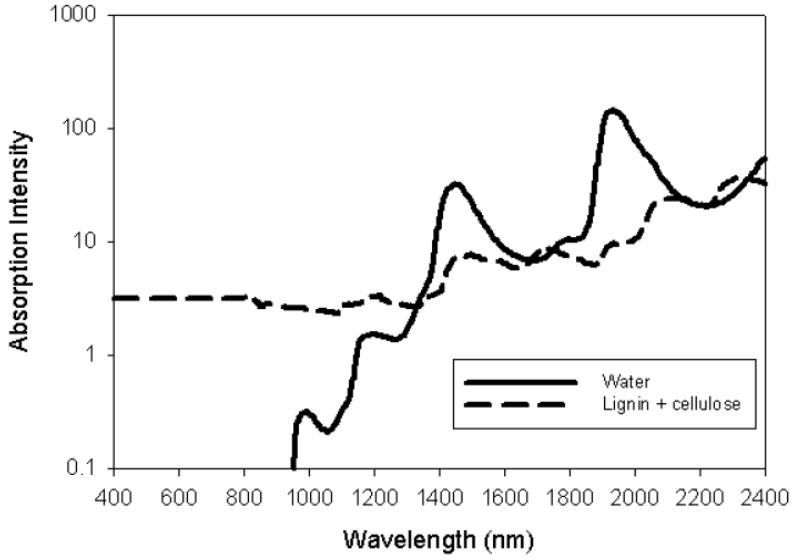

Graphic 4: Relative Light Absorption Intensity of Leaf Water and Carbon (Cellulose and Lignin)

- **NITROGEN**

Leaves contain nitrogen bound in the chlorophyll pigment, proteins, and other molecules. Nitrogen concentrations in foliage are linked to maximum photosynthetic rate and net primary production. VIs sensitive to chlorophyll content (which is approximately 6% nitrogen) are often broadly sensitive to nitrogen content as well. Some proteins that contain nitrogen affect the spectral properties of leaves in the 1500 nm to 1720 nm range.

- **COMBINED LEAF LEVEL ABSORPTION**

The interaction of radiation with foliage is primarily a function of the reflectance properties of leaf components. In the visible range, the main signal comes from the absorption of incident radiation by the leaf pigments chlorophyll, carotenoids, and anthocyanins. In the near-infrared, the primary contribution comes from the absorption of water. The reflectance in

the shortwave infrared range is partially determined by water, but also receives significant contributions from the reflectance of nitrogen and various forms of carbon. The next graphic shows an example of the reflectance spectra of both mature and young leafs.

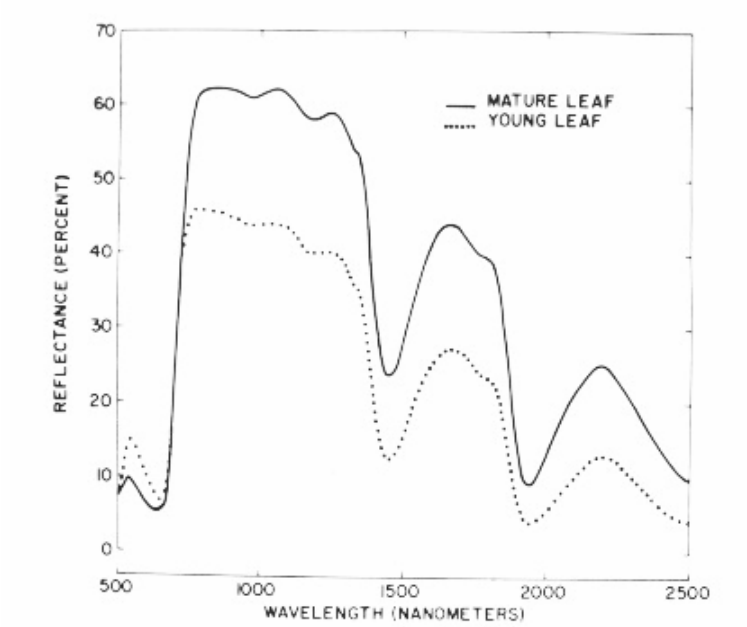

Graphic 5: Reflectance spectra of mature and young leafs

5.1.2. Canopies

The canopy is the habitat found at the uppermost level of a forest, especially rainforest. Canopy trees refer to the tallest layer of trees in a forest, which are distinguished from secondary trees which occupy a lower ecological niche. Only emergent - of which there are typically just one or two per hectare - reach above the canopy.

The canopy of a rainforest is typically 10m thick, and intercepts around 95% of sunlight. With an abundance of water and a near ideal temperature, light and minerals are the two restricting factors on a tree's growth. Plants grow rapidly to reach the canopy, but have no need to grow any taller after reaching the light.

The canopy is home to a unique flora and fauna not found in other layers of a forest. Trees in the canopy are able to photosynthesise very rapidly thanks to the large amount of light, so it supports the widest diversity of plant as well as animal life in most rainforests. Many rainforest animals have evolved to live solely in the canopy, and will never touch the ground.

However, the term canopy has lately acquired a most generic meaning, and now it is used in scientific literature to design the upper level of almost all vegetation, cultivations included.

Leaf reflectance properties (controlled by properties of pigments, water, and carbon) play a significant role in reflectance at the canopy level. Additionally, the amount of foliage and the architecture of the canopy are also meaningful in determining the scattering and absorption properties of vegetation canopies. Different ecosystems, whether they are forest, grassland, or agricultural field, have different reflectance properties, even though the properties of individual leaves are usually quite similar.

Vegetation with mostly vertical foliage, such as grass, reflects light differently than other with more horizontally-oriented foliage, seen frequently in trees and tropical forest plants. The variation in reflectance caused by different canopy structures, much like individual leaf reflectance, is highly variable with wavelength.

There are a variety of vegetation properties of interest to scientists at the canopy level, and many of these have direct effects on canopy reflectance properties. The most significant is leaf area index (LAI). The LAI is the green leaf area per unit ground area, which represents the total amount of green vegetation present in the canopy. The LAI is an important property of vegetation, and has the strongest effect on overall canopy reflectance, as seen on Graphic 6.

Whereas vegetation strongly reflects light in the near-infrared portion of the spectrum, canopies strongly absorb photons in the visible and SWIR-2 ranges. This results in a much shallower penetration of photons into the canopy in these wavelengths. As such, VIs using spectral data from the visible and SWIR-2 are very sensitive to upper-canopy conditions. In contrast, photons are scattered in the near-infrared and SWIR-1 range. Therefore, these photons measured by a remote sensing instrument come from reflections throughout much of a vegetation canopy.

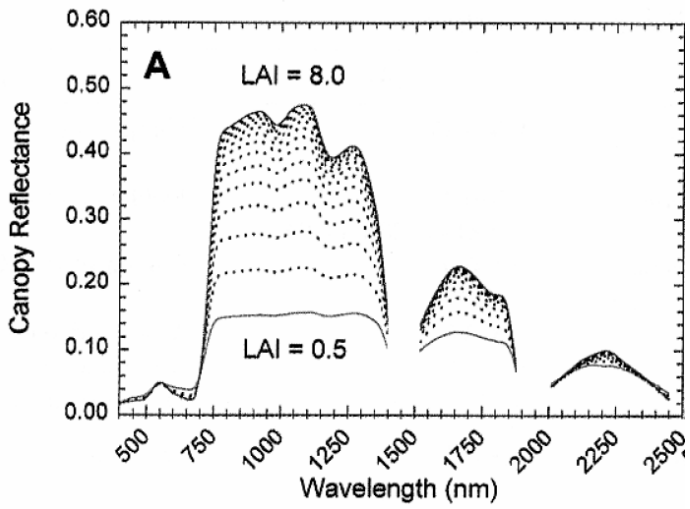

Graphic 6: Example effect of increasing LAI on Canopy Reflectance

More aspects on Leaf Area Index have been studied 3.3 above on section 3.3: Leaf area index and its significance in plantations.

5.1.3. Non-Photosynthetic Vegetation

The previous sections primarily discuss live, green vegetation, but many ecosystems contain as much, or more, senescent or dead vegetation (also known as non-photosynthetic vegetation, or NPV) as they do green vegetation. Examples include grasslands, shrublands, savannas, and open woodlands, which collectively cover over half of the global vegetated land surface.

This material is often called non-photosynthetic vegetation because it could be truly dead or simply dormant (such as some grasses between rainfall events). Also included in the NPV category are woody structures in many plants, including tree trunks, stems, and branches.

NPV is composed largely of the carbon-based molecules lignin, cellulose, and starch. As such, it has a similar reflectance signature to these materials, with most of the variation in the shortwave infrared range. In many canopies, much of the NPV is obscured below a potentially closed leaf canopy; the wavelengths used to measure NPV (shortwave infrared) are often unable to penetrate through the upper canopy to interact with this NPV. As such, only exposed NPV has a significant effect on the spectral reflectance of vegetated ecosystems. When exposed, NPV scatters photons very efficiently in the shortwave infrared range, in direct contrast to green vegetation which absorbs strongly in the shortwave infrared range.

In general, photons in the visible wavelength region are efficiently absorbed by live, green vegetation. Likewise, photons in the SWIR-2 region of the spectrum are efficiently absorbed by water. In contrast to live vegetation, dead, dry, or senescent vegetation scatters photons very efficiently throughout the spectrum, with the most scattering occurring in the SWIR-1 and SWIR-2 ranges. The change in canopy reflectance due to increasing amounts of NPV is shown in the next graphic.

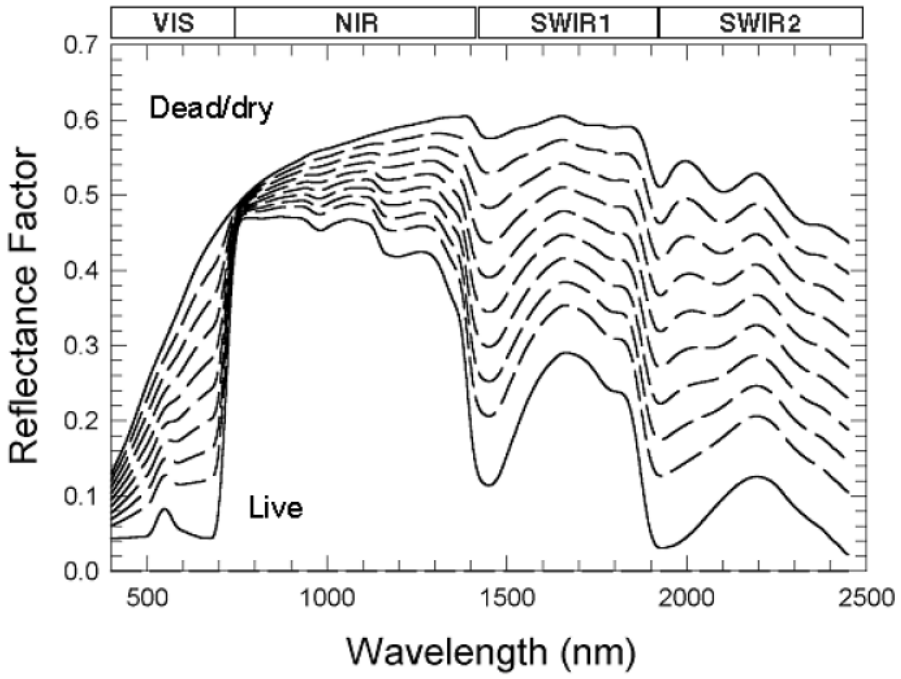

Graphic 7: Changes in a Canopy's Reflectance as it Transitions from Live/Green to Dry/Dead Status

5.2. Vegetation indices

Vegetation Indices (VIs) are combinations of surface reflectance at two or more wavelengths designed to highlight a particular property of vegetation. They are derived using the reflectance properties of vegetation described in section 5.1.1 Plant foliage. Each of the VIs is designed to accentuate a particular vegetation property.

More than 150 VIs have been published in scientific literature, but only a small subset have substantial biophysical basis or have been systematically tested. Many of these indices are currently unknown or under-used in the commercial, government, and scientific communities.

The studied indices are grouped into categories that calculate similar properties. The categories and indices are:

Broadband Greenness (6 indices):

- Simple Ratio Index
- Normalized Difference Vegetation Index
- Normalized Vegetation Index
- Enhanced Vegetation Index
- Atmospherically Resistant Vegetation Index
- Sum Green Index

Narrowband Greenness (7 indices):

- Red Edge Normalized Difference Vegetation Index
- Modified Red Edge Simple Ratio Index
- Modified Red Edge Normalized Difference Vegetation Index
- Vogelmann Red Edge Index 1
- Vogelmann Red Edge Index 2
- Vogelmann Red Edge Index 3
- Red Edge Position Index

Light Use Efficiency (3 indices):

- Photochemical Reflectance Index
- Structure Insensitive Pigment Index

- Red Green Ratio Index

Canopy Nitrogen (1 index):

- Normalized Difference Nitrogen Index

Dry or Senescent Carbon (3 indices):

- Normalized Difference Lignin Index
- Cellulose Absorption Index
- Plant Senescence Reflectance Index

Leaf Pigments (4 indices):

- Carotenoid Reflectance Index 1
- Carotenoid Reflectance Index 2
- Anthocyanin Reflectance Index 1
- Anthocyanin Reflectance Index 2

Canopy Water Content (4 indices):

- Water Band Index
- Normalized Difference Water Index
- Moisture Stress Index
- Normalized Difference Infrared Index

Each category of indices typically provides multiple techniques to estimate the absence or presence of a single vegetation property. For different properties and field conditions, some indices within a category provide results with higher validity than others. By comparing the results of different VIs in a category-and correlating these to field conditions measured on site- you can assess which indices in a particular category do the best job of modelling the variability

in your scene. By using the VI in any category which best models the measured field conditions for a few measurements, you can significantly increase the quality of the results from any further processing.

All VIs require high-quality reflectance measurements from either multispectral or hyperspectral sensors. Measurements in radiance units that have not been atmospherically corrected are unsuitable, and typically provide poor results.

The next sections describe the studied VIs, grouped by category. Information about each index includes the formulation, expected range, usage, limitations, etc… Except for the broadband greenness VI descriptions, the wavelength (in nanometres) is represented as a subscript in the reflectance identifier for all inputs to the VI formulae (for example, ρ_{680} means the reflectance at 680 nm). To indicate that the broadband greenness indices require less precise wavelength bands, the formulae use the subscripts NIR, RED, and BLUE to indicate the spectral region of the reflectance input used to calculate the VI.

5.2.1. Broadband greenness indices

The broadband greenness VIs are among the simplest measures of the general quantity and vigour of green vegetation. They are combinations of reflectance measurements that are sensitive to the combined effects of foliage chlorophyll concentration, canopy leaf area, foliage clumping, and canopy architecture. These VIs are designed to provide a measure of the overall amount and quality of photosynthetic material in vegetation, which is essential for understanding the state of vegetation for any purpose. These VIs are an integrative measurement of these factors and are well correlated with the fractional absorption of photosynthetically active radiation (FAPAR) in plant canopies and vegetated pixels. They do not provide quantitative information on any one biological or environmental factor contributing to the FAPAR, but broad correlations have been found between the broadband greenness VIs and canopy LAI, as an example.

Broadband greenness VIs compare reflectance measurements from the reflectance peak of vegetation in the near-infrared range to another measurement taken in the red range, where chlorophyll absorbs photons to store into energy through photosynthesis. Use of near-infrared measurements, with much greater penetration depth through the canopy than red, allows sounding of the total amount of green vegetation in the column until the signal saturates at very high levels. Because these features are spectrally quite broad, many of the broadband greenness indices can work effectively, even with image data collected from broadband multispectral

sensors, such as AVHRR, Landsat TM, and QuickBird. Applications include vegetation phenology (growth) studies, land-use and climatological impact assessments, and vegetation productivity modelling.

The broadband greenness equations in the next sections represent the surface reflectance in an image band with a centre wavelength as follows: ρ_{NIR}=800 nm, ρ_{RED}=680 nm and ρ_{BLUE}=450 nm. Increases in leaf chlorophyll concentration or leaf area, decreases in foliage clumping, and changes in canopy architecture each can contribute to ρ_{NIR} decreases and ρ_{RED} increases, thereby causing an increase in the broadband greenness values.

Index	Index Description
Simple Ratio Index	Ratio of green leaf scattering in near-infrared, chlorophyll absorption in RED.
Normalized Difference Vegetation Index	Normalized difference of green leaf scattering in near-infrared, chlorophyll absorption in RED.
Normalized Vegetation Index	NDVI density-normalized
Enhanced Vegetation Index	An enhancement on the NDVI to better account for soil background and atmospheric aerosol effects.
Atmospherically Resistant Vegetation Index	An enhancement of the NDVI to better account for atmospheric scattering.
Sum Green Index	Integral of scattered light in the GREEN spectral range is sensitive to gaps in vegetation canopy.

Table 9: Broadband greenness indices

- **SIMPLE RATIO INDEX**

The Simple Ratio (SR) index is an old and well known VI. The SR is the ratio of the highest reflectance; absorption bands of chlorophyll makes it both easy to understand and effective over a wide range of conditions. As with the NDVI, it can saturate in dense vegetation when LAI becomes very high. SR is defined by the following equation:

$$SRI = \frac{R_{NIR}}{R_{RED}}$$

Equation 2: Simple ratio index

The value of this index ranges from 0 to more than 30. The common range for green vegetation is 2 to 8.

- **NORMALIZED DIFFERENCE VEGETATION INDEX**

The Normalized Difference Vegetation Index (NDVI) is one of the oldest, most well known, and most frequently used VIs. The combination of its normalized difference formulation and use of the highest absorption and reflectance regions of chlorophyll make it robust over a wide range of conditions. It can, however, saturate in dense vegetation conditions when LAI becomes high. NDVI is defined by the following equation:

$$NDVI = \frac{R_{NIR} - R_{RED}}{R_{NIR} + R_{RED}}$$

Equation 3: Normalized Difference Vegetation Index

The value of this index ranges from -1 to 1. The common range for green vegetation is 0.2 to 0.8.

- **NORMALIZED VEGETATION INDEX**

The vegetation index density-normalized (IVN) is a new developed VI. It takes care of the density of vegetation, deleting this way the dependence of this factor:

$$IVN = \frac{R_{NIR} - R_{RED}}{R_{NIR} + R_{RED}} \Big/ D$$

Equation 4: Normalized Vegetation Index

- **ENHANCED VEGETATION INDEX**

The Enhanced Vegetation Index (EVI) was developed to improve the NDVI by optimizing the vegetation signal in high LAI regions by using the blue reflectance to correct for soil background signals and reduce atmospheric influences, including aerosol scattering. This VI is therefore most useful in high LAI regions, where the NDVI may saturate. EVI is defined by the following equation:

$$EVI = 2.5\left(\frac{\rho_{NIR} - \rho_{RED}}{\rho_{NIR} + 6\rho_{RED} - 7.5\rho_{BLUE} + 1}\right)$$

Equation 5: Enhanced vegetation index

The value of this index ranges from -1 to 1. The common range for green vegetation is 0.2 to 0.8.

- **ATMOSPHERICALLY RESISTANT VEGETATION INDEX**

The Atmospherically Resistant Vegetation Index (ARVI) is an enhancement to the NDVI that is relatively resistant to atmospheric factors (for example, aerosol). It uses the reflectance in blue to correct the red reflectance for atmospheric scattering. It is most useful in regions of high atmospheric aerosol content, including tropical regions contaminated by soot from slash-and-burn agriculture. ARVI is defined by the following equation:

$$ARVI = \frac{\rho_{NIR} - (2\rho_{RED} - \rho_{BLUE})}{\rho_{NIR} + (2\rho_{RED} - \rho_{BLUE})}$$

Equation 6: Atmospherically Resistant Vegetation Index

The value of this index ranges from -1 to 1. The common range for green vegetation is 0.2 to 0.8.

- **SUM GREEN INDEX**

The Sum Green (SG) index is one of the simplest vegetation indices used for detecting changes in vegetation greenness. Because light is strongly absorbed by green vegetation in this spectral region, the SG index is highly sensitive to small changes in vegetation canopy opening, such as what might occur with forest disturbance. The SG index is the mean of reflectance across the 500 nm to 600 nm portion of the spectrum.

This sum is then normalized by the number of bands to convert it back to units of reflectance. The value of this index ranges from 0 to more than 50 (in units of % reflectance). The common range for green vegetation is 10 to 25 percent reflectance.

5.2.2. Narrowband Greenness indices

Narrowband greenness VIs are a combination of reflectance measurements sensitive to the combined effects of foliage chlorophyll concentration, canopy leaf area, foliage clumping, and canopy architecture. Similar to the broadband greenness VIs, narrowband greenness VIs are designed to provide a measure of the overall amount and quality of photosynthetic material in vegetation, which is essential for understanding the state of vegetation. These VIs use reflectance measurements in the red and near-infrared regions to sample the red edge portion of the reflectance curve. The red edge is a name used to describe the steeply sloped region of the vegetation reflectance curve between 690 nm and 740 nm that is caused by the transition from chlorophyll absorption and near-infrared leaf scattering. Use of near-infrared measurements, with much greater penetration depth through the canopy than red measurements, allows estimation of the total amount of green material in the column.

Narrowband greenness VIs are more sophisticated measures of general quantity and vigour of green vegetation than the broadband greenness VIs. Making narrowband measurements in the red edge allows these indices to be more sensitive to smaller changes in vegetation health than the broadband greenness VIs, particularly in conditions of dense vegetation where the broadband measures can saturate. Narrowband greenness VIs are intended for use with high spectral resolution imaging data, such as that acquired by hyperspectral sensors.

Index	Index Description
Red Edge Normalized difference Vegetation Index	A modification of the NDVI using reflectance measurements along the red edge.
Modified Red Edge Simple Ratio Index	A ratio of reflectance along the red edge with blue reflection correction.
Modified Red Edge Normalized Difference Vegetation Index	A modification of the Red Edge NDVI using blue to compensate for scattered light.
Vogelmann Red Edge Index 1	A shoulder of the RED-to-NIR transition that is indicative of canopy stress.
Vogelmann Red Edge Index 2	A shape of the near-infrared transition that is indicative of the onset of canopy stress and senescence.
Vogelmann Red Edge Index 3	A shape of near-infrared transition that is indicative of the onset of canopy stress and senescence.
Red Edge Position Index	The location of the maximum derivative in near-infrared transition, which is sensitive to chlorophyll concentration.

Table 10: Narrowband greenness indices

- **RED EDGE NORMALIZED DIFFERENCE VEGETATION INDEX**

The Red Edge Normalized Difference Vegetation Index ($NDVI_{705}$) is a modification of the traditional broadband NDVI. It is intended for use with very high spectral resolution reflectance data, such as from hyperspectral sensors. Applications include precision agriculture, forest monitoring, and vegetation stress detection. This VI differs from the NDVI by using bands along the red edge, instead of the main absorption and reflectance peaks. The $NDVI_{705}$ capitalizes on the sensitivity of the vegetation red edge to small changes in canopy foliage content, gap fraction, and senescence. $NDVI_{705}$ is defined by an equation similar to the NDVI:

$$NDVI_{705} = \frac{\rho_{750} - \rho_{705}}{\rho_{750} + \rho_{705}}$$

Equation 7: Red Edge NDVI

The value of this index ranges from -1 to 1. The common range for green vegetation is 0.2 to 0.9.

- **MODIFIED RED EDGE NORMALIZED DIFFERENCE VEGETATION INDEX**

The Modified Red Edge Normalized Difference Vegetation Index ($mNDVI_{705}$) is a modification of the Red Edge NDVI. It differs from the Red Edge NDVI by incorporating a correction for leaf specular reflection. The $mNDVI_{705}$ capitalizes on the sensitivity of the vegetation red edge to small changes in canopy foliage content, gap fraction, and senescence. Applications include precision agriculture, forest monitoring, and vegetation stress detection. The $mNDVI_{705}$ index is defined by the following equation:

$$mNDVI_{705} = \frac{\rho_{750} - \rho_{705}}{\rho_{750} + \rho_{705} - 2\rho_{445}}$$

Equation 8: Modified Red Edge NDVI

The value of this index ranges from -1 to 1. The common range for green vegetation is 0.2 to 0.7.

- **VOGELMANN RED EDGE INDICES**

The Vogelmann Red Edge Indices (VOG_X) are a narrowband reflectance measurements that are sensitive to the combined effects of foliage chlorophyll concentration, canopy leaf area, and water content. Applications include vegetation phenology (growth) studies, precision agriculture, and vegetation productivity modelling. VOG's are defined by the following equations:

$$VOG_1 = \frac{\rho_{740}}{\rho_{720}}$$

Equation 9: Vogelmann Red Edge Index 1

$$VOG_2 = \frac{\rho_{734} - \rho_{747}}{\rho_{715} + \rho_{726}}$$

Equation 10: Vogelmann Red Edge Index 2

$$VOG_3 = \frac{\rho_{734} - \rho_{747}}{\rho_{715} + \rho_{720}}$$

Equation 11: Vogelmann Red Edge Index 3

The value of these indices ranges from 0 to 20. The common range for green vegetation is 4 to 8.

- **RED EDGE POSITION INDEX**

The Red Edge Position (REP) index is a narrowband reflectance measurement that is sensitive to changes in chlorophyll concentration. Increased chlorophyll concentration broadens the absorption feature and moves the red edge to longer wavelengths. The red edge position refers to the wavelength of steepest slope within the range 690 nm to 740 nm. The common range for green vegetation is 700 nm to 730 nm.

Results are reported as the wavelength of the maximum derivative of reflectance in the vegetation red edge region of the spectrum in microns from .69 microns to .74 microns.

Applications include crop monitoring and yield prediction, ecosystem disturbance detection, photosynthesis modelling, and canopy stress caused by climate and other factors.

5.2.3. Light Use Efficiency Indices

The light use efficiency VIs are designed to provide a measure of the efficiency with which vegetation is able to use incident light for photosynthesis. Light use efficiency is highly related to carbon uptake efficiency and vegetative growth rates, and is somewhat related to fractional absorption of photosynthetically active radiation (FAPAR). These VIs help us to estimate growth rate and production, which is useful in precision agriculture. These VIs use reflectance measurements in the visible spectrum to take advantage of relationships between different pigment types to assess the overall light use efficiency of the vegetation.

Index	Index Description
Photochemical Reflectance Index	Useful to estimate absorption by leaf carotenoids (especially xanthophyll) pigments, leaf stress, and carbon dioxide uptake.
Structure Insensitive Pigment Index	Indicator of leaf pigment concentrations normalized for variations in overall canopy structure and foliage content.
Red Green Ratio Index	Ratio of reflectance in RED-to-GREEN sensitive to ratio of anthocyanin to chlorophyll.

Table 11: Light use efficiency indices

- **PHOTOCHEMICAL REFLECTANCE INDEX**

The Photochemical Reflectance Index (PRI) is a reflectance measurement that is sensitive to changes in carotenoid pigments (particularly xanthophyll pigments) in live foliage. Carotenoid pigments are indicative of photosynthetic light use efficiency, or the rate of carbon dioxide uptake by foliage per unit energy absorbed. As such, it is used in studies of vegetation productivity and stress. Applications include vegetation health in evergreen shrub lands, forests, and agricultural crops prior to senescence. PRI is defined by the following equation:

$$PRI = \frac{\rho_{531} - \rho_{570}}{\rho_{531} + \rho_{570}}$$

Equation 12: Photochemical Reflectance Index

The value of this index ranges from -1 to 1. The common range for green vegetation is -0.2 to 0.2.

- **STRUCTURE INSENSITIVE PIGMENT INDEX**

The Structure Insensitive Pigment Index (SIPI) is a reflectance measurement designed to maximize the sensitivity of the index to the ratio of bulk carotenoids (for example, alpha-carotene and beta-carotene) to chlorophyll while decreasing sensitivity to variation in canopy structure (for example, leaf area index). Increases in SIPI are thought to indicate increased canopy stress (carotenoid pigment). Applications include vegetation health monitoring, plant physiological stress detection and crop production and yield analysis. SIPI is defined by the following equation:

$$SIPI = \frac{\rho_{800} - \rho_{445}}{\rho_{800} - \rho_{680}}$$

Equation 13: Structure Insensitive Pigment Index

The value of this index ranges from 0 to 2. The common range for green vegetation is 0.8 to 1.8.

- **RED GREEN RATIO INDEX**

The Red Green Ratio (RG Ratio) index is a reflectance measurement that indicates the relative expression of leaf redness caused by anthocyanin to that of chlorophyll. The RG Ratio has been used to estimate the course of foliage development in canopies.

The RG Ratio index is an indicator of leaf production and stress, and may also indicate flowering in some canopies. Applications include plant growth cycle (phenology) studies, canopy stress detection, and crop yield prediction. Results are reported as the mean of all bands in the red range divided by the mean of all bands in the green range.

The value of this index ranges from 0.1 to more than 8. The common range for green vegetation is 0.7 to 3.

5.2.4. Canopy Nitrogen Indices

The Canopy Nitrogen VI is designed to provide a measure of nitrogen concentration of remotely sensed foliage. Nitrogen is an important component of chlorophyll and is generally present in high concentration in vegetation that is growing quickly. The section 5.1.1: Plant

foliage (above) provides more information on the importance of nitrogen in vegetation. This VI uses reflectance measurements in the shortwave infrared range to measure relative amounts of nitrogen contained in vegetation canopies.

Index	Index Description
Normalized Difference Nitrogen Index	It does show strong sensitivity to changing nitrogen status when the canopy is green (not senescent) and closed in architecture

Table 12: Canopy Nitrogen Indices

- **NORMALIZED DIFFERENCE NITROGEN INDEX**

The Normalized Difference Nitrogen Index (NDNI) is designed to estimate the relative amounts of nitrogen contained in vegetation canopies. Reflectance at 1510 nm is largely determined by nitrogen concentration of leaves, as well as the overall foliage biomass of the canopy. Together, leaf nitrogen concentration and canopy foliar biomass are combined in the 1510 nm range to predict total canopy nitrogen content. This is compared to a reference reflectance at 1680 nm, which should contain a similar signal due to foliar biomass, but without the influence of nitrogen absorption. The NDNI is experimental, but it does show strong sensitivity to changing nitrogen status when the canopy is green (not senescent) and closed in architecture. Applications include precision agriculture, ecosystem analysis, and forest management. NDNI is defined by the following equation:

$$NDNI = \frac{\log\left(\frac{1}{\rho_{1510}}\right) - \log\left(\frac{1}{\rho_{1680}}\right)}{\log\left(\frac{1}{\rho_{1510}}\right) + \log\left(\frac{1}{\rho_{1680}}\right)}$$

Equation 14: Normalized Difference Nitrogen Index

The value of this index ranges from 0 to 1. The common range for green vegetation is 0.02 to 0.1.

5.2.5. Dry or Senescent Carbon Indices

The dry or senescent carbon VIs are designed to provide an estimate of the amount of carbon in dry states of lignin and cellulose. Lignin is a carbon-based molecule used by plants for

structural components; cellulose is primarily used in the construction of cell walls in plant tissues. Dry carbon molecules are present in large amounts in woody materials and senescent, dead, or dormant vegetation. These materials are highly flammable when dry. Increases in these materials can indicate when vegetation is undergoing senescence.

These VIs can be used for fire fuel analysis and detection of surface litter. They use reflectance measurements in the shortwave infrared range to take advantage of known absorption features of cellulose and lignin. These indices provide suspect results in wet environments, or when the dry materials are obscured by a green canopy.

Index	Index Description
Normalized Difference Lignin Index	Detects leaf lignin increases at the 1754 nm feature relative to 1680 nm canopy structure region.
Cellulose Absorption Index	Detects absorption features due to cellulose above 2000 nm.
Plant Senescence Reflectance Index	Uses a ratio of carotenoids to chlorophyll to detect onset and degree of plant senescence.

Table 13: Dry or senescent carbon indices

- **NORMALIZED DIFFERENCE LIGNIN INDEX**

The Normalized Difference Lignin Index (NDLI) is designed to estimate the relative amounts of lignin contained in vegetation canopies. Reflectance at 1754 nm is largely determined by lignin concentration of leaves, as well as the overall foliage biomass of the canopy. Together, leaf lignin concentration and canopy foliar biomass are combined in the 1750 nm range to predict total canopy lignin content. Applications include ecosystem analysis and detection of surface plant litter. The NDLI, defined by the following equation, is still highly experimental:

$$NDLI = \frac{\log\left(\frac{1}{\rho_{1754}}\right) - \log\left(\frac{1}{\rho_{1680}}\right)}{\log\left(\frac{1}{\rho_{1754}}\right) + \log\left(\frac{1}{\rho_{1680}}\right)}$$

Equation 15: Normalized Difference Lignin Index

The value of this index ranges from 0 to 1. The common range for green vegetation is 0.005 to 0.05.

- **CELLULOSE ABSORPTION INDEX**

The Cellulose Absorption Index (CAI) is a vegetation index indicating exposed surfaces containing dried plant material. Absorptions in the 2000 nm to 2200 nm range are sensitive to cellulose. Applications include crop residue monitoring, plant canopy senescence, fire fuel conditions in ecosystems, and grazing management. CAI is defined by the following equation:

$$CAI = 0.5\left(\frac{\rho_{2000} - \rho_{2200}}{\rho_{2100}}\right)$$

Equation 16: Cellulose Absorption Index

The value of this index ranges from -3 to more than 4. The common range for green vegetation is -2 to 4.

- **PLANT SENESCENCE REFLECTANCE INDEX**

The Plant Senescence Reflectance Index (PSRI) is designed to maximize the sensitivity of the index to the ratio of bulk carotenoids (for example, alpha-carotene and beta-carotene) to chlorophyll. An increase in PSRI indicates increased canopy stress (carotenoid pigment), the onset of canopy senescence, and plant fruit ripening. Applications include vegetation health monitoring, plant physiological stress detection and crop production and yield analysis. PSRI is defined by the following equation:

$$PSRI = \frac{\rho_{680} - \rho_{500}}{\rho_{750}}$$

Equation 17: Plant Senescence Reflectance Index

The value of this index ranges from -1 to 1. The common range for green vegetation is -0.1 to 0.2.

5.2.6. Leaf Pigments indices

The leaf pigment VIs are designed to provide a measure of stress-related pigments present in vegetation. Stress-related pigments include carotenoids and anthocyanins, which are

present in higher concentrations in weakened vegetation. These VIs do not measure chlorophyll, which is measured using the greenness indices. Carotenoids function in light absorption processes in plants, as well as in protecting plants from the harmful effects of high light conditions. Anthocyanins are water-soluble pigments abundant in newly forming leaves and leaves undergoing senescence. Applications for leaf pigment VIs include crop monitoring, ecosystem studies, analyses of canopy stress, and precision agriculture. Stress pigments can indicate the presence of vegetation stress, often before it is observable using the unaided eye. The VIs use reflectance measurements in the visible spectrum to take advantage of the absorption signatures of stress-related pigments.

Index	Index Description
Carotenoid Reflectance Index 1	Detects a relative difference in absorption indicative of changes in leaf total carotenoid concentration relative to chlorophyll concentration
Carotenoid Reflectance Index 2	Similar to CRI1, but uses a different wavelength to estimate the chlorophyll content.
Anthocyanin Reflectance Index 1	Changes in GREEN absorption relative to RED indicate leaf anthocyanins.
Anthocyanin Reflectance Index 2	A variant of the ARI1, which is sensitive to changes in GREEN absorption relative to RED, indicating leaf anthocyanins.

Table 14: Leaf Pigments indices

- **CAROTENOID REFLECTANCE INDEX 1**

The Carotenoid Reflectance Index 1 (CRI_1) is a reflectance measurement that is sensitive to carotenoid pigments in plant foliage. Higher CRI_1 values mean greater carotenoid concentration relative to chlorophyll. CRI_1 is defined by the following equation:

$$CRI_1 = \left(\frac{1}{\rho_{510}}\right) - \left(\frac{1}{\rho_{550}}\right)$$

Equation 18: Carotenoid Reflectance Index 1

The value of this index ranges from 0 to more than 15. The common range for green vegetation is 1 to 12.

- **CAROTENOID REFLECTANCE INDEX 2**

The Carotenoid Reflectance Index 2 (CRI_2) is a reflectance measurement that is sensitive to carotenoid pigments in plant foliage. CRI_2 is a modification of CRI_1, and provides better results in areas of high carotenoid concentration. Higher CRI_2 values mean greater carotenoid concentration relative to chlorophyll. CRI_2 is defined by the following equation:

$$CRI_2 = \left(\frac{1}{\rho_{510}}\right) - \left(\frac{1}{\rho_{700}}\right)$$

Equation 19: Carotenoid Reflectance Index 2

The value of this index ranges from 0 to more than 15. The common range for green vegetation is 1 to 11.

- **ANTHOCYANIN REFLECTANCE INDEX 1**

The Anthocyanin Reflectance Index 1 (ARI_1) is a reflectance measurement that is sensitive to anthocyanins in plant foliage. Increases in ARI_1 indicate canopy changes in foliage via new growth or death. ARI_1 is defined by the following equation:

$$ARI_1 = \left(\frac{1}{\rho_{550}}\right) - \left(\frac{1}{\rho_{700}}\right)$$

Equation 20: Anthocyanin Reflectance Index 1

The value of this index ranges from 0 to more than 0.2. The common range for green vegetation is 0.001 to 0.1.

- **ANTHOCYANIN REFLECTANCE INDEX 2**

The Anthocyanin Reflectance Index 2 (ARI_2) is a reflectance measurement that is sensitive to anthocyanins in plant foliage. Increases in ARI_2 indicate canopy changes in foliage via new growth or death. The ARI_2 is a modification of the ARI_1 which detects higher concentrations of anthocyanins in vegetation. ARI_2 is defined by the following equation:

$$ARI_2 = \rho_{800}\left[\left(\frac{1}{\rho_{550}}\right) - \left(\frac{1}{\rho_{700}}\right)\right]$$

Equation 21: Anthocyanin Reflectance Index 2

The value of this index ranges from 0 to more than 0.2. The common range for green vegetation is 0.001 to 0.1.

5.2.7. Canopy Water Content Indices

The canopy water content VIs are designed to provide a measure of the amount of water contained in the foliage canopy. Water content is an important quantity of vegetation because higher water content indicates healthier vegetation that is likely to grow faster and be more fire-resistant. Canopy water content VIs use reflectance measurements in the near-infrared and shortwave infrared regions to take advantage of known absorption features of water and the penetration depth of light in the near-infrared region to make integrated measurements of total column water content.

Index	Index Description
Water Band Index	Absorption intensity at 900 nm increases with canopy water content.
Normalized Difference Water Index	The rate of increase at 857 nm absorption relative to 1241 nm is a direct metric of total volumetric water content of vegetation.
Moisture Stress Index	Detects changes at 1599 nm absorption that is sensitive to the onset of moisture stress in vegetation
Normalized Difference Infrared Index	Absorption intensity at 1649 nm increases with canopy water content.

Table 15: Canopy Water Content Indices

- **WATER BAND INDEX**

The Water Band Index (WBI) is a reflectance measurement that is sensitive to changes in canopy water status. As the water content of vegetation canopies increases, the strength of the absorption around 970 nm increases relative to that of 900 nm. Applications include canopy stress analysis, productivity prediction and modelling, fire hazard condition analysis, cropland management, and studies of ecosystem physiology. WBI is defined by the following equation:

$$WBI = \frac{\rho_{900}}{\rho_{970}}$$

Equation 22: Water Band Index

The common range for green vegetation is 0.8 to 1.2.

- **NORMALIZED DIFFERENCE WATER INDEX**

The Normalized Difference Water Index (NDWI) is sensitive to changes in vegetation canopy water content because reflectance at 857 nm and 1241 nm has similar but slightly different liquid water absorption properties. The scattering of light by vegetation canopies enhances the weak liquid water absorption at 1241 nm. Applications include forest canopy stress analysis, leaf area index studies in densely foliated vegetation, plant productivity modelling, and fire susceptibility studies. NDWI is defined by the following equation:

$$NDWI = \frac{\rho_{857} - \rho_{1241}}{\rho_{857} + \rho_{1241}}$$

Equation 23: Normalized Difference Water Index

The value of this index ranges from -1 to 1. The common range for green vegetation is -0.1 to 0.4.

- **MOISTURE STRESS INDEX**

The Moisture Stress Index (MSI) is a reflectance measurement that is sensitive to increasing leaf water content. As the water content of leaves in vegetation canopies increases, the strength of the absorption around 1599 nm increases. Absorption at 819 nm is nearly unaffected by changing water content, so it is used as the reference. Applications include canopy stress analysis, productivity prediction and modelling, fire hazard condition analysis, and studies of ecosystem physiology. The MSI is inverted relative to the other water VIs; higher values indicate greater water stress and less water content. MSI is defined by the following equation:

$$MSI = \frac{\rho_{1599}}{\rho_{819}}$$

Equation 24: Moisture Stress Index

The value of this index ranges from 0 to more than 3. The common range for green vegetation is 0.4 to 2.

- **NORMALIZED DIFFERENCE INFRARED INDEX**

The Normalized Difference Infrared Index (NDII) is a reflectance measurement that is sensitive to changes in water content of plant canopies. The NDII uses a normalized difference formulation instead of a simple ratio, and the index values increase with increasing water content. Applications include crop agricultural management, forest canopy monitoring, and vegetation stress detection. NDII is defined by the following equation:

$$NDII = \frac{\rho_{819} - \rho_{1649}}{\rho_{819} + \rho_{1649}}$$

Equation 25: Normalized Difference Infrared Index

The value of this index ranges from -1 to 1. The common range for green vegetation is 0.02 to 0.6.

6. Use of multispectral imagery to obtain acidity and brix maps

6.1. Image preparation

For the imagery analysis and study, I have used the software: ENVI version 4.2, year 2005, ERDAS IMAGINE version 8.7 year 2003, and ARCVIEW GIS version 3.2, year 1999. The process followed for the image preparation has been:

- Radiometric correction and data units change
- Projection and coordinates changes. Georeferencing.
- Orthorectification by control points insertion

6.1.1. Radiometric correction and data units change

One of the top radiometric priorities of the high-spatial resolution, commercial remote sensing industry is to achieve a superior level of image quality in all imagery products. Errors in detector gain and offset correction during product generation create noticeable image artefacts such as banding and streaking that degrade the overall image quality.

Banding and streaking can be minimized by relative radiometric calibration, however, this calibration is only a temporary solution as the gain and offset of each detector will drift over time.

The next figure shows an example. The top half of the figure is a raw image spanning the boundary between detector chip assemblies (DCA) two and three of the blue band. Banding can be seen where the right side of the image is brighter than the left side. Also, several vertical streaks are visible. When a radiometric correction is applied (bottom half of the figure), the banding and streaking are minimized to create a seamless image devoid of visible artefacts.

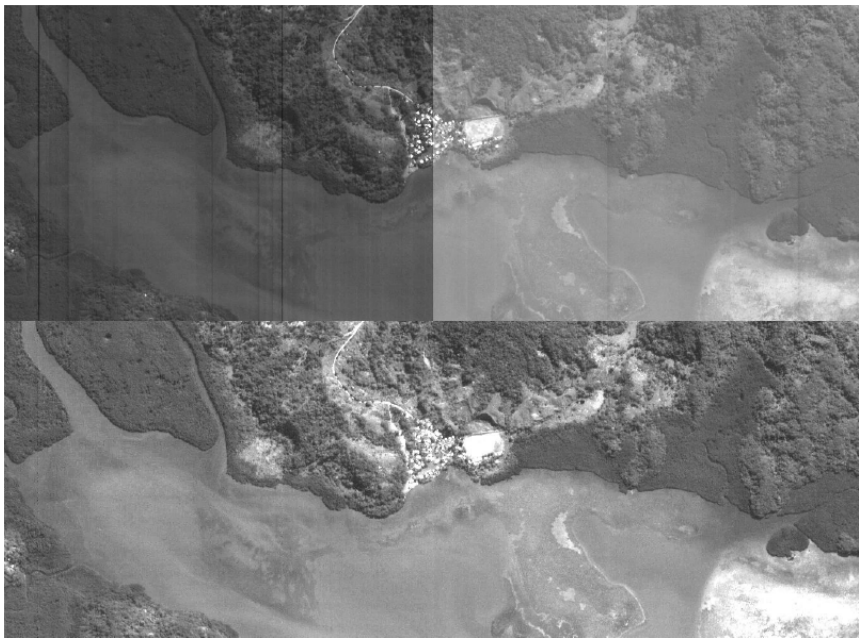

Image 7: Example of QuickBird imagery radiometric correction

The exact mathematical process followed to apply the radiometric correction to the images can be found on document *"QuickBird relative radiometric performance and on-orbit long term trending"*, Keith S. Krause, Earth Observing Systems XI SPIE Vol. 629 (2006).

It is also necessary to change the range of the data values, changing from the distribution standard (relative radiance) to absolute radiance. The units are converted

$$\text{from}\left[\frac{W}{m^2 \cdot str}\right] \text{ into}\left[\frac{\mu W}{cm^2 \cdot nm \cdot str}\right].$$

The following nominal bandpass widths are used:

- Pan band: 398 nm
- Multispectral Band 1 (Blue): 68 nm
- Multispectral Band 2 (Green): 99 nm
- Multispectral Band 3 (Red): 71 nm
- Multispectral Band 4 (NIR): 114 nm

As a practical method, it is possible to use of the ENVI implementation of this algorithm, accessible from *Basic Tools* → *Pre-processing Utilities* → *Calibration Utilities* → *QuickBird Radiance*. The calibration is performed using the calibration factors in the QuickBird metadata file (the absCalFactor in the .imd file), and the gain factors that were applied can be found in the ENVI Header file of the calibrated image.

6.1.2. Projection and coordinates changes

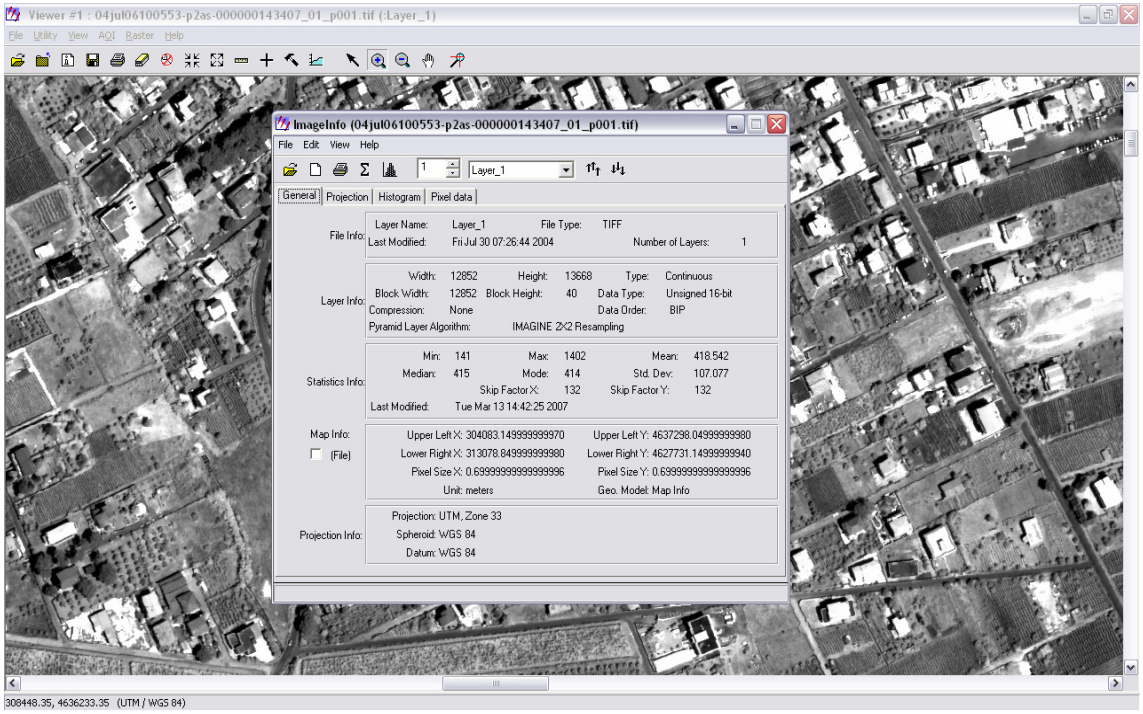

Figure 13: ERDAS header information dialog, where the chosen projection, spheroid and datum are showed.

Before applying georeferencing, it is necessary to establish the projection system to which the image belongs, choosing the one that best represents the study zone. The standard projection system in the firm where I have done this project is the UTM, and the spheroid WGS 84. The study zone, Frascati, corresponds with the quadrant 33 north.

The Universal Transverse Mercator (UTM) coordinate system is a grid-based method of specifying locations on the surface of the Earth. It is used to identify locations on the earth, but differs from the traditional method of latitude and longitude in several respects. The UTM system is not a single map projection. The system instead employs a series of sixty zones, each of which is based on a specifically defined Transverse Mercator projection.

The UTM system divides the surface of the Earth between 80° S latitude and 84° N latitude into 60 zones, each 6° of longitude in width and centred over a meridian of longitude. Zones are numbered from 1 to 60. Zone 1 is bounded by longitude 180° to 174° W and is centred on the 177th West meridian. Zone numbering increases in an easterly direction.

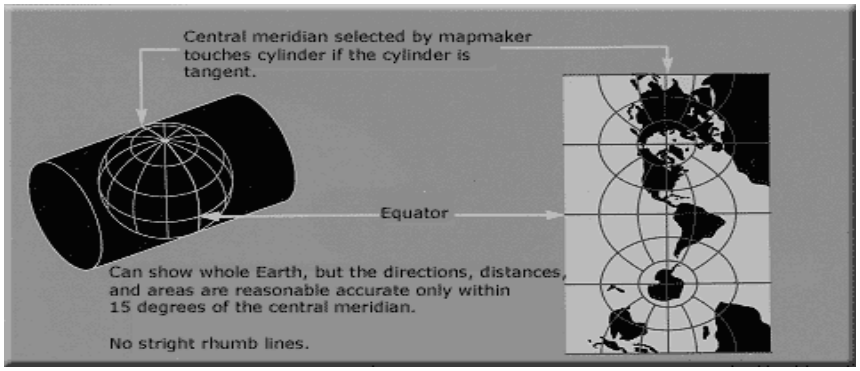

Figure 14: UTM description

Each of the 60 longitude zones in the UTM system is based on a Transverse Mercator projection, which is capable of mapping a region of large north-south extent with a low amount of distortion. By using narrow zones of 6° in width, and reducing the scale factor along the central meridian to 0.9996, (a reduction of 1:2500) the amount of distortion is held below 1 part in 1,000 inside each zone. Distortion of scale increases to 1.0010 at the outer zone boundaries along the equator.

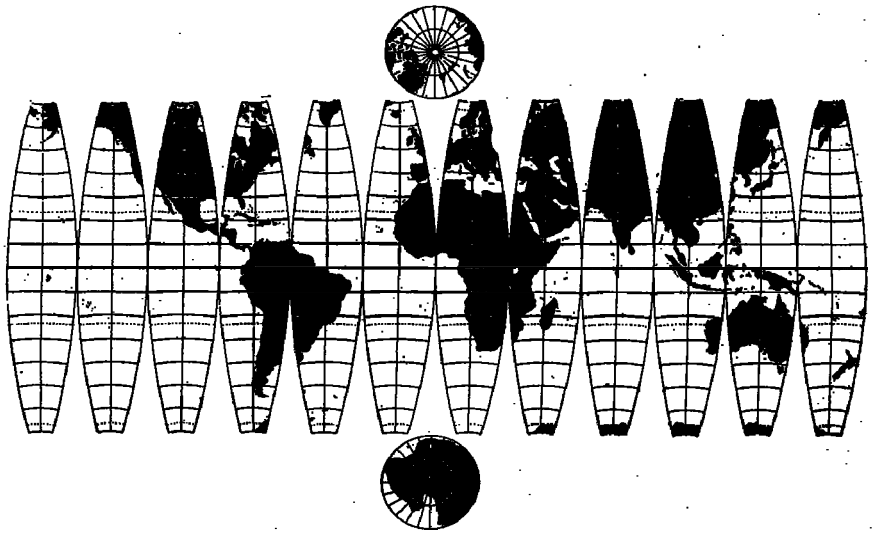

Figure 15: Example image of UTM with 12 divisions. The real has 60.

The reduction in the scale factor along the central meridian creates two lines of true scale located approximately 180 km on either side of (and approximately parallel to) the central meridian. The scale factor is too small inside these lines and too large outside of these lines, but the overall distortion scale inside the entire zone is minimized.

The UTM system also segments each longitude zone into 20 latitude zones. Each latitude zone is 8 degrees high, and is lettered starting from "C" at 80° S, increasing up the English alphabet until "X", omitting the letters "I" and "O" (because of their similarity to the digits one and zero). The last latitude zone, "X", is extended an extra 4 degrees, so it ends at 84° N latitude, thus covering the northern most land on Earth. Latitude zones "A" and "B" do exist, as do zones "Y" and Z". They cover the western and eastern sides of the Antarctic and Arctic regions respectively. A convenient trick to remember is that the letter "N" is the first letter in the northern hemisphere, so any letter coming before "N" in the alphabet is in the southern hemisphere, and any letter "N" or after is in the northern hemisphere.

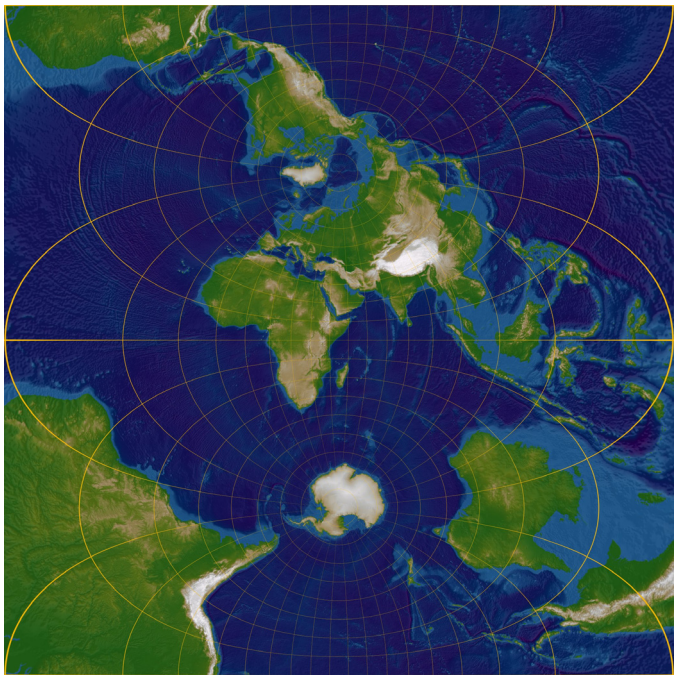

Figure 16: World Map in Universal Transverse Mercator projection

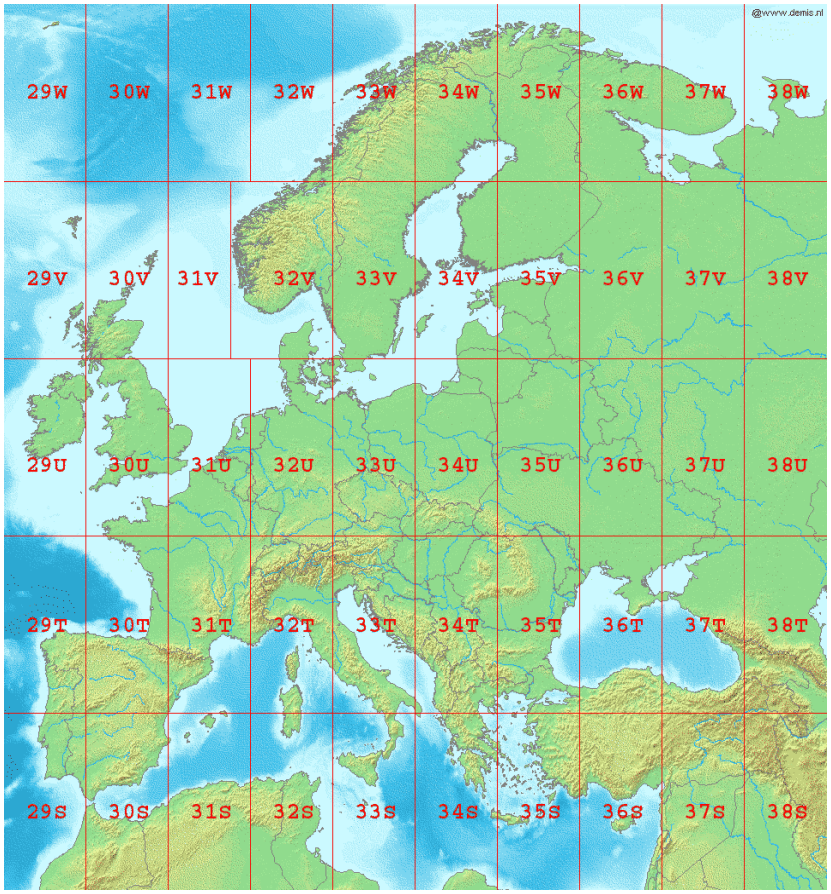

Figure 17: Europe division in UTM zones

These longitude and latitude zones are uniform over the globe, except in two areas. One of them is the southwest coast of Norway, where the UTM zone 32V is extended further west, and the zone 31V is correspondingly shrunk to cover only open water. In the next figure is also shown that the study area of this project corresponds with zone 33T.

Calculation of a map projection requires definition of the spheroid (or ellipsoid) in terms of the length of axes and eccentricity squared (or radius of the reference sphere). Several principal spheroids are in use by one or more countries. Differences are due primarily to calculation of the spheroid for a particular region of the Earth's surface. Only recently have satellite tracking data provided spheroid determinations for the entire Earth. However, these spheroids may not give the best fit for a particular region.

The spheroid used in this project is WGS-84 (World Geodetic System 1984), a recent recalculation of the WGS-72, and with these values:

- Sphere semi-major axis: 6378137.0
- Sphere semi-minor axis: 6356752.31424517929

6.1.3. Orthorectification and georeferencing by control points insertion

Digital satellite images and aerial photographs play an important role in general mapping, as well as GIS data acquisition and visualization. First, they help provide a solid visual effect. Many people are more able to put spatial concepts into perspective when they see photos. In addition, the secondary and perhaps more vital role is to provide a basis for gathering spatial information. Examples of this are features such as roads, vegetation, and water. Before this information can be gathered in a manner that is useful for a mapping or GIS system, the satellite image data or aerial photographs must be prepared in a way that removes distortion from the image. This process is called orthorectification. Without this process, you wouldn't be able to do such functions as make direct and accurate measurements of distances, angles, positions, and areas.

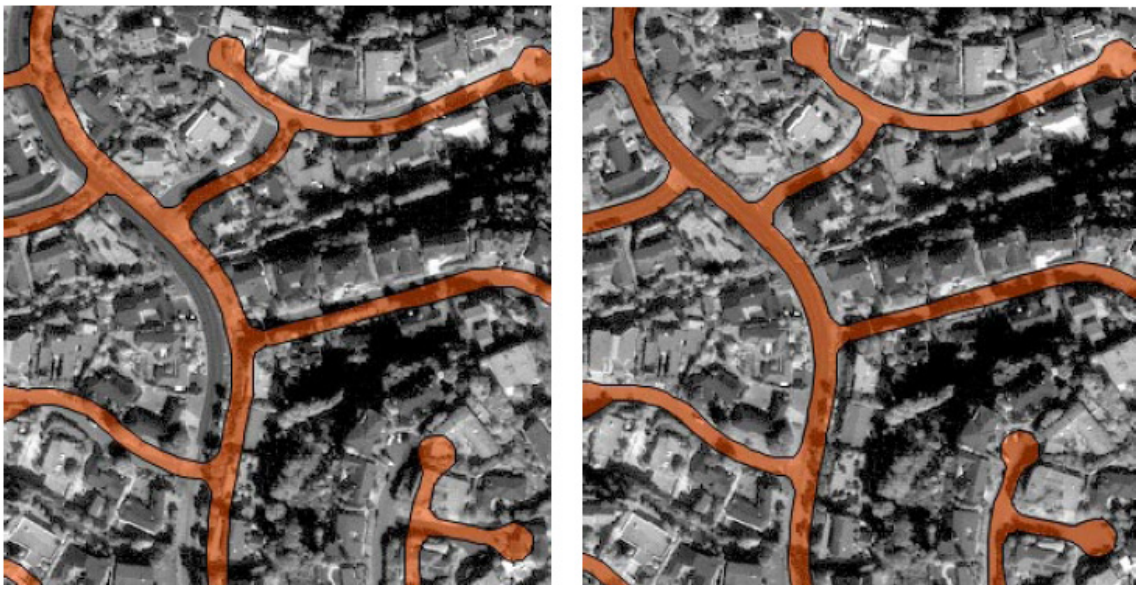

Image 8: Differences between original and orthorectified images when overlaid with a planimetric street vector

The topographical variations in the surface of the earth and the tilt of the satellite or aerial sensor affect the distance with which features on the satellite or aerial image are displayed. The more topographically diverse the landscape is, the more distortion inherent in the photograph.

Image data acquired by airborne and satellite image sensors are affected by systematic sensor and platform-induced geometry errors, which introduce terrain distortions when the image sensor is not pointing directly at the Nadir location of the sensor.

Terrain displacement can be hundreds of meters. For example, if the IKONOS satellite sensor acquires image data over an area with a kilometre of vertical relief, with the sensor having an elevation angle of 60° (30° from Nadir), the image product will have nearly 600 meters of terrain displacement. Additional terrain displacement can result from errors in setting the reference elevation. Low elevation angles of images, imperfect terrain models, and variability of sensor azimuth and elevation angles within an image limit accuracy potential if image orthorectification is attempted. For this reason, when new high resolution satellite image data is acquired over rough terrain, high elevation angles of the sensor is required.

Georeferencing refers to the process of assigning map coordinates to image data. The image data may already be projected onto the desired plane, but not yet referenced to the proper coordinate system. Rectification, by definition, involves georeferencing, since all map projection systems are associated with map coordinates. Image-to-image registration involves

georeferencing only if the reference image is already georeferenced. Georeferencing, by itself, involves changing only the map coordinate information in the image file. The grid of the image does not change.

However, there are some disadvantages. During rectification, the data file values of rectified pixels must be resampled to fit into a new grid of pixel rows and columns. Although some of the algorithms for calculating these values are highly reliable, some spectral integrity of the data can be lost during rectification. If map coordinates or map units are not needed in the application, then it may be wiser not to rectify the image. An unrectified image is more spectrally correct than a rectified image.

- **THE POLYNOMIAL TRANSFORMATION**

The ground control points (GCPs) are specific pixels in an image for which the output map coordinates (or other output coordinates) are known. GCPs consist of two (X,Y) pairs of coordinates:

- Source coordinates—usually data file coordinates in the image being rectified

- Reference coordinates—the coordinates of the map or reference image to which the source image is being registered

The term map coordinates is sometimes used loosely to apply to reference coordinates and rectified coordinates. These coordinates are not limited to map coordinates. For example, in image-to-image registration, map coordinates are not necessary.

In the polynomial method, polynomial equations are used to convert source file coordinates (X,Y) to rectified map coordinates (X_0,Y_0). Depending upon the distortion in the imagery, the number of GCPs used, and their locations relative to one another, complex polynomial equations may be required to express the needed transformation.

$$x_0 = \sum_{i=0}^{t}\sum_{j=0}^{i} a_k \cdot x^{i-j} \cdot y^j \qquad y_0 = \sum_{i=0}^{t}\sum_{j=0}^{i} b_k \cdot x^{i-j} \cdot y^j$$

$$k = \frac{i\cdot(i+j)}{2} + j$$

Equation 26: Generic t-order polynomial functions used to rectify an image

In these equations, t is the polynomial order, and a_k and b_k are coefficients. A transformation matrix is computed from the GCPs. The matrix consists of coefficients that are used in polynomial equations to convert the coordinates. The size of the matrix depends upon the order of transformation. The goal in calculating the coefficients of the transformation matrix is to derive the polynomial equations for which there is the least possible amount of error when they are used to transform the reference coordinates of the GCPs into the source coordinates. It is not always possible to derive coefficients that produce no error. For example, in Graphic 8 below, GCPs are plotted on a graph and compared to the curve that is expressed by a polynomial.

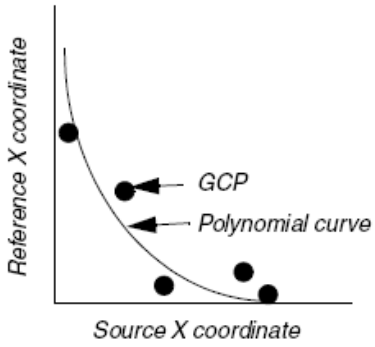

Graphic 8: Example of a polynomial adjust of some GCP

The next figure illustrates the effect of some possible outputs when applying the transformation to the original image:

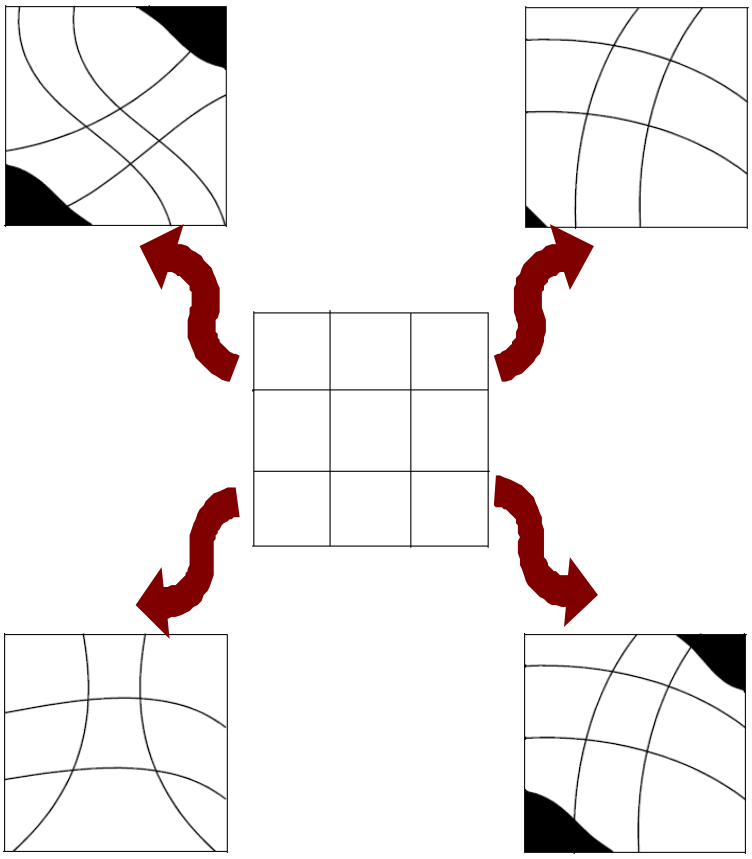

Figure 18: Some possible polynomial transformations

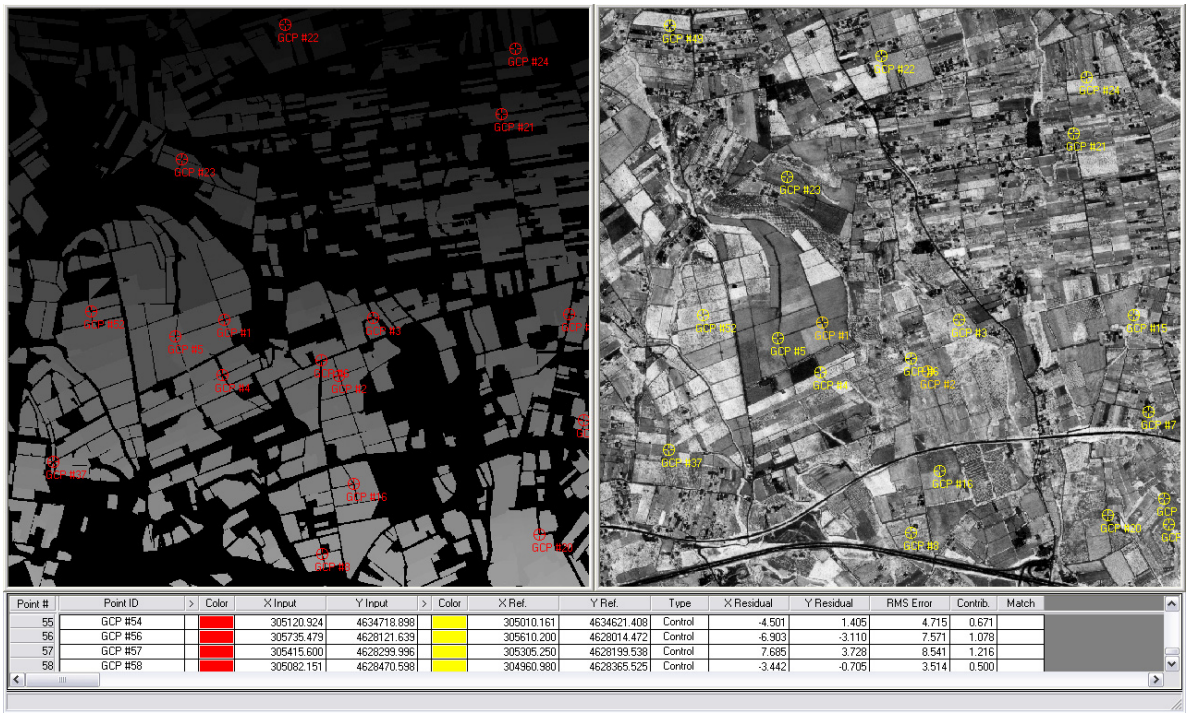

Figure 19: Example step of the process of entering GCPs in ERDAS

6.2. IVN processing

The process followed to obtain the IVN maps has kept three steps. The first is to get the NDVI maps of the study zone from the multispectral imagery available. On the second stage, from the cadastral data of the zone, we have extracted a vectorial image with the density of each vineyard. Finally we have to relate these two images to achieve the final IVN map with this equation:

$$IVN = \frac{\frac{R_{NIR} - R_{RED}}{R_{NIR} + R_{RED}}}{D} = \frac{NDVI}{D}$$

Equation 27: Process followed to obtain IVN, where D is the canopy density of the considered field

6.2.1. NDVI calculation

On the duration of this project, we have used two different ways to calculate the NDVI maps from the multispectral imagery available. The first one is using IDL programming, and the other is employing the ENVI Band Math tool. The first option is more versatile, and we can introduce all the changes that we want, whereas the second way is faster, handier and easier.

- **FIRST METHOD**

The first option consists on writing a little IDL program which calculates the NDVI pixel per pixel. For the programming with IDL I've used the interface IDL for Windows, version 6.2, distributed with ENVI. The first program written has been:

```
PRO GEOVINE
file_path=dialog_pickfile(filter='*.tif')

temp=strsplit(file_path, '\',/extract)
dim=size(temp,/dimension)
name=temp(dim(0)-1)
image=read_tiff(file_path,GEOTIFF=geo_tag)
```

```
dimension=size(image,/dimension)
ndvi=fltarr(dimension(1),dimension(2))
band1=fltarr(dimension(1),dimension(2))
band2=fltarr(dimension(1),dimension(2))
band3=fltarr(dimension(1),dimension(2))
band4=fltarr(dimension(1),dimension(2))

FOR i=0, dimension(1)-1 DO BEGIN
        band1(i,*)=image(0,i,*)
        band2(i,*)=image(1,i,*)
        band3(i,*)=image(2,i,*)
        band4(i,*)=image(3,i,*)
ENDFOR

nozero=where( band4 ne 0)
zero=where(band3 eq 0)

;VEGETATION INDEX
ndvi(*)=(band4(*)-band3(*))/(band3(*)+band4(*))

file_out=dialog_pickfile(filter='*.tif',/write)
write_tiff, file_out+'.tif', ndvi,/float

END
```

This IDL program takes a multispectral image and assigns it to the variable *image*. Then, reads each band from *image* and assigns them to the variables *bandX*, with X symbolizing the number of each band (0=blue, 1=green, 2=red, 3=infrared). Afterwards, it does the calculation of the NDVI with the definition of the index, to finally save it as a tiff image.

The obtained image will be the NDVI, with data range between -1 and 1, and will be naturally represented on greyscale colours, with the black for the -1 and the white for the 1. Below is showed a part of the studied zone and the NDVI map obtained with this first method.

Image 9: Zone selected to see the NDVI results of cultivars, houses and roads

Image 10: NDVI of the same zone obtained with the first method

In images 9 to 11 three points are clearly visible:

- ❶: Zone with cultivated field and quite leafy vegetation, high NDVI values.
- ❷: Field probably cultivated but without vegetation, NDVI results lower.
- ❸: Building. Minimal NDVI values.

Since the human eye is not capable to differentiate more than 20 or 30 levels of grey, the density slicing technique is generally used to represent this kind of images. Thus, all the grey levels are converted in a full-coloured range, to convert the image more comprehensible.

This can be done adding some lines to the IDL program showed before. In this case, the range that we have used varies from blue (low levels of NDVI) to red (high levels of NDVI: leafy vegetation). The program then becomes:

```
PRO GEOVINE
file_path=dialog_pickfile(filter='*.tif')

temp=strsplit(file_path, '\',/extract)
dim=size(temp,/dimension)
name=temp(dim(0)-1)
image=read_tiff(file_path,GEOTIFF=geo_tag)

dimension=size(image,/dimension)
ndvi=fltarr(dimension(1),dimension(2))
band1=fltarr(dimension(1),dimension(2))
band2=fltarr(dimension(1),dimension(2))
band3=fltarr(dimension(1),dimension(2))
band4=fltarr(dimension(1),dimension(2))

FOR i=0, dimension(1)-1 DO BEGIN
        band1(i,*)=image(0,i,*)
        band2(i,*)=image(1,i,*)
        band3(i,*)=image(2,i,*)
        band4(i,*)=image(3,i,*)
ENDFOR

nozero=where( band4 ne 0)
```

```
zero=where(band3 eq 0)

;VEGETATION INDEX
ndvi(*)=(band4(*)-band3(*))/(band3(*)+band4(*))

good=where(ndvi ge -1 or ndvi le 1,complement=bad)
top_value=max(ndvi(good), min=bottom_value)

;SAVING COLOUR IMAGE
ndvi=temporary(fix((!D.TABLE_SIZE-1)*(ndvi(*,*)-
bottom_value)/(top_value-bottom_value)))

ared=bindgen(256)
agreen=bindgen(256)
ablue=bindgen(256)

Obj = OBJ_NEW('IDLgrPalette', aRed, aGreen, aBlue )
Obj->IDLgrPalette::LoadCT, 27
Obj->IDLgrPalette::GetProperty,Blue_values=ablue
Obj->IDLgrPalette::GetProperty,Red_values=ared
Obj->IDLgrPalette::GetProperty,Green_values=agreen

file_out=dialog_pickfile(filter='*.tif',/write)
write_tiff, file_out+'.tif',
ndvi,GEOTIFF=geo_tag,red=ared,green=agreen,blue=ablue
obj_destroy,Obj

END
```

Applying the new program to the same zone than before, we obtain this more understandable NDVI map:

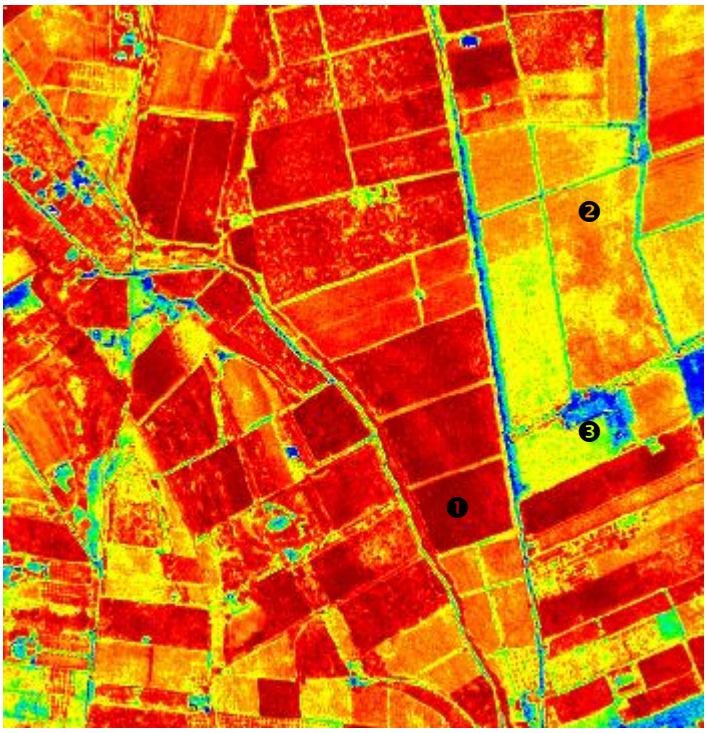

Image 11: NDVI of the same zone applying the second program proposed

- **SECOND METHOD**

The second method to obtain NDVI is the use of Band Math tool in ENVI, in the menu *Basic Tools*. With this utility, it is possible to directly do a mathematical calculation of an image without programming it on IDL.

The formula that we must introduce to do the NDVI calculation is the following. Of course, we must assign the band 4 (infrared) to the variable *b1* and the band 3 (red) to the variable *b2*.

$$\frac{float(b1) - float(b2)}{float(b1) + float(b2)}$$

Equation 28: Formula to introduce in ENVI Band Math to calculate NDVI

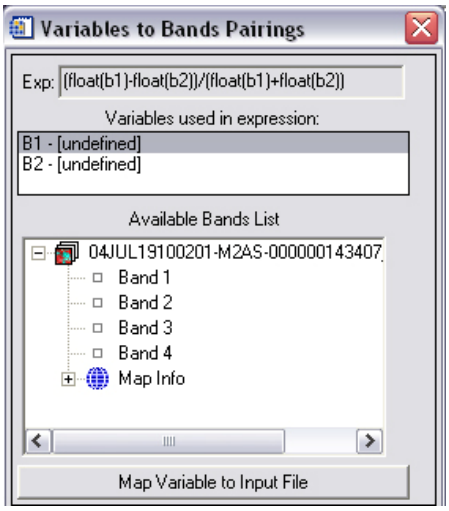

Figure 20: ENVI window to assign variables to bands in Band Math

The resulting image is identical to the one obtained with the IDL program, seen on Image 10. Furthermore, ENVI has various ways to apply the density-slicing technique, and thus it's not necessary to program it on IDL as long as you don't want to do your own changes.

One of the ways, the easier, is to apply the colour tables pre-programmed on ENVI. You choose a colour table and the stretch bottom or up values to obtain the desired final image. To do this, in the Image Window, you must do *Tools* → *Colour Mapping* → *ENVI Colour tables*.

Other way, more configurable, is *Tools* → *Colour Mapping* → *Density Slice.* There, it's possible to choose the colours you want and the data range that represent.

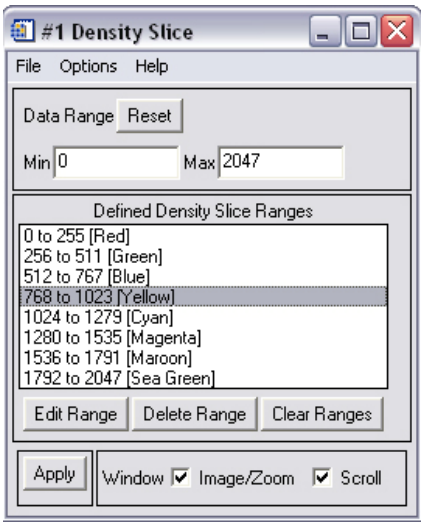

Figure 21: ENVI density slice window to select colours and ranges

To better adjust the ranges, it is very advisable to perform a statistical analysis before. To see more information of this kind of analysis, see Section 7.2: Statistical study, on page 110.

In Image 12 is presented an example zone of the study area, where it has been calculated the NDVI with the Band Math tool and finally it has been applied the colour scheme "Green/White Linear", but reversing the predefined ranges, with the scope of assign the green colour to the zones with high NDVI (dense vegetation), and the white to the low NDVI (roads, buildings, etc…).

Image 12: NDVI zone obtained with Band Math, and applying the Green/White linear colour scheme

6.2.2. Shape data preparation and density development

The second step when calculating IVN maps consists on extracting the density of each field and linking it to the original image. This is possible with the cadastral data that the city council has available.

How has been studied before, in section 4.2.3, the shapefile does not only contain the shape of each field, but also a big amount of information. For example, this file allows us to

know, of each field, data as the field number, the city council where it has been inscribed, the area, the perimeter, the number of cultivated plants, the density, the register year, the type of wine installation (*filare, tendone …)*, etc…

Attributes of Unità_vitate_doc.shp

Particella	Shape	Comune_nom	Area	Perimeter	Num_ceppi	Supvit_mq	Density	Sup_map	Anno_dic	Anno_imp
00315	Polygon	Roma	398.325390000000030	83.324349999999995	104	390.00	2667	398.00	1998	1993
00303	Polygon	Roma	601.992100000000050	125.395880000000010	150	600.00	2500	601.00	1998	1983
00140	Polygon	Frascati	1617.951360000000000	200.481519999999990	1264	1618.00	7812	1615.00	1998	1956
00338	Polygon	Roma	1767.722790000000000	267.652769999999980	884	1768.00	5000	1765.00	1998	1978
00578	Polygon	Frascati	2687.127810000000000	253.182199999999990	490	3062.00	1600	2682.00	1998	1974
00412	Polygon	Roma	1202.315250000000100	219.296280000000000	700	1260.00	5556	1200.00	1998	1995
00324	Polygon	Roma	340.399890000000030	79.639399999999995	106	395.00	2684	340.00	1998	1993
00413	Polygon	Roma	42.650820000000003	31.536860000000001	25	45.00	5556	43.00	1998	1995
00004	Polygon	Roma	6850.675059999999600	349.803220000000010	913	7680.00	1189	6839.00	1998	1980
01150	Polygon	Roma	6471.766529999999900	331.839990000000000	3398	6795.00	5001	6461.00	1998	1965
00154	Polygon	Frascati	4149.357119999999700	329.147969999999990	664	4149.00	1600	4142.00	1998	1996
00311	Polygon	Roma	519.020359999999980	98.106049999999996	231	519.00	4451	518.00	1998	1963
00177	Polygon	Frascati	2415.193299999999900	219.727250000000000	483	2415.00	2000	2411.00	1998	1992
00323	Polygon	Roma	352.577519999999990	81.755420000000001	94	355.00	2648	352.00	1998	1993
00001	Polygon	Roma	1997.641270000000100	237.704990000000010	357	2234.00	1598	1994.00	1998	1975
00107	Polygon	Frascati	339.504920000000030	90.648679999999999	106	357.00	2969	339.00	1998	1996
00486	Polygon	Roma	1688.330470000000100	163.518000000000000	1103	1688.00	6534	1685.00	1998	1965
00383	Polygon	Roma	521.575100000000020	103.307779999999990	100	530.00	1887	521.00	1998	1993
01150	Polygon	Roma	2521.812800000000200	241.909050000000010	1323	2645.00	5002	2517.00	1998	1965
00083	Polygon	Frascati	725.045589999999950	143.141789999999990	484	870.00	5563	724.00	1998	1980
00391	Polygon	Frascati	332.304590000000020	104.821659999999990	346	332.00	10422	332.00	1998	1940
00414	Polygon	Roma	44.350709999999999	36.725160000000002	14	44.00	3182	44.00	1998	1990
00397	Polygon	Roma	1152.253539999999900	338.344290000000000	1371	1535.00	8932	1536.00	1999	1968
00414	Polygon	Roma	48.297719999999998	34.575069999999997	28	50.00	5600	48.00	1998	1995
00412	Polygon	Roma	1441.672300000000000	230.674749999999990	444	1442.00	3079	1439.00	1998	1990
00135	Polygon	Frascati	5644.349290000000100	359.008940000000000	1763	5925.00	2976	5635.00	1998	1996
00340	Polygon	Roma	1422.641290000000000	255.401670000000000	712	1423.00	5004	1421.00	1998	1960
00347	Polygon	Roma	350.408279999999990	79.095259999999996	110	410.00	2683	350.00	1998	1993

Table 16: ARCGIS view of some cadastral dates on the shapefiles

Our goal is an image that represents a canopy density map of the test zone; this operation can be performed extracting some attributes from the database associated to each field. Obviously, the density is the same inside one field, because we don't have information about intra-field variable density, but this will be different from other field.

This is achievable this way:

- With ARCGIS, we have deleted all the other columns of information and leaving only the density. To do that, we have opened the shapefile attributes table and with *Table* → *Start editing,* it is possible to select the columns and delete them. After that, we must do *Table* → *Stop editing*, and save the changes. The column "Shape", with the type of shape (Polygon, line, point), shouldn't be deleted. Furthermore, we must also delete the registers that, because of any reason, are incoherent. For example, it would be ridiculous to calculate the IVN from a field whose density value according to the cadastral data is 65 vineyards per square meter… In general, we have considered correct a maximum of 2 or 3 vineyards per square meter, although the normal value is 0,3 or 0,4.

- In ERDAS, we have imported the resultant shapefile, which at this moment should have only two attribute columns (Shape and density). To do that, we use the tool Import/Export, and just before launch the process, we activate the checkbox *Create polygon topology and import polygon attributes*.

- At this moment, we have the file, that continues being vectorial, in arcinfo format. Now we have to change it to raster: in ERDAS, in the menu *Vector → Vector to Raster*. After selecting it, in the box *Convert Vector Layer to Raster Layer*, we must specify that the input types are polygons, the pixel size, and that we want a continuous output image, to allow ERDAS to fill in the fields, and not only the boundary. Also, it is here where we select the attribute that will done its value to the new raster image. We must select, obviously, Density. When we have done the import to ERDAS, there are some other attributes created, as Density# or Density-ID, that are identifiers and are not interesting for us; we must choose only "Density".

- The process has finished. A new raster image has been created, in format img. If we want it in other format, such as GeoTIFF or ENVI's hdr, we will change it with the ERDAS Import/Export utility again or with ENVI.

Below it is presented a zone of an image where this process has been applied, comparing it with the calculated NDVI for the same zone.

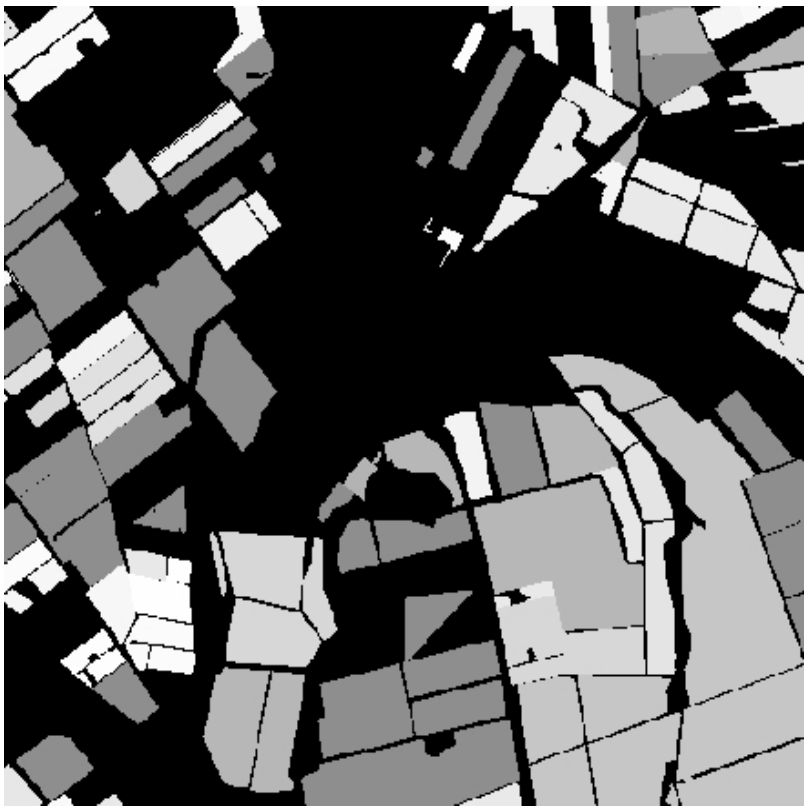

Image 13: Raster image of the density obtained.

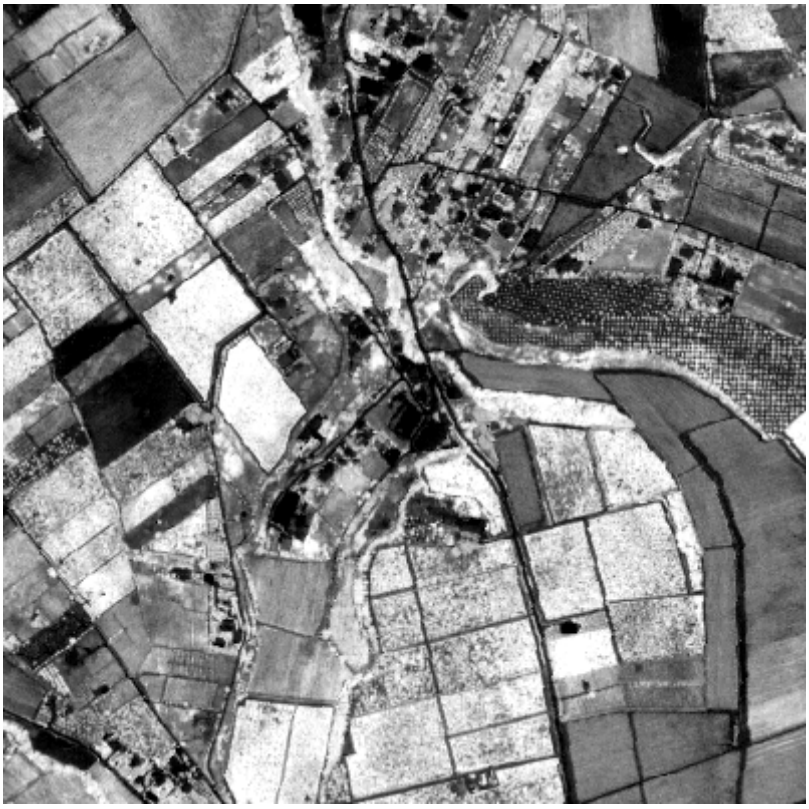

Image 14: NDVI of the same zone

6.2.3. Results

At this point we have the two images that we need to calculate the IVN map. On one hand, the NDVI, and on the other, the raster density image discussed before. Now we must link them to obtain the IVN. However, we must check again that the images are perfectly coregistered. If not, we must re-open the shapefile with ARCGIS and modify the fields that are not perfectly coregistered with the satellite image, and then apply again the method proposed before to obtain the raster image.

If all of this is correct, to obtain the IVN we must open the NDVI image and the density image, and then use the Band Math tool to divide them, as the definition of IVN requires (see Equation 28). As we can see in the Table 16, we must scale the density data to have it on square meter units, which corresponds to divide it by 10000.

$$\frac{b1*10000}{float(b2)}$$

Equation 29: Formula to introduce in ENVI Band Math to obtain the IVN map

In this case, we will assign the variable *b1* to the only band we have in the NDVI image, and the variable *b2* to the density. In the next two images, some zones of the resulting IVN image are showed. The second has been obtained applying the density-slicing technique.

Image 15: Detail of the obtained IVN map

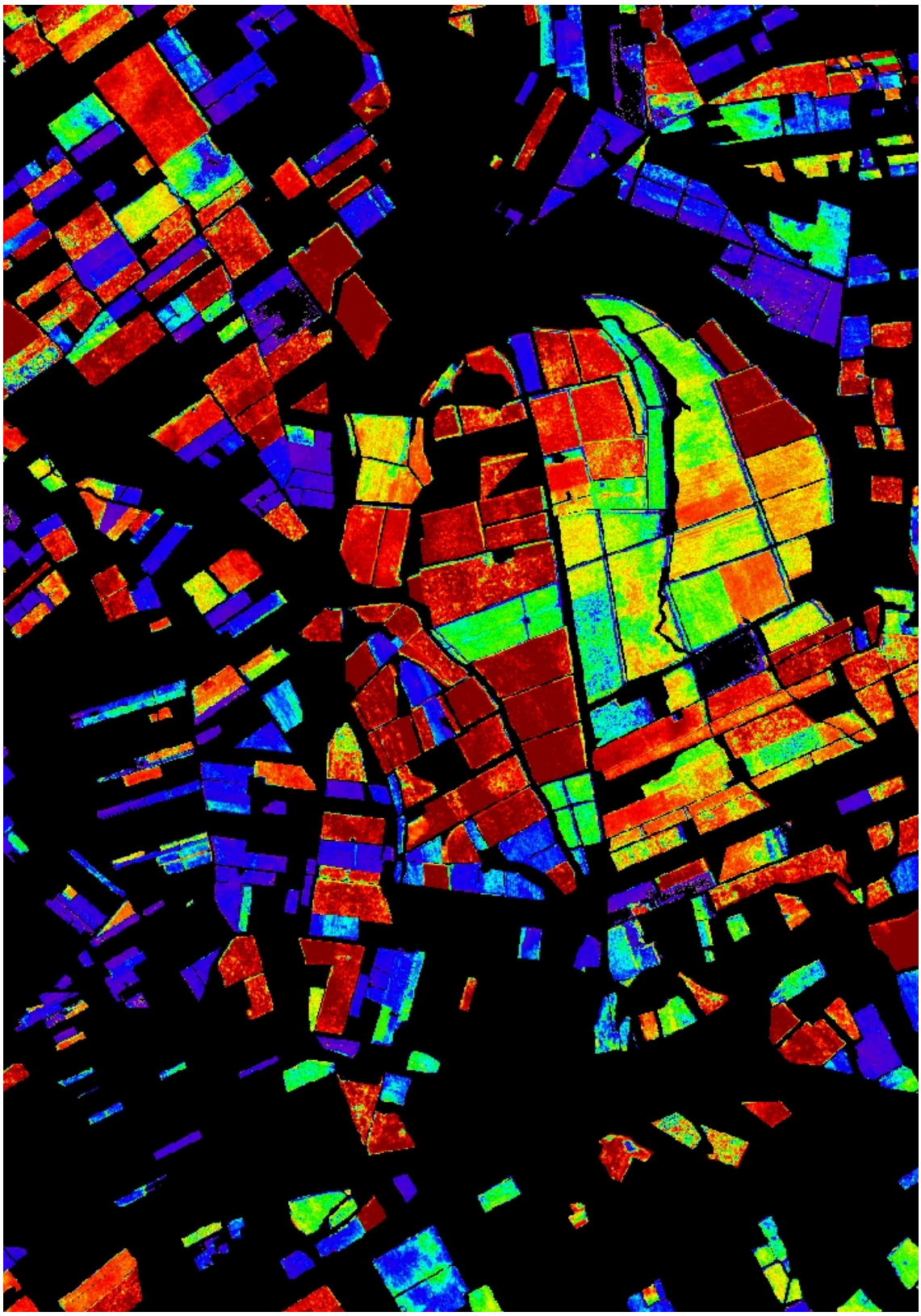

Image 16: Density slicing of the obtained image, with the violet representing low IVN values and the red high values.

6.3. Applications and pansharpening

It is possible to realize an analysis of the IVN maps obtained that will give us the opportunity to monitor some important crop parameters. Specifically, diverse studies have demonstrated that the brix grade, explained on section 3.2: Brix and its importance in crops, or the acidity, commented on 3.1: Acidity and its influence in wine, have good statistical correlation values with the enounced vegetation index.

However, first of doing it, we must delete the bottom values of the image. The black zones out of the vineyards have result in infinite pixel value. To make the analysis correctly, we must take them to the value zero. To do that, we must build a mask which has to include all the intra-field zones.

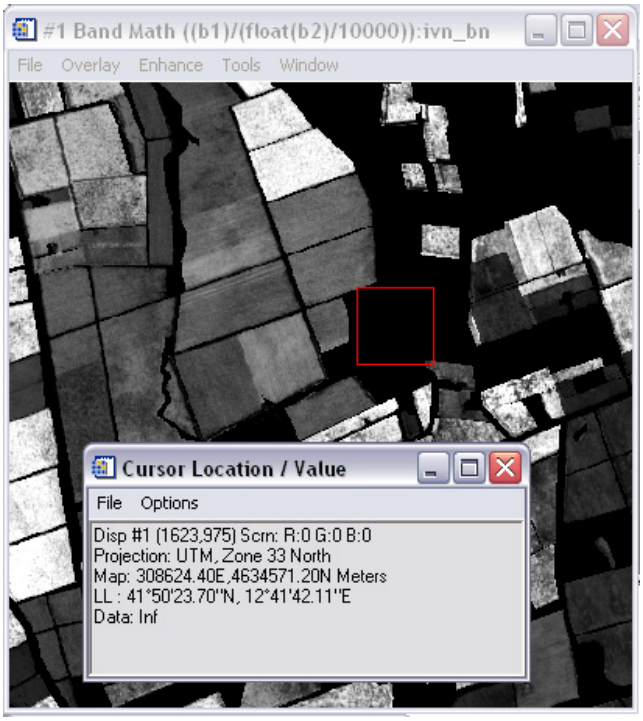

Figure 22: The IVN value in the intra-field zone has result infinite.

The process followed to correct this data has been:

- To build the mask in ENVI we must do *Basic Tools* → *Masking* → *Build Mask*. After that, instead of import data ranges or establish the values manually, we can do *Options* → *Mask Finite Values*, as we want to filter the zones with a non real number, and select

the IVN file. It is also necessary to verify first that the selected zones (those with the real value), are going to be masked as "active". To do that, we must check *Options* → *Selected Areas On*.[1]

- Once the mask is created, we must apply it. To do that in ENVI, we go to *Basic Tools* → *Masking* → *Apply Mask*, selecting the IVN file and the recently created mask. The value that we must specify to the masked pixels is 0.

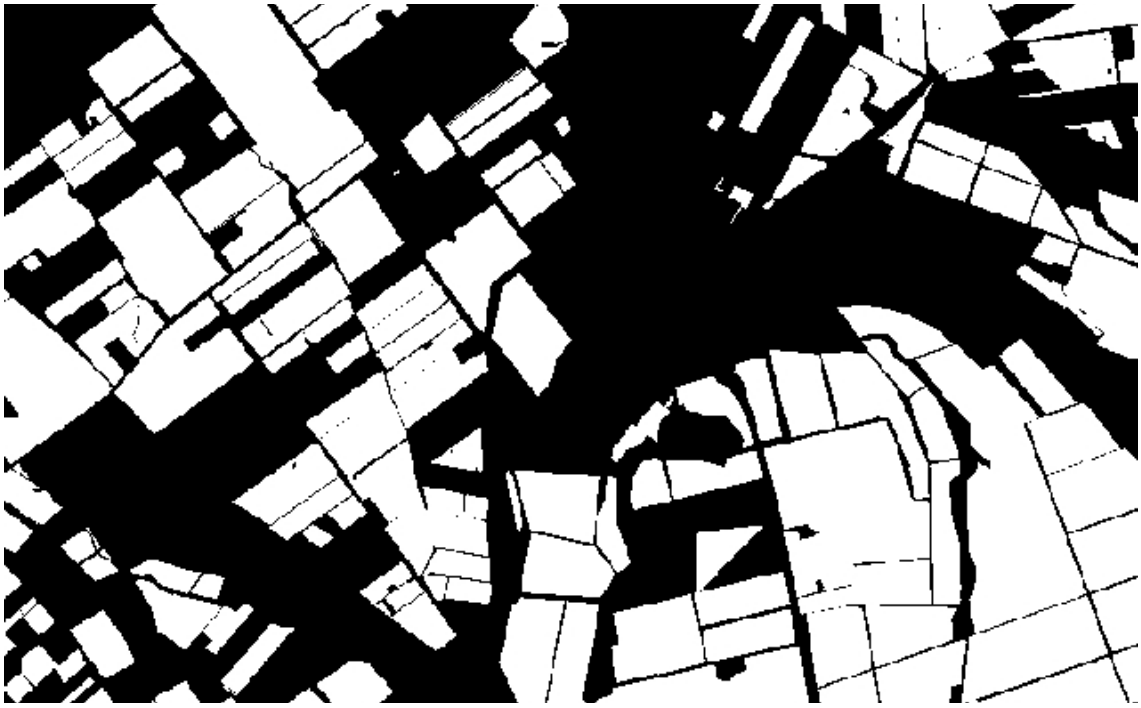

Image 17: Created mask to delete the zones with infinite or NaN values

6.3.1. Brix

According to the Franciacorta experience, exposed on *L.Brancadoro, O. Failla, P. Dosso y F. Serina "Use of satellite in precision agriculture: the Franciacorta experience", of VIth terroir international congress 2006*, or in *Ing. P. Rossi, Terradat, SRL "Viticoltura di precissione assistita da satellite" Workshop Citimap2006*, it is possible to establish the next relation between the Normalized Vegetation Index IVN and the brix grade with a great statistical result (R^2=0,73):

[1] As the masks are maps of ones and zeros that take up not so much memory space, are especially convenient to be stored in RAM; there is not need to save them on hard disk if we don't want to keep them.

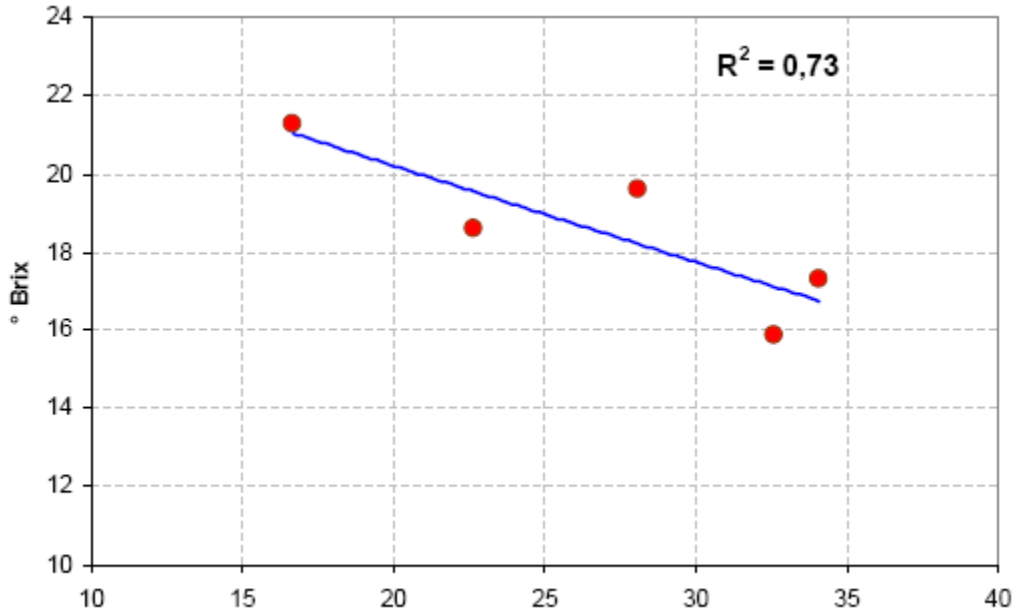

Graphic 9: Lineal relation obtained to calculate the Brix grade from the IVN map

Of this relation, we can obtain the following dependence formula, allowing the direct calculation of brix grade of grapes:

$$B = -0.24 \cdot IVN + 25$$

Equation 30: Lineal regression formula to obtain the brix grade from IVN index

The final step consists on the application of this formula to our image, for example with the Band Math tool of ENVI. Such as we have done in previous situations, it is better to apply a pseudo-colour scheme to appreciate correctly all the details. The next image corresponds to the map of the brix grade of the Frascati DOC vineyards:

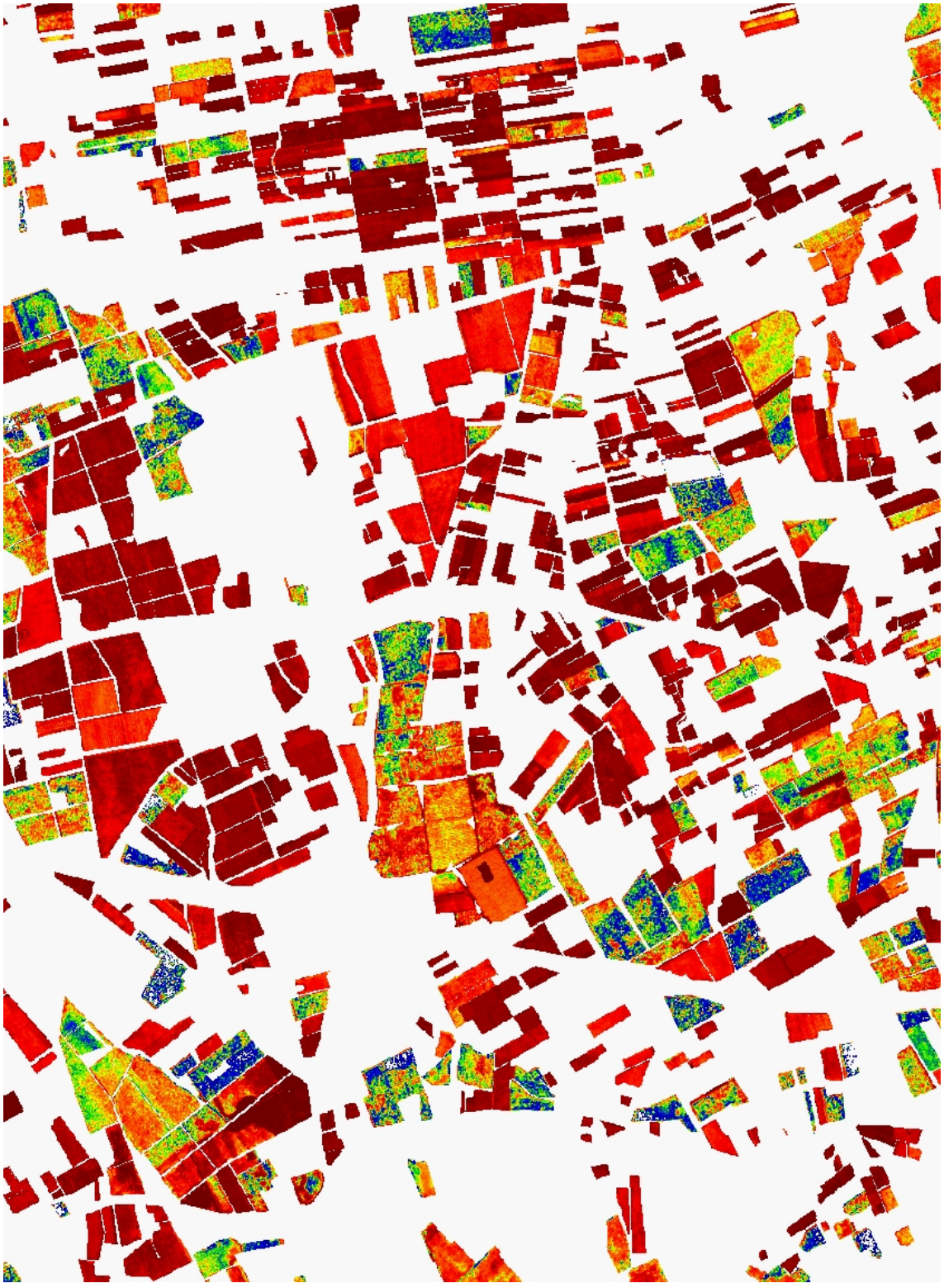

Image 18: FIRST RESULT, Brix grade of the grapes on Frascati DOC vineyards

6.3.2. Acidity

Attending to the acidity case, the same publications have demonstrated that it is also possible to correlate the IVN index with the acidity on vineyard grapes. In this case, the statistic values obtained are even better, reaching values as R^2=0,93.

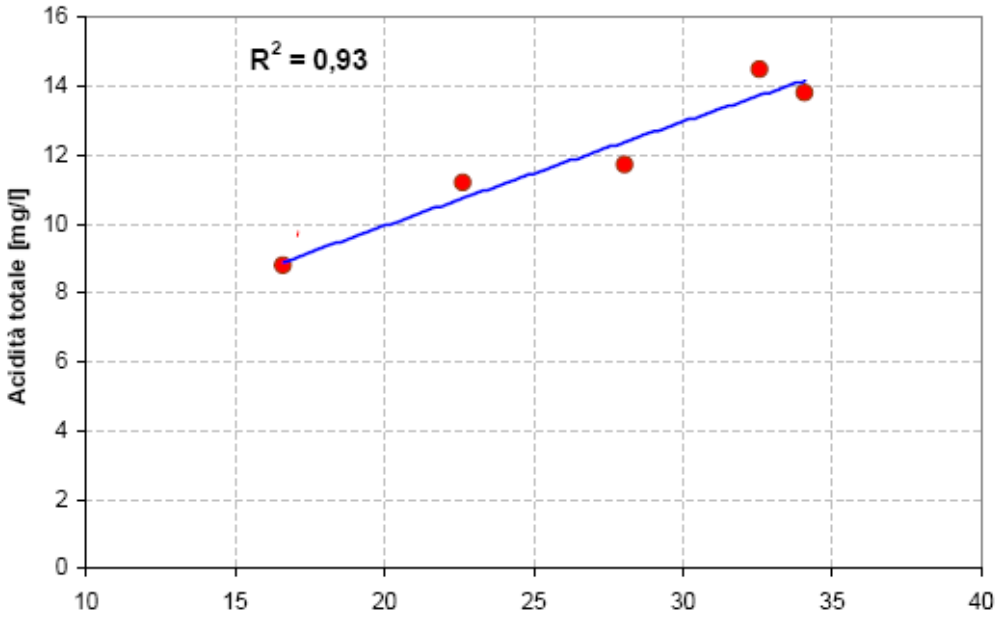

Graphic 10: Lineal relation obtained to calculate the Acidity grade from the IVN map

In this case, the equation obtained will be the following:

$$A = 0.314 \cdot IVN + 3.310$$

Equation 31: Lineal regression formula to obtain the acidity grade from IVN index

As in the brix study, we apply this equation to the IVN image using the Band Math tool in ENVI; as well we represent the image with a density slicing colour scheme to better appreciate the differences.

Below is presented the result map of the grape acidity in grapes of Frascati DOC Vineyards:

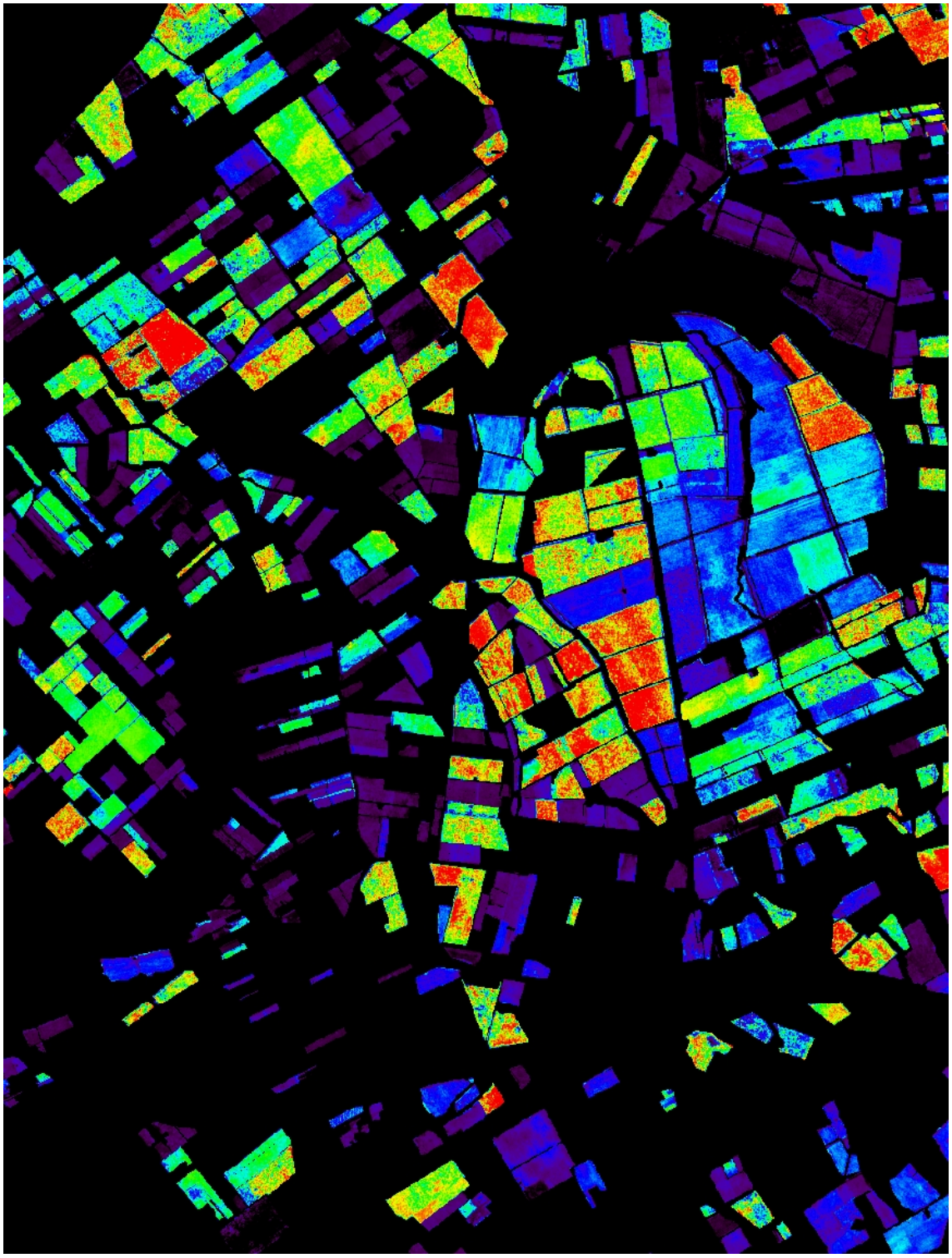

Image 19: SECOND RESULT, Acidity grade of the grapes on Frascati DOC vineyards

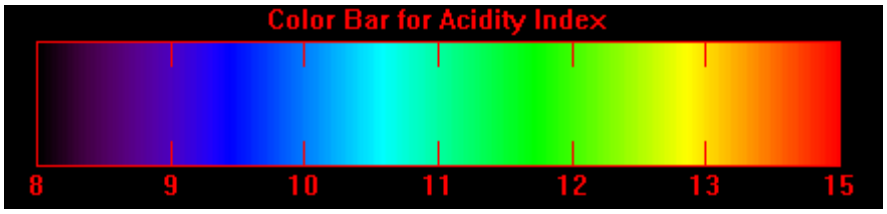

6.3.3. Pansharpening

Remote-sensing image fusion techniques aim at integrating the information conveyed by data acquired with different spatial and spectral resolution sensors. The most straightforward goal is photo-analysis, but also automated tasks such as features extraction and segmentation/classification have been found to benefit from fusion. In our case, we are going to use the pansharpening technique to allow a better visualization of intra-field variability and so, simplify the qualitative study.

A variety of image fusion techniques is devoted to merge multi-spectral (MS) and panchromatic (Pan) images, which exhibit complementary characteristics of spatial and spectral resolutions. When exactly three MS bands are concerned, the most straightforward fusion method is to resort to an Intensity-Hue-Saturation (IHS) transformation. This procedure is equivalent to inject the difference between the sharp Pan and the smooth intensity into the re-sampled MS bands. Since the histogram-matched Pan and the intensity component do not generally have the same radiometry, when the fusion product is displayed in colour composition, large spectral distortion, (colour changes) may be noticed.

This occurs because the spectral response of the intensity, as synthesised by means of the MS bands, may be far different from that of Pan. Thus, also radiance offsets, slowly space-varying, and not only spatial details, are locally injected. When more than three spectral bands are available, IHS fusion may be applied to three consecutive spectral components at a time, or better the IHS transformation may be replaced with principal component analysis (PCA). This one does not avoid spectral distortion, even if it may be less noticeable. Generally speaking, if spectral responses are not perfectly overlapped with the Pan bandwidth, as it happens with Ikonos and QuickBird, IHS- and PCA-based methods yield poor results in terms of spectral fidelity.

One of the most sophisticated and performing MS + Pan fusion method based on the component substitution strategy is Gram-Schmidt (GS) spectral sharpening invented by Laben and Brover in 1998 and patented by Eastman Kodak. It is widespread being implemented in the ENVI package. The GS method has two operational modes, depending on how the low-resolution version of the Pan image used in the forward GS transformation is defined.

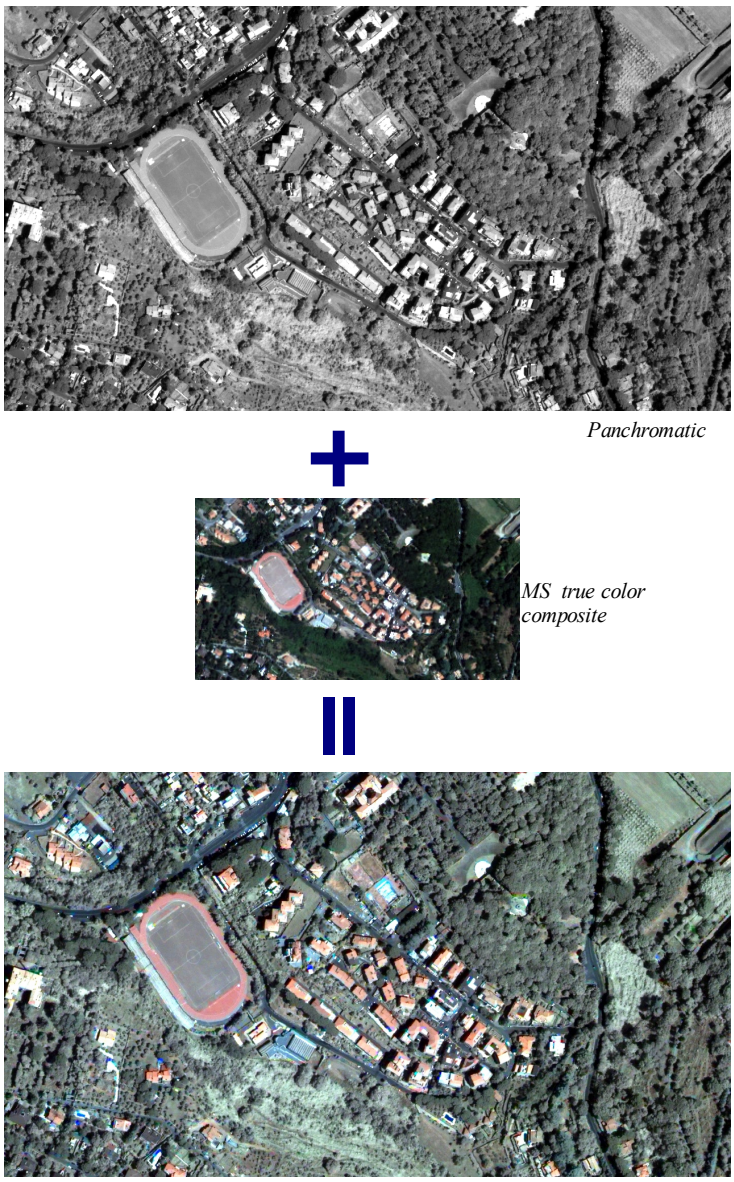

Figure 23: Pansharpening method illustration

The Gram-Schmidt Spectral Sharpening method can be explained with four steps:

- First, a panchromatic band is simulated from the lower spatial resolution spectral bands.
- Second, a Gram-Schmidt transformation is performed on the simulated panchromatic band and the spectral bands, where the simulated panchromatic band is employed as the first band.
- Third, the high spatial resolution panchromatic band is swapped with the first Gram-Schmidt band.

- And finally, the inverse Gram-Schmidt transform is then applied to form the pan-sharpened spectral bands.

Some details of the result images are shown below.

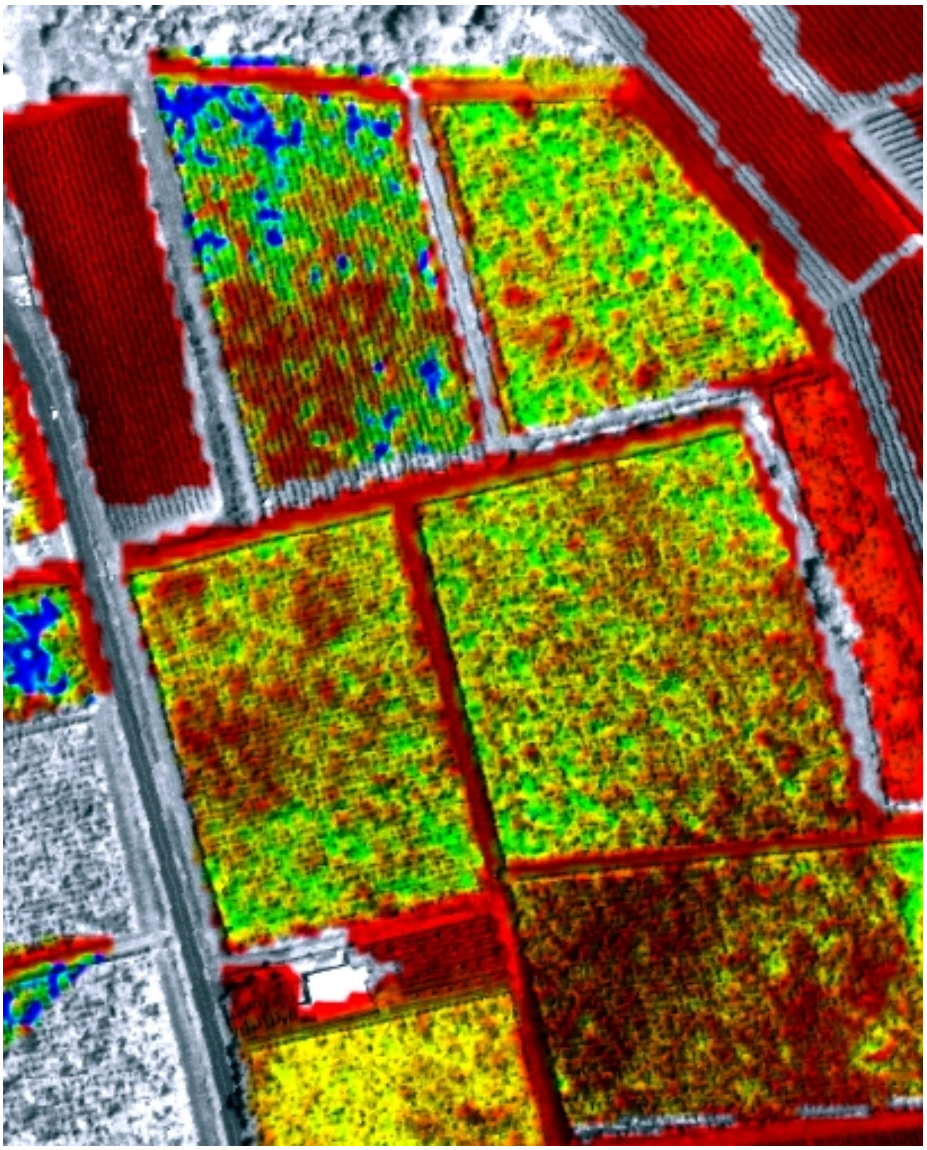

Images 20 21 22: Brix details

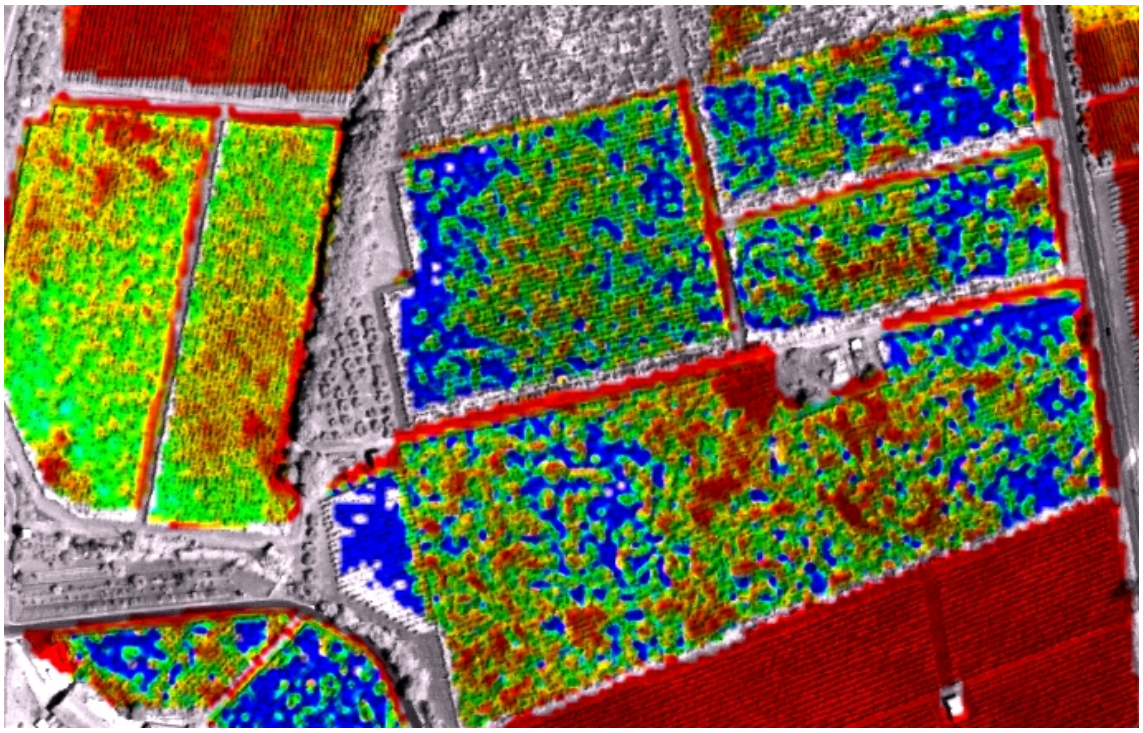

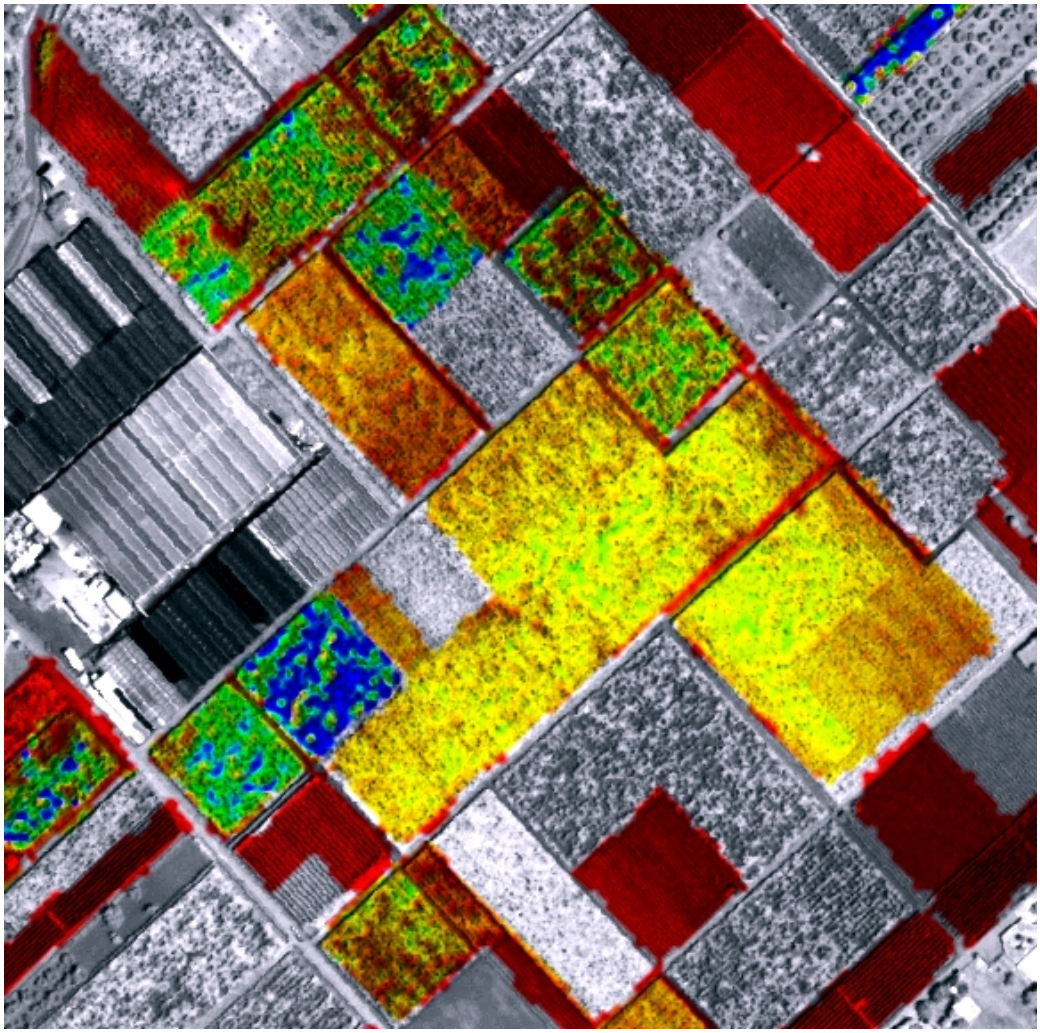

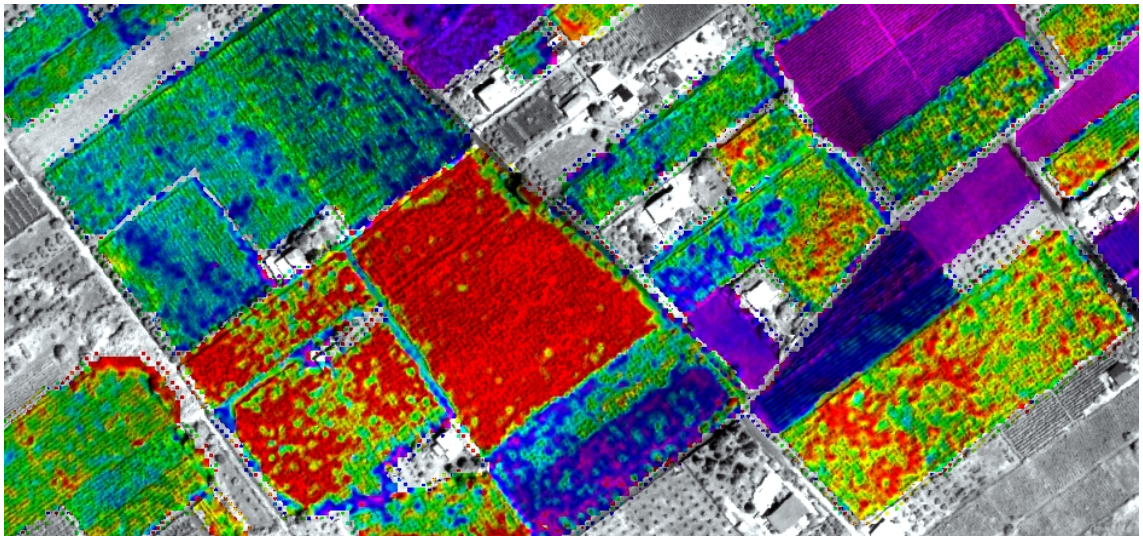

Images 23 24 25: Acidity details

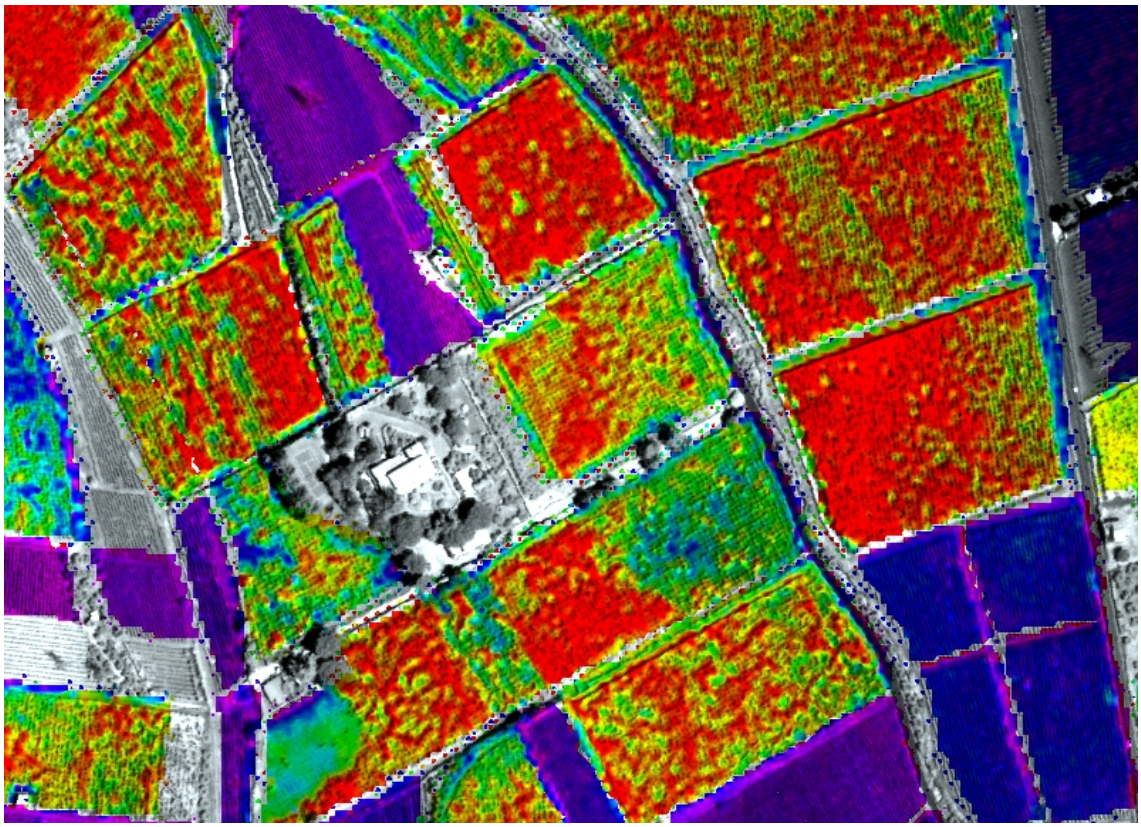

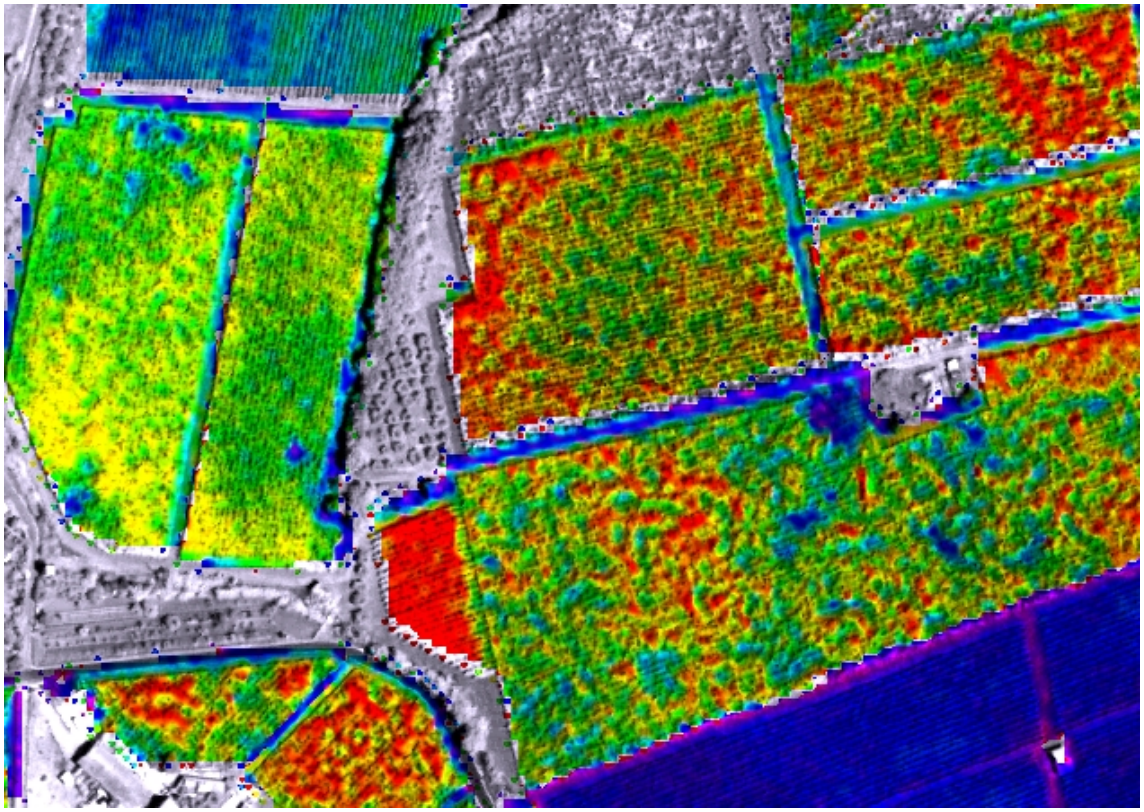

7. Use of hyperspectral imagery to obtain leaf area index maps

As commented before, in section 3.3: Leaf area index and its significance in plantations, there is a considerable interest in assessing LAI, because of its importance in evaluating crop growth and production.

In "*Relationship between leaf area index and proper vegetation indices across a wide range of cultivars"* Changwei Tan; Wenjiang Huang; Liangyun Liu; Jihua Wang; Chunjiang Zhao, Geoscience and Remote Sensing Symposium, 2004. IGARSS apos;04. Proceedings. 2004 IEEE International, an operational approach was proposed to evaluating LAI for different cultivars under different nitrogen treatments and developmental stages by selecting ten familiar remote sensing vegetation indices (VIs).

The result indicated that VIs had the potential for faithfully estimating LAI, and the estimation power of VIs for assessing LAI was better in some stages than others, which primarily depended on the LAI dynamic variation during the process of the growth. As the estimation power of VIs was systematically verified with the other independent data set, the VIs could accurately evaluate LAI. The ratio spectral index of R_{810}/R_{560} was the best index to estimate LAI, which was wondrously sensitive to LAI dynamic variation almost without the influence of cultivars, growth stages and nitrogen treatments. The exponential regression model for LAI based on R_{810}/R_{560} was also established, with a mean determination of coefficient (R^2)

of 0.9573 (P value=0.01) and a mean root mean square error (RMSE) of 0.0365. Therefore, the spectral index of R_{810}/R_{560} could be considered as a sensitive indicator of LAI.

The model proposed on this article was:

$$LAI = 0.765 \cdot e^{0.2637 \cdot \frac{R_{810}}{R_{560}}}$$

Equation 32: Regression formula to obtain LAI from ratio index R_{810} / R_{560}

As presented on Table 5: Band configuration in the operating mode 3 of sensor CHRIS at page 29, we have available the Band L4 (mean wavelength of 551 nm) which can serve to approximate the R_{560} term on Equation 32.

However, the term R_{810} is a bit distanced from the nearest two bands in this range; the band L_{14} is centred on 781nm and the L_{15} on 872nm. As in this part of our study we have the scope of doing a qualitative job, we have interpolated the value at 810nm from the enounced nearest two bands.

7.1. Image preparation

As done with the QuickBird images, the CHRIS ones have also to be prepared and corrected first of analyzing them. The process followed has been the same that in the other case:

- As explained on section 6.1.2: Projection and coordinates changes on page 74, the images have been switched in their projections to the standard in which we work: projection UTM with spheroid WGS 84. The Frascati zone corresponds to the quadrant 33 north.

- After that, a georeferencing has been applied and the orthorectification with the polynomial method has also been used inserting ground control points. The process is explained on section 6.1.3 on page 78.

However, in this case we have found more difficulties to decide the ground control points to use: because of the low spatial resolution of the CHRIS data, it is more difficult to recognise points as crossroads or particular buildings. Nevertheless, the images weren't much distorted because the CHRIS data standard distribution is almost corrected. We have introduced a total amount of 20 points.

7.2. Statistical study

To qualitatively interpolate the value at 810 nm, we have followed a statistical study of the image, using the statistics tool implemented in ENVI. It is accessible under the menu *Basic Tools* → *Statistics* → *Compute Statistics.* Basic statistics and/or tabulated histogram information (frequency distributions) can be calculated for single-band or multi-band images. The minimum, maximum, and mean spectra can only be calculated for multi-band images. Similarly, covariance statistics, which include eigenvectors and a correlation matrix, can only be calculated for multi-band images. The statistics are calculated in double-precision.

After the file has been selected, subsetted, and masked as desired, the Compute Statistics Parameters dialog appears. This dialog contains the following selections:

- Basic Stats - This check box indicates basic statistics (the minimum, maximum, mean, and standard deviation for all bands) are calculated for your data. These basic statistics are always calculated. This option is always set.

- Histograms - To calculate the histogram of each band. The frequency distribution calculations also return the number of points, cumulative points, percent for each bin, and cumulative percentage for each DN (digital number) in the image histogram. The number of histogram bins used in the calculation is set in the ENVI Configuration File (see Setting ENVI Preferences for more information).

- Covariance - To calculate the covariance matrix, the correlation matrix, eigenvalues, and eigenvectors. When this check box is selected, a Covariance Image check box also appears in the dialog. Select the Covariance Image check box to return the covariance and correlation matrices, and the eigenvectors as images in the Available Bands List. The dimensions of the resulting images are nb by nb, where nb is the number of bands

of the input data. The eigenvectors are associated with the rows in the output eigenvector image.

- Samples Resize Factor and Lines Resize Factor - The values in these text boxes indicate the factors used for resizing the samples and the lines of the image while calculating the statistics. To improve the performance for larger images, specify a value of less than 1 to skip pixels. For example, a factor of 0.5 indicates only every other pixel is used to calculate the statistics.

- Output to the Screen - To display the statistics report on the screen. When this check box is selected, a Statistics Results dialog is used to display the resulting statistics.

- Output to a Statistics File - To save the statistics report to an ENVI format statistics file. This file format is used by ENVI to improve the speed of some ENVI processes. When this check box is selected, the Enter Output Stats Filename section appears in the dialog. The default file extension for statistics files is .sta.

- Output to a Text Report File - To save the statistics report to a text file. When this check box is selected, the Enter Output Text Filename section appears in the dialog.

- Queue - Select this button to place the statistics calculation process in the ENVI Queue Manager.

- Report Precision - This button enables you to change the data precision displayed in the output statistics report. The Set Report Precision dialog appears when you click this button. You can use the Data Precision increment button to set the number of digits to display after the decimal point, and the Floating Report toggle button to designate the format (Normal or Scientific) for the numbers in the ASCII report. A Normal number is a number in decimal format (for example, 25.88), whereas a Scientific number is a single digit followed by a decimal value, the letter e, and the exponential power (for example, 2.588e+001).

  For our purpose, only a basic statistical study is needed.

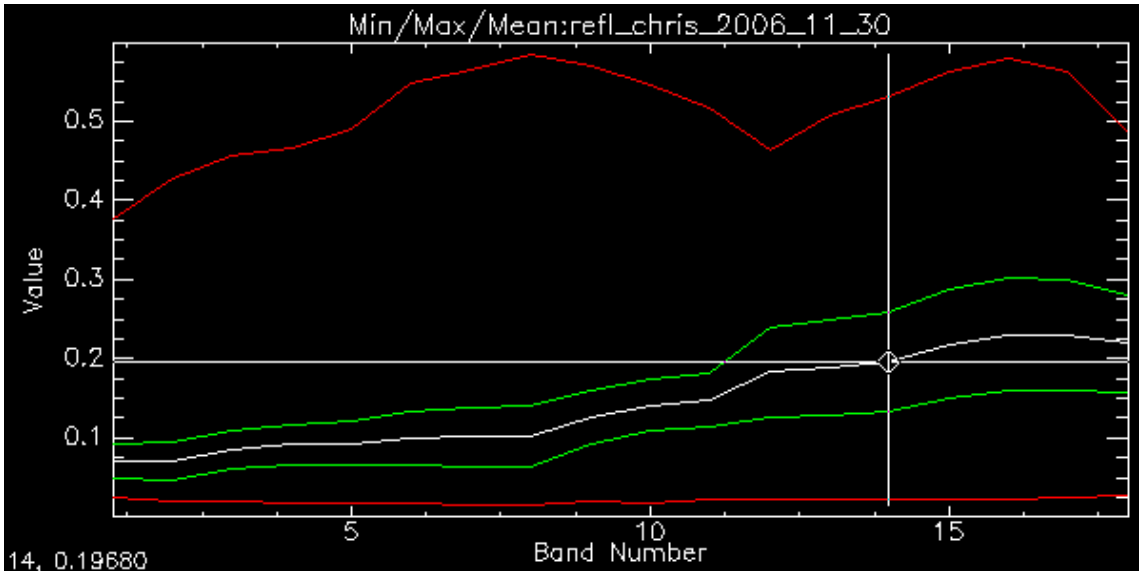

Graphic 11: Statistical result of one of the CHRIS images, specifying the value at band 14

In the graphics obtained, we can observe the mean value in a white line and the maximum and minimum values in a red line. There are also showed in two green lines the results of adding or subtracting the standard deviation to the mean value in each band.

The more important part of the generated statistical text file is the next table, with the mean, max, min and standard deviation values specified for each band.

	Min	Max	Mean	Stdev
Band1	0.024364	0.377210	0.070430	0.021179
Band2	0.020201	0.426614	0.071615	0.023941
Band3	0.020753	0.455662	0.085131	0.023761
Band4	0.018732	0.466925	0.091868	0.024762
Band5	0.017624	0.490269	0.093347	0.027105
Band6	0.016851	0.548925	0.100168	0.033862
Band7	0.015538	0.565135	0.100957	0.037055
Band8	0.014624	0.585221	0.102671	0.039081
Band9	0.019309	0.570646	0.126929	0.033388
Band10	0.018307	0.544594	0.141060	0.032196
Band11	0.023149	0.515401	0.148554	0.033291
Band12	0.023114	0.463954	0.183240	0.056168
Band13	0.022357	0.507363	0.189230	0.060151
Band14	0.021525	0.530602	0.196804	0.062653
Band15	0.022335	0.562863	0.218799	0.068360
Band16	0.023185	0.578816	0.230070	0.071235
Band17	0.024983	0.562835	0.229345	0.070027
Band18	0.029278	0.487529	0.219211	0.061482

Table 17: Basic Stats table of one CHRIS image, part of the statistical text file generated

The process followed to interpolate the hypothetical value at 810 nm has been, for each image:

- Compute the basic statistics of the image.
- Locate the mean values at bands 14 and 15.
- Establish a linear regression curve, considering the centre wavelengths of these bands (781nm and 872nm).
- Calculate the value at 810 nm.
- Evaluate the difference between the 781 nm and 810 nm values.
- Use Band Math to add a new band, result of adding to all pixels at band 14 the difference obtained in the previous step.

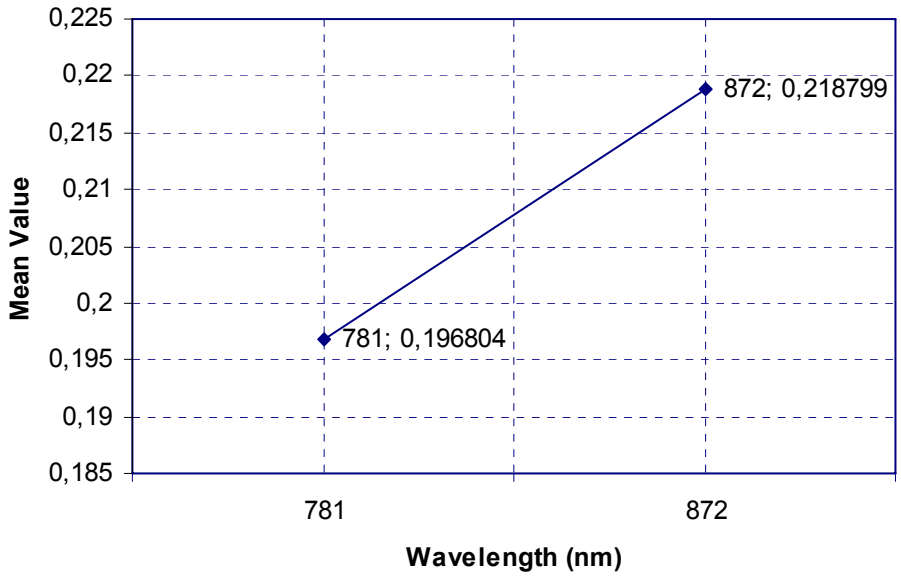

Graphic 12: Lineal regression curve of values in Table 17

The value that we could expect at 810 nm wavelength, in this image, should be 0.2038134. The difference between this value and the one at band 14 is 0.2038134-0.196804=0.00794. Therefore, the formula to write on Band Math must be, only for this image:

$$b1 + 0.00794$$

Equation 33: Formula to introduce in Band Math to simulate an 810nm band for the same image

Obviously, the variable b1 must be assigned to the band 14.

7.3. LAI estimation

Once this has been done for all images, the Equation 32 could be used to finally calculate the LAI map.

The formula that must be introduced in Band Math is the next one:

$$0.765 * \exp(0.2637 * (b1 / b2))$$

Equation 34: Formula to introduce in Band Math to finally calculate LAI maps

We now should assign the variable b2 to the band 4 and the variable b1 to the new band that we have created simulating the 810 nm. To see a more detailed explanation of the use of Band Math, refer to the section 6.2.1: NDVI calculation (second method).

The last step should be the application of a colour scheme, to take advantage of the density-slicing technique. The scheme selected has been the white-green linear. The result images are showed below.

Image 26: LAI June

Image 27: LAI August

Image 28: LAI October

Image 29: LAI November

At this point, it is also possible to apply the image sharpening method described on section 6.3.3: Pansharpening. The selected algorithm in this case has been the HSV. We have used this one to transform the RGB image to HSV colour space, replace the value band with the high-resolution image, automatically resample the hue and saturation bands to the high-resolution pixel size using a cubic convolution technique, and finally transform the image back to RGB colour space. The output RGB image has the pixel size of the input high-resolution data.

However, the image sharpening in this case does not offer a superb result, because of the high difference on pixel size. The CHRIS image has pixels of 21x21 meters, and on the other hand, the pixel size on panchromatic QuickBird is 0.6x0.6 meters.

This way, the images obtained could serve to study a big area, such as the entire DOC, and in some cases, where the pansharpening achieve a good result, also for the intra-field investigation. As an example, below there are showed some details of the image resulted, suitable to the intra-field analysis:

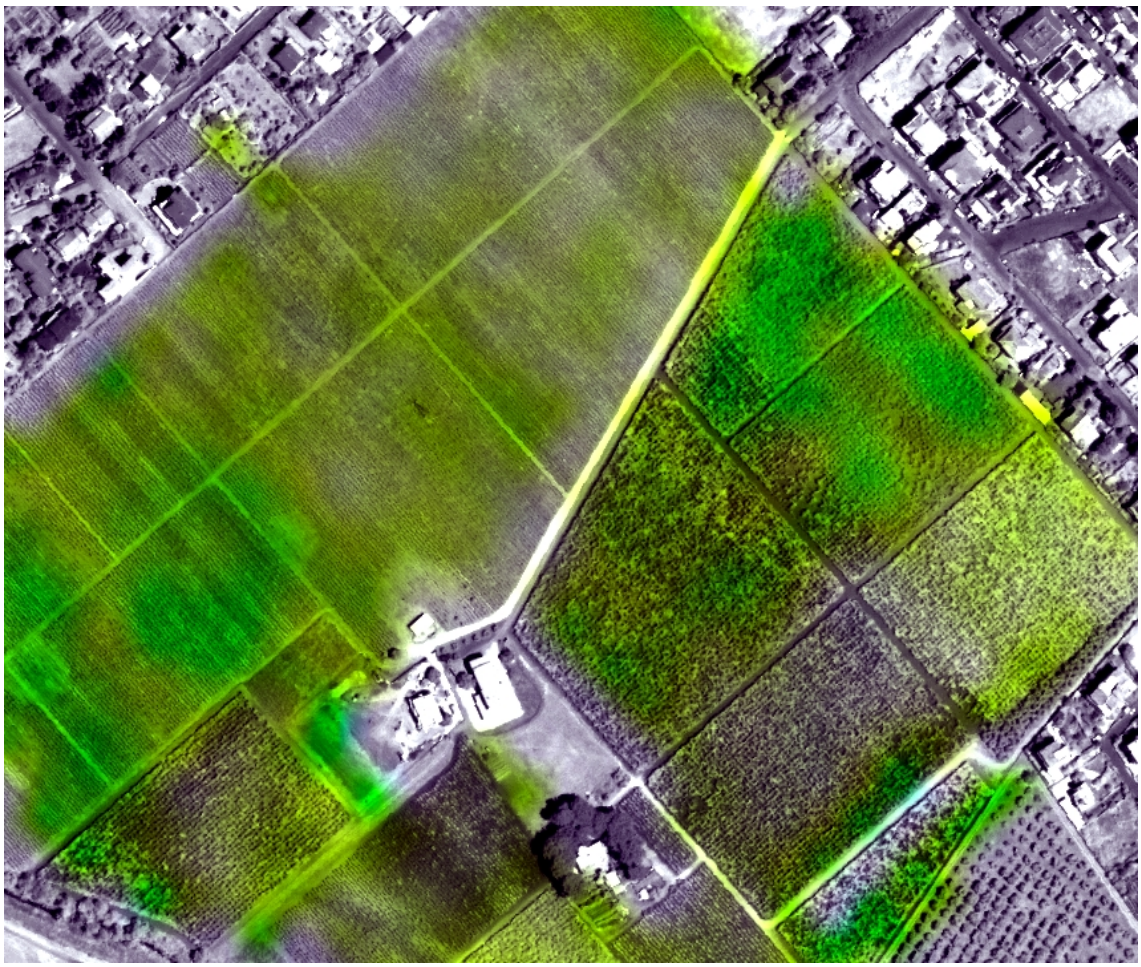

Image 30: LAI pansharpening detail 1

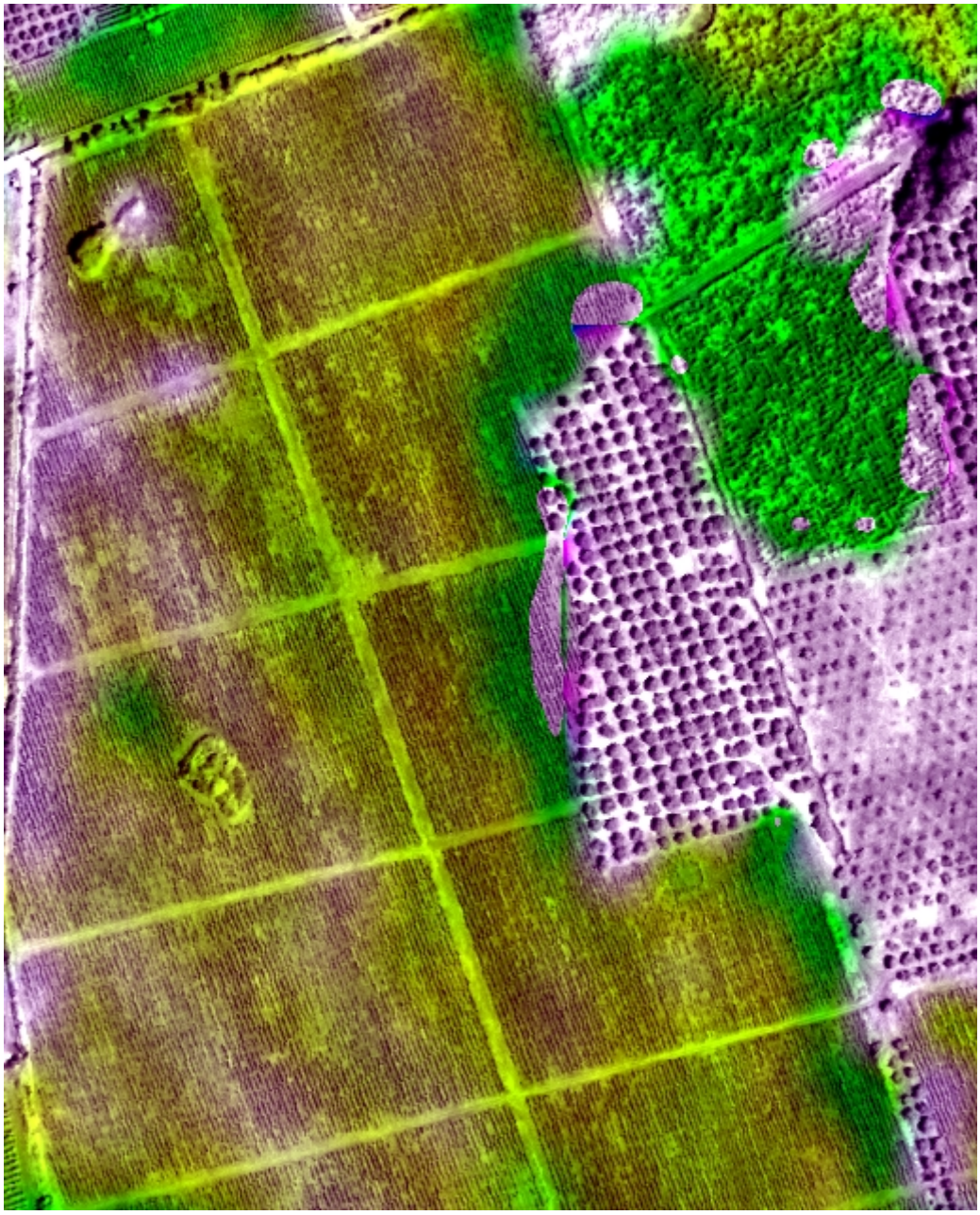

Image 31: LAI pansharpening detail 2

8. Conclusions

In a modern society, the base of a sustainable development is the management of the territory, and the decisions to be adopted must rely on truthful and consistent information, obtained from reliable and trustworthy data.

The spatial remote sensing is a source of this data (actualized and with reasonable costs), that combined with other data sources as orthophotography, cartography, GPS and cadastres, allows us to obtain information (elaborated data). To do that, it is necessary to have the suitable tools and algorithms that will facilitate the provision, analysis and query of this information to or from the different entities involved on the local or regional vineyard management.

This final year thesis has studied the use of multispectral and hyperspectral satellite imagery to assess vineyard condition and grape characteristics in the Frascati region. These vineyards belong to a Controlled Guarantee of Origin of Italian vines.

The project has been developed in collaboration with the firm GEO-K, in the European Spatial Agency (ESA) headquarters on Rome, from January to June 2007, and some results are available, together with other information from other projects, in the site at address www.geovine.org.

It has been demonstrated that it is possible to obtain a valuable utility to the administration and decision-making of a vineyard zone, but also to the intra-field management because of the high spatial resolution of the imagery used.

It has been developed and explained the proceedings to obtain maps of the brix grade and the acidity of the grapes in vineyards with QuickBird multispectral acquisitions. Also, the steps to get the important parameter called Leaf Area Index from CHRIS sensor imagery have been described.

Finally, it has been applied a colour scheme to the resulting maps and in some cases it has been discussed the convenience of using a sharpening technique to evidence the intra-field spatial variability.

Therefore, it has been demonstrated that the employment of satellite imagery together with other support data and tools will fast offer benefits to apply in the different work scales, as the elaboration or actualization of vineyards inventory, the zoning of areas depending of the potential of the terrain to cultivate vines or the prediction of the harvest, or even the acknowledgement of the variability existing on a cultivation, allowing the improvement in the management of DOCs, the products marketing and the quality of the produced wine.

9. The way ahead

There are suitable perfections that can be applied to this project. Some future lines that surely will improve the final result can be these enounced below.

- It is possible to apply neural networks to establish the relationships between the several variables used along the entire project, instead of interpolating values with lineal regression curves. This surely will offer values that will be better simulate the originals.

- Regarding to the LAI obtaining, it will be better to have a band between the 14 and the 15, that will be better fit the factor R_{810}.

- Also talking about the LAI, if we had available at this wavelengths imagery with a higher spatial resolution, the HSV pansharpening of the result image would be more accurate. This way, the viewing of the intra-field variability would be easier and more precise.

10. References

- Generic aspects:
  - About remote sensing in general, it has been interesting and very didactic, although perhaps a bit basic, the tutorial of the Canada Centre for Remote Sensing, and also the equivalent of the NASA:

    [I] *"Fundamentals of Remote Sensing". Canada Centre for Remote Sensing. Natural Resources Canada.* Accessible from: http://ccrs.nrcan.gc.ca/resource/tutor/fundam/index_e.php

    [II] *"Remote Sensing Tutorial", Dr. Nicholas Short's, NASA.* Accessible from http://rst.gsfc.nasa.gov/
  - It has been also useful the study of the synopsis of the projects that the European commission is carrying out:

    [III] *"Space applications for the environment". Development of Earth Observation Technologies within the Fifth Framework Programme. UE Publications office.* http://publications.eu.int
  - More specified on remote sensing applied to farming, but certainly also with a generic approach, it can be consulted:

    [IV] *"Handbook of precision agriculture, Principles and Applications". Ancha Srinivansan, Haworth Press Inc., 2006*

    [V] *"Applications of Remote Sensing to Agribusiness", Jack F. Paris, Spatial Information, Visualization & Analysis Resources Centre, California State University Monterey Bay.*

[VI] *"The Mediterranean precision farming potential", Mr. Christos G. Karydas, Mediterranean Agronomic Institute of Chania, Greece.*

- Concerning the satellites which sensors and images I have used to do this project:
  - QuickBird. The next documents or web pages have a lot of information about the characteristics of these images, and also about sensors, launches, orbits, etc…:

    [VII] "*QuickBird Imagery Products-Product Guide" Digital Globe Inc.* Accessible from http://www.digitalglobe.com/product/product_docs.shtml

    [VIII] http://www.digitalglobe.com/about/quickbird.html
  - About CHRIS sensor and ESA's satellite PROBA:

    [IX] *"Chris Data Format", March 2005,* accessible from http://earth.esa.int/proba/

    [X] Web about the sensor CHRIS: http://earth.esa.int/object/index.cfm?fobjectid=4216

    [XI] *"The Compact High Resolution Imaging Spectrometer (CHRIS):the future of hyperspectral satellite sensors", Barbara Van Mol and Kevin Ruddick, Presented at the Airborne Imaging Spectroscopy Workshop, Bruges, October 2004*

    [XII] *"First results from the PROBA/CHRIS Hyperspectral/Multiangular Satellite System", Luis Guanter, Luis Alonso, José Moreno, IEEE Geoscience and Remote Sensing Letters, Vol2-3, Julio 2005*

    [XIII] *"On the Potential of CHRIS/PROBA for Estimating Vegetation Canopy Properties from Space", M. J. Barnsley et al. Remote Sensing Reviews, 2000, Vol. 00, Overseas Publishers Association.*

- About satellite imagery:
  - Regarding the radiometric correction of QuickBird images, the more specific document that I have consulted has been:

    [XIV] *"QuickBird relative radiometric performance and on-orbit long term trending", Keith S. Krause, DigitalGlobe, Inc. Earth Observing Systems XI.*
  - About the geometric rectifications, this is the best article that I have found:

    [XV] *"Rectificación y ortorrectificación de imágenes de satélite: análisis comparativo y discusión", Cuartero, A., Felicísimo, A. M. (2003), GeoFocus (Artículos), nº 3, 2003, p. 45-57. ISSN: 1578-5157*
  - About the projections and coordinate systems, as well as the help of the programs ENVI and ERDAS, I have seen the next web page:

    [XVI] http://hosting.soonet.ca/eliris/gpsgis/Lec2Geodesy.html
  - Information about Pan sharpening GS method:

[XVII] *"MS + Pan Image Fusion by an Enhanced Gram-Schmidt Spectral Sharpening" Bruno Aiazzil et alt. Institute of Applied Physics "Nello Carrara", IFAC-CNR and Department of Electronics & Telecommunications, University of Florence.*

- In relation to the vegetation indices:
  - This is the basic original article of NDVI:

    [XVIII] *"Monitoring the vernal advancements and retrogradation of natural vegetation". Rouse, J. W., Haas, R. H., Schell, J. A., Deering, D. W., & Harlan, J. C. NASA/GSFC final report.*
  - About EVI can be seen:

    [XIX] *"Enhanced Vegetation Index", Terrestrial Biophysics & Remote Sensing Lab. University of Arizona.* http://tbrs.arizona.edu/project/MODIS/evi.php
  - About FAPAR (Fraction of Absorbed Photosynthetically Active Radiation), I would advise to visit the next page:

    [XX] http://fapar.jrc.it
  - The University of Nebraska offers some information about SVI:

    [XXI] *"Standard Vegetation Index". University of Nebraska-Lincoln. 2005 CALMIT.* http://casde.unl.edu/imagery/svi/index.php
- Concerning the Leaf Area Index (LAI):
  - From a theoretical perspective:

    [XXII] *"Estimation of Global Leaf Area Index and Absorbed Par Using Radiative Transfer Models". Ranga B. Myneni, Ramakrishna R. Nemani, and Steven W. Running. IEEE Transactions on Geoscience and Remote Sensing, Vol. 35, NO. 6, 1997*
  - The next article has been very useful in the development of this project:

    [XXIII] *"Relationship between Leaf Area Index and proper Vegetation Indices across a wide range of cultivars", Changwei Tan, Wenjiang Huang, Liangyun Liu, Jihua Wang, Chunjiang Zhao. Geoscience and Remote Sensing Symposium, 2004. IGARSS '04. Proceedings. 2004 IEEE International*
  - With SAR there have been also a lot of studies. Although in this project it hasn't been used, it is advisable to know:

    [XXIV] *"Estimation of leaf area index over agricultural areas from polarimetric SAR images", Sasan S. Saatchl, Robert Treuhalfl, Myron C. Dobson, Geoscience and Remote Sensing Symposium, 1994. IGARSS '94. Surface and Atmospheric Remote Sensing: Technologies, Data Analysis and Interpretation, IEEE.*

- More concretely, and regarding the theme that concerns us, there have been published a lot of articles that investigate the obtaining of parameters on vineyards by remote sensing images, from satellites or airborne. Next I have tried to do a small synopsis of the more relevant documents that I have found:

  [XXV] *"Airborne/Spaceborne remote sensing for the grape and wine industry" David Lamb, Andrew Hall and John Louis. Australian Regional Institute Ltd.* *http://www.regional.org.au/au/gia/18/600lamb.htm*

  [XXVI] *"Vineyard monitoring and management beyond 2000 Workshop", David Lamb,2000 WaggaWagga, Australia*

  [XXVII] *"Precision vineyard management from space",Simoneta Cheli, Luigi Fusco, Stefano Sandrelli, ESA bulletin 123, august 2005*

  [XXVIII] *"2005 Progress Report: Using Precision Agriculture Tools to Increase Vineyard Production Efficiency", Terence R. Bates Dept. of Horticultural Sciences. Cornell University Vineyard Laboratory, New York (USA)*

  [XXIX] *"Assessing vineyard condition with hyperspectral indices: Leaf and canopy reflectance simulation in a row-structured discontinuous canopy", P.J. Zarco-Tejada et Alt. Remote Sensing of Environment 99 (2005) 271 – 287*

  - About BACCHUS project:

    [XXX] *"Proyecto Bacchus. Aproximación metodológica al inventariado y gestión del viñedo". S. Montesinos, M. Bea, L. Fernández, GEOSYS S.L. Presentado en la Asociación Española de Teledetección, Cáceres septiembre de 2003.*

    [XXXI] *"Bacchus: una herramienta para mejorar el inventario y la gestión de la viña", Montesinos, Salomon, et alt. Presentado en el V Foro Mundial de la Viña. Logroño, Marzo de 2006.*

    [XXXII] *"Il Progetto BACCHUS, Applicazioni sull'area del Frascati", Fulvio Comandini, ESA, Space for Wine, Frascati, April 2005*

  - About the investigation Project on Franciacorta, Italy:

    [XXXIII] *"Use of satellite in precision agriculture: the Franciacorta experience", L.Brancadoro, O. Failla, P. Dosso y F. Serina, VIth terroir international congress 2006.*

    [XXXIV] *"Viticoltura di precissione assistita da satellite", Ing. P. Rossi, Terradat, SRL, Workshop Citimap2006.*

  - With the purpose of detecting senile or dead vineyards, it has been written:

    [XXXV] *"Airborne Remote Sensing of Vineyards for the Detection of Dead Vine Trees", Jocelyn Chanussot, Patrick Bas and Lionel Bombrun, Geoscience and*

Remote Sensing Symposium, 2005. IGARSS '05. Proceedings. 2005 IEEE International.

- With some discrimination objectives, such as between vineyards and other cultivars, or between diverse types of vineyards, it has been written:

  [XXXVI] *"Texture Orientation and Period Estimator for Discriminating Between Forests, Orchards, Vineyards, and Tilled Fields" Roger Trias-Sanz, IEEE Transactions On Geoscience And Remote Sensing, Vol. 44, NO. 10, Oct 2006*

  [XXXVII] *"Use of Hyperspectral Imagery for Mapping Grape Varieties in the Barossa Valley, South Australia" F.M. Lacar, M.M. Lewis and I.T. Grierson. Geoscience and Remote Sensing Symposium, 2001. IGARSS '01. IEEE 2001 International.*

  [XXXVIII] *"Use of Hyperspectral Reflectance for Discrimination between Grape Varieties" F.M. Lacar, M.M. Lewis, I.T. Grierson, IEEE Applied Imagery Pattern Recognition Workshop, 2002. Proceedings. 31st*

  [XXXIX] *"Vine plot detection in aerial images using Fourier analysis" C. Delenne, G. Rabatel, V. Agurto, M. Deshaye.,* accessible from *http://www.commission4.isprs.org/obia06/Papers/*

- Focusing the management aspects, but also very interesting, it can be consulted:

  [XL] *"Applied Research into the Integration of Spatial Information Systems with Viticultural Research &Vineyard Management Systems", Lloyd Smith, Peter Firns. http://www.business.otago.ac.nz/SIRC05/*

  [XLI] *"Spatial Aspects of Vineyard Management and Wine Grape Production", Lloyd Smith & Peter Whigham, http://www.business.otago.ac.nz/SIRC05/*

  [XLII] *"Vineyard and Winery Management: A Case Study in GIS Implementation", Donald A. Gordon, VESTRA Resources, Inc. http://gis2.esri.com/library/userconf/proc97/proc97/to450/pap411/p411.htm*

- About the relationship between vineyards and proper indices as NDVI, LAI, or vegetative vigour:

  [XLIII] *"Vineyard canopy density mapping with IKONOS satellite imagery", Lee F. Johnson et alt. Presented at the Third International Conference on Geospatial Information in Agriculture and Forestry, Denver, USA, November 200"*

  [XLIV] *"Toward the Improved Use of Remote Sensing and Process Modelling in California's Premium Wine Industry", Lee F. Johnson et alt., accessible from http://geo.arc.nasa.gov/sge/vintage/*

[XLV] *"Image-Based Decision Tools for Vineyard Management", Lee F. Johnson et alt., Written for presentation at the 2003 ASAE Annual International Meeting, Las Vegas, USA.*

- The next document has been specially interesting because of the resemblance with the theme developed in this project:

  [XLVI] *"Hyperspectral remote sensing for vineyard management", Sedat A. Arkun, Iain J. Dunk and Stephen M. Ranson, Australian Regional Institute Ltd.* *http://www.regional.org.au/au/gia/18/586arkun.htm*

- With Radar there also have been a lot of work in this sense, such as:

  [XLVII] *"SMOS REFLEX 2003: L-Band Emissivity Characterization of Vineyards", Mercè Vall-llossera, Adriano Camps, et alt., IEEE Transactions On Geoscience And Remote Sensing, Vol. 43, No. 5, May 2005*

- Other consulted documents:
  - Information about Frascati DOC:

    [XLVIII] *http://www.consorziofrascati.it/*

  - Shapefile information

    [XLIX] *"ESRI Shapefile technical description" Environmental Systems Research Institute inc. July 1998*
    http://www.esri.com/library/whitepapers/pdfs/shapefile.pdf

  - I have used also the online help of the programs used in this project: ENVI, version 4.2, year 2005, ERDAS IMAGINE version 8.7, year 2003, and ARC VIEW GIS, version 3.2, year 1999.

11. Figure index

11.1. Images

11.2. Graphics

11.3. Figures

11.4. Tables

11.5. Equations